

CATALYTIC HYDROFUNCTIONALIZATION AND SMALL MOLECULE REACTIVITY
AT A LOW-VALENT COBALT CENTER SUPPORTED BY A BIS(CARBENE) CCC
PINCER LIGAND

BY

ABDULRAHMAN IBRAHIM

DISSERTATION

Submitted in partial fulfillment of the requirements
for the degree of Doctor of Philosophy in Chemistry
in the Graduate College of the
University of Illinois at Urbana-Champaign, 2017

Urbana, Illinois

Doctoral Committee:

Assistant Professor Alison R. Fout, Chair
Assistant Professor Kami L. Hull
Professor Kenneth S. Suslick
Professor Scott E. Denmark

Abstract

The ubiquity of noble metal catalysts in both industrial and academic settings is a testament to their impressive reactivity, versatility, and modularity. Recent advances in cross-coupling catalyses have principally been achieved with this privileged class of compounds, in large part due to the ability of noble metals to engage in well-defined two-electron redox events that are amenable to analysis and prediction. In contrast, the reactivity of first-row transition metals is mostly characterized by one-electron redox changes that can be deleterious and has precluded the systemic incorporation of these more earth-abundant and affordable metals in certain settings.

Considerations of the intrinsic electronic structure of these base metals provides insight into their apparently orthogonal redox reactivity to second and third-row transition metals. For many first-row transition metal compounds, the presence of a weak ligand field engenders a high-spin electron configuration and one-electron events at the expense of two-electron elementary steps. Accordingly, our lab and many others have endeavored to utilize a strong ligand field approach whereby a highly-donating ligand set is installed at the first-row transition metal center to impart a strong ligand field and thereby disfavor one-electron redox changes.

Early work focused on the synthesis and characterization of cobalt derivatives of the (^{DIPP}CCC) pincer ligand, (^{DIPP}CCC = bis(diisopropylphenyl-benzimidazol-2-ylidene)phenyl), a platform which provides highly-donating carbenes and an aryl carbon linkage to the coordinated metal. Multinuclear NMR spectroscopies, cyclic voltammetry, X-ray crystallography, and EPR spectroscopies have established the successful isolation of Co(I), Co(II), and Co(III) derivatives with this ligand platform. The diamagnetic natures of the Co(I) and Co(III) compounds, (^{DIPP}CCC)Co(N₂) and (^{DIPP}CCC)CoCl₂py, respectively, confirmed the ability of the CCC ligand framework to support low-spin electron configurations at the first-row transition metal center and

motivated additional studies into the reactivity of the Co(I) dinitrogen compound.

Initial studies explored the catalytic competency of the (^{DIPP}CCC)CoN₂ species, specifically towards hydrosilylation and hydroboration, two processes typically mediated by precious metal catalysts. Hydrosilylation of terminal alkene substrates proceeded in good yields with secondary and tertiary silanes, an important feat for earth-abundant catalysts for which examples of hydrosilylation with tertiary silanes and hydrosiloxanes are relatively uncommon. Interestingly, the catalyst exhibited high chemoselectivity and 1,2-regioselectivity even towards challenging substrates bearing unprotected hydroxyl, amino, nitrile, formyl, and conjugated diene functionality, a consequence of both steric and electronic factors. A variety of experiments, including ²⁹Si NMR and two-dimensional NMR spectroscopy experiments, confirmed oxidative addition of silane and established that this catalysis likely proceeds through a Chalk-Harrod-type mechanism, thereby establishing that a Co(I)/Co(III) redox couple is operative for this process.

Extension of this catalysis towards hydroboration was successful. In addition to exhibiting a chemoselectivity and regioselectivity similar to that of the hydrosilylation protocol, the (^{DIPP}CCC)Co(N₂) catalyst was also found to be competent towards nitrile reduction, a challenging process for earth-abundant metal catalysts. Mechanistic studies establish the intermediacy of a cobalt hydride, as well as the negotiation of insertion, isomerization, and β-hydride elimination processes. These results allowed us to propose a mechanism, similar to that proposed for the hydrosilylation protocol, whereby the cobalt catalyst accesses a Co(I)/Co(III) redox couple, highlighting the ability of this bis(carbene) CCC pincer platform to impart noble-metal-type reactivity onto base metals.

Finally, the stoichiometric reactivity of the Co^I complex towards potential two-electron oxidants was probed in order to assess the viability of Co(I)/Co(III) redox couple with additional

substrates and advance our understanding of the reactivity of these interesting compounds.

To My Family

Acknowledgements

It is impossible to overstate how grateful I am to my parents and siblings. Their words of advice and encouragement have been a solace for me throughout my life and graduate school career. I am extremely fortunate to have them as my family and I could not have gotten to this point without them.

I would also like to thank my advisor Professor Alison Fout for her support and guidance throughout my time at the University of Illinois. She provided me with the opportunity to be a part of a project that was both exciting and intellectually fulfilling. Her support and the support of my committee members, Professor Kenneth Suslick, Professor Kami Hull, and Professor Scott Denmark, have been invaluable to my growth as a chemist and I am grateful for all the insights that they shared with me.

I would also like to thank my colleagues, Zack Gordon, Gabriel Espinosa Martinez, Kenan Tokmic, Courtney Ford, Bailey Jackson, Michael Drummond, Jack Killion, Joe Nugent, Tabitha Miller, and Safiyah Muhammad, as well as previous Fout group members Dr. Yun Ji Park and Professor Ellen Matson. I deeply appreciated all their support, suggestions, and discussions about chemistry and life. I will always be grateful for their conversation and am lucky to count them as my friends.

Additionally, I would like to thank Lingyang Zhu for her help with more advanced NMR spectroscopy experiments, Dr. Danielle Gray and Dr. Jeffery Bertke for their help with crystallographic characterizations, and Dr. Mark Nilges for his help with EPR spectroscopy experiments.

Finally, I am forever grateful for the support of Connie Knight, Stacy Dudzinski, and the IMP office secretaries, Beth Myler, Karen Watson, Theresa Struss, and Katie Trabaris. Their

kindness and warmth have made navigating departmental requirements an easy and pleasant experience.

Table of Contents

Chapter 1: Approaches to circumvent one-electron reactivity at first-row transition metal centers	1
Chapter 2: Synthesis and characterization of cobalt CCC bis(carbene) pincer complexes	20
Chapter 3: Catalytic hydrosilylation with (^{DIPP} CCC)CoN ₂ : substrate scope and mechanistic insights	43
Chapter 4: Catalytic hydroboration with (^{DIPP} CCC)CoN ₂ : evidence for insertion, isomerization, and β-hydride elimination processes	76
Chapter 5: Reactivity of (^{DIPP} CCC)CoN ₂ towards dichalcogenides and other potential two-electron oxidants	103

Chapter 1

Approaches to circumvent one-electron reactivity at first-row transition metal centers

1.1 The origin of one-electron reactivity at first-row transition metals

Noble metal centers have long held a privileged role in synthesis, small molecule activation, and catalysis, resulting in their frequent use in both academic and commercial settings. Indeed, some of the most well-known catalysts or organometallic complexes, such as Wilkinson's catalyst,¹ Vaska's complex,² and Karstedt's catalyst,³ feature noble metal centers. The ubiquitous nature of these compounds is, in many ways, attributable to their predictability or modularity, engaging in well-defined two-electron redox processes that render them particularly amenable to rational ligand design and modification to achieve desirable regio-, stereo-, and chemoselectivities in chemical transformations. Pathways such as oxidative addition and reductive elimination have been systematically studied, enabling significant advances in the field of catalytic C–N bond formation for example.⁴ The work of different groups, such as the Hartwig lab and the Buchwald lab, has established the profound impact of ligand design on a catalyst's competency towards redox processes.^{4,5} As a result, substantial attention has been given to the electronic and steric parameters of coordinating ligands in many catalytic systems, systematizing the effects of different ligand characteristics on overall function and structure of these compounds.^{6,7} Needless to say, a consideration of the fundamental electronic structures of these metals is required to appreciate their intrinsic tendency to engage in well-defined redox processes, particularly in relation to base metals.

A comparison of the reactivity of second- and third-row transition metals has long established that, for a given ligand set, second-row metals generally react more rapidly than their third-row congeners.⁸ An investigation carried out by Wolczanski and coworkers probed the origin

of this general trend, specifically focusing on the olefin substitution chemistry of a niobium complex and its tantalum analogue to make inferences about the nominally swifter reactivity of second-row transition metal complexes.⁸ Interestingly, this study demonstrated that, despite higher olefin binding energies, the niobium complex exhibited greater levels of olefin substitution. This effect was attributed to a greater density of states (DOS) at the niobium complex compared to tantalum (Figure 1.1). This greater DOS, which can lower transition state energies by allowing greater mixing of surfaces near the transition states, is, in turn, attributed to the weaker field strength of second-row transition metals, as well as the greater mixing of 6s and 5d metal orbitals in third-row transition metal complexes compared to analogous mixing of 5s and 4d orbitals in second-row congeners.

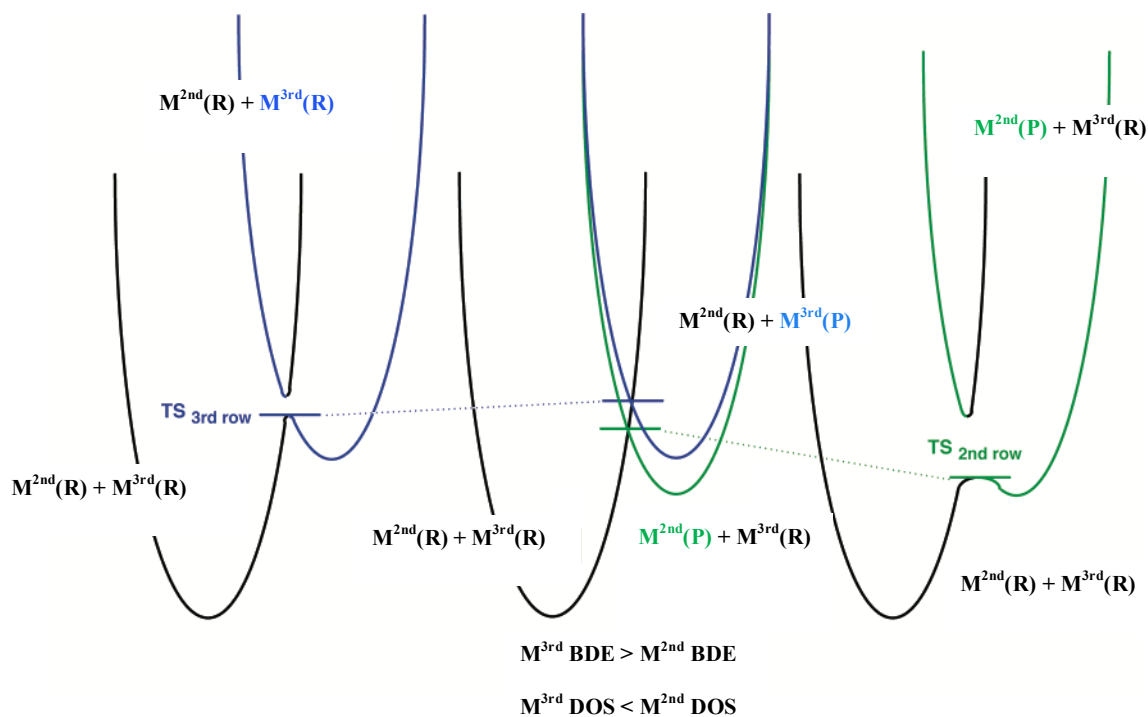


Figure 1.1 Density of states at second and third-row transition metal compounds

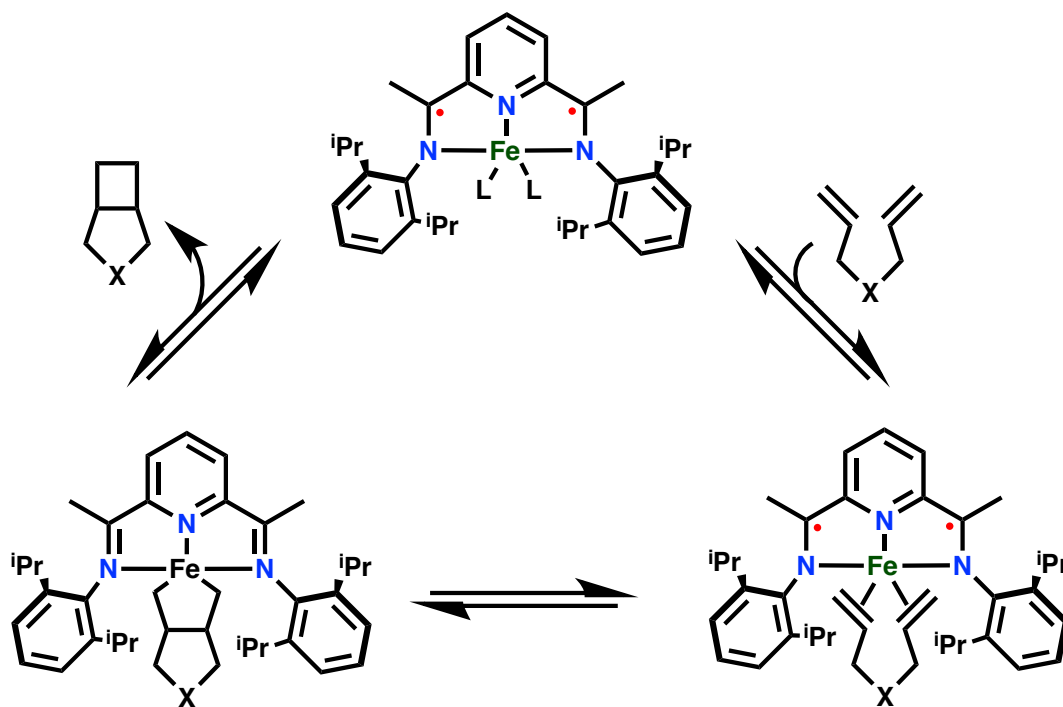
Interestingly, this trend of greater DOS is also borne out in a comparison of first- and second-row transition metals.⁹ First-row transition metals possess a greater DOS, as evidenced by

UV spectroscopic studies.⁹ As in the case of second-row transition metals, this greater DOS is coincident with a weaker ligand field strength. However, in the case of first-row transition metal complexes, the ligand field strength is now sufficiently weak to generally promote high-spin electron configurations and render one-electron events, as opposed to two-electron events, more likely. In some cases, this complementarity to the two-electron reactivity of second- and third-row transition metals has been used to great effect.¹⁰ Nevertheless, the disruptive effect of one-electron redox changes has also precluded the systemic incorporation of more earth-abundant first-row transition metals in certain catalytic contexts.⁹ Recent research efforts have focused on mitigating or circumventing the proclivity of base metals to engage in one-electron chemistry, particularly considering the scarcity and the energy-intensive nature of the extraction processes for noble metals.¹¹ Moreover, the generally reduced toxicity and biocompatibility of first-row transition metals has provided a further impetus for conferring noble metal reactivity on first-row transition metal centers.

1.2 A redox-active ligand approach towards two-electron reactivity

Recent studies by Chirik^{12,13,14}, Heyduk^{15,16}, and others^{17,18} have provided some early notable successes in the use of base metal systems towards two-electron processes. The prominent use of amidophenolate cobalt complexes by Soper¹⁹ and aryl-substituted bis(imino)pyridine iron compounds by Chirik, for example, has facilitated alkene and alkyne hydrogenation²⁰, hydrosilylation, olefin cyclization²¹ (Scheme 1.1), and atom and group transfers at first-row metal centers.²² Such work features a prominent use of redox non-innocent ligands, whereby the ligand can serve as an electron reservoir, providing the reducing equivalents, i.e. electrons, to accommodate two-electron elementary steps that may otherwise be inaccessible to the ligated base metal. This approach signifies a departure from the more classical formulation of ligands as

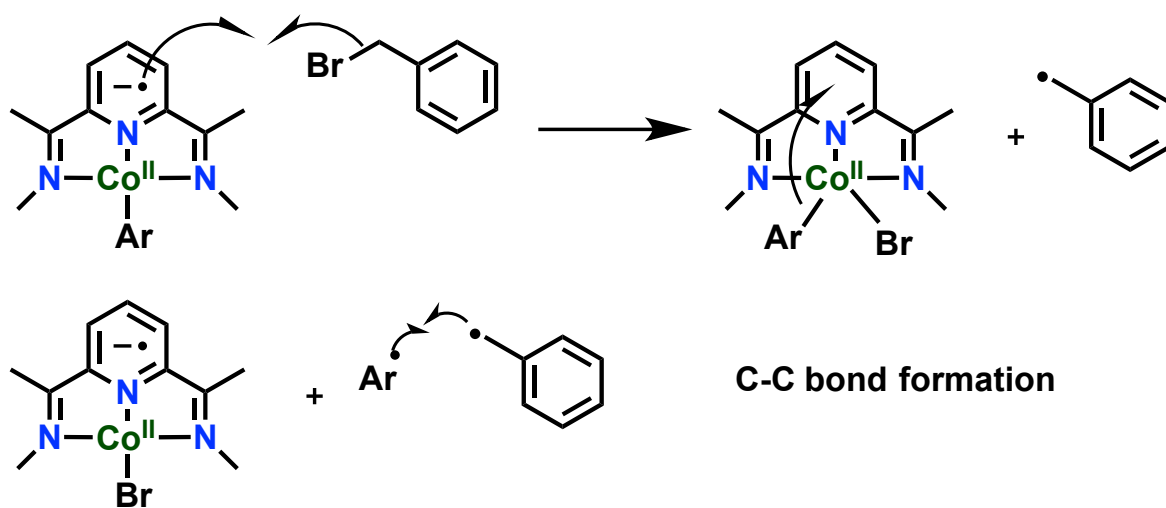
“spectators” and is informed by Nature’s own prominent use of redox-active amino acids at the active sites of different enzymes.²³ Thus, in contrast to a conventional oxidative addition process whereby the metal oxidation state changes by two units, the redox-active ligand and metal each supply an electron for a net two-electron process.



Scheme 1.1 Fe-catalyzed [2 + 2] cycloaddition

In addition to providing a platform by which base metals can access chemical space typically restricted to noble metal compounds, studies of base metal complexes bearing redox non-innocent ligands have shown that these compounds can undergo unusual pathways over the course of a chemical transformation, in some cases providing potentially novel synthetic routes to products of interest. Desage-El Murr, Fensterbank, and coworkers reported an iron complex that is competent towards Csp^2-Csp^2 bond formation between benzene and aryl bromides.²⁴ Spectroscopic and DFT studies suggest an uncommon inner-sphere mechanism for the C–H activation step rather than a homolytic aromatic substitution pathway, where the transition state

involves three components – an HMDS⁻ anion (HMDS = hexamethyldisilazide), the iron complex, and benzene. Similarly, Budzelaar reported a bis(imino)pyridine cobalt complex that couples aryl chlorides and activated benzyl or allyl chlorides and bromides.²⁵ This is thought to proceed by halide abstraction from the bis(imino)pyridine cobalt aryl complex, (L[•])Co^{II}Ar to generate (L)Co^{II}(Ar)(Br) (Scheme 1.2). Loss of an aryl radical from this complex, facilitated by the oxidizing nature of the ligand in the L⁰ oxidation state, enables radical recombination with a benzyl radical to generate the Csp²–Csp³ bond formation. Similar nickel-mediated cross-coupling studies²⁶ lend further credence to the notion that such unconventional mechanistic pathways, particularly in the field of cross-coupling catalysis, are not necessarily metal-specific; the use of redox-innocent ligands is often accompanied by divergent chemical pathways. This, in turn, may enable access to new selectivities and synthetic schemes.



Scheme 1.2 C-C coupling with a bis(imino)pyridine cobalt complex

Interestingly, investigations have shown that, in some contexts, a ligand with potential to engage in redox-activity need not participate directly to engender interesting reactivity. Bielawski and co-workers reported a nickel catalyst with an N-heterocyclic carbene ligand that incorporates a

redox-active naphthoquinone moiety and performs aryl-aryl Kumada cross-coupling.²⁷ Although an electronic contribution from the ligand is not invoked to achieve product formation, the addition of cobaltocene reductant to the complex arrested catalysis, demonstrating that modulation of catalytic reactivity can be achieved even in the absence of direct ligand assistance from the redox-active moiety.

Despite the advantages concomitant with the use of the redox-active ligand approach, some challenges have precluded its utilization to a more significant extent. The ambiguous nature of redox processes upon the complexation of non-innocent platforms means that the role of the ligand is not always clearly established.²⁸ Coupled to the presence of frequently elusive paramagnetic intermediates that are less amenable to examination by conventional methods, this renders mechanistic analyses of these systems less tractable. Additionally, a potential pitfall of this strategy is that the added electronic complexity of such systems may translate into greater chemical complexity, introducing side reactions that mitigate system efficacy.²⁹ Such difficulties have limited the optimization and extension of these types of systems to larger-scale synthetic processes.²⁸ Nevertheless, the unusual reactivity observed with redox non-innocent platforms renders this a promising field for further development.

1.3 A strong-field approach with base metals

1.3.1 Phosphorous-based ligands with first-row transition metal complexes

Notwithstanding the successes of the redox-active approach, studies probing the fundamental ability of first-row metals to engage in two-electron processes like oxidative addition and reductive elimination have been explored. Given the intrinsically weaker ligand field of first-row transition metals, ligands capable of inducing a stronger ligand field, i.e. possessing orbitals that better overlap with the 3d orbitals of the first-row transition metal, should disfavor one-

electron pathways upon complexation and, thereby, result in metal-centered two-electron reactivity more akin to that of second- and third-row transition metal complexes.⁹ A consideration of angular overlap arguments is highly informative in this regard. As seen in Figure 1.2, carbon-based and phosphorous-based (as opposed to nitrogen or oxygen-based) orbitals, for example, are especially well-suited to interact with the orbitals of a first-row transition metal given their proximity in energy.⁹ Consequently, carbon-based and phosphine-based ligands, are best able to impart a strong ligand field for first-row transition metals.

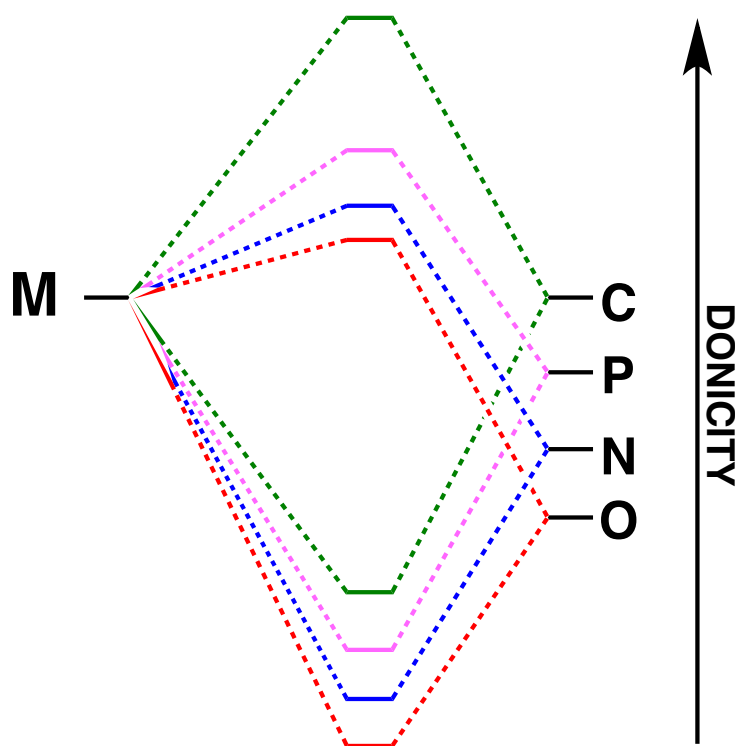
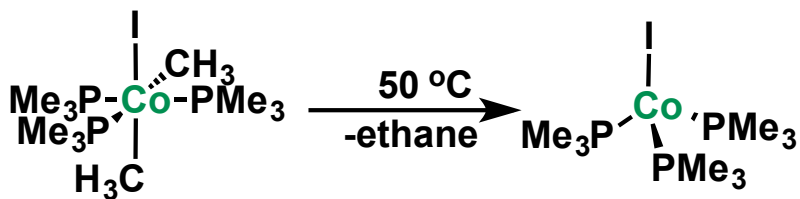


Figure 1.2 Angular orbital overlap between metal and ligand orbitals

The use of phosphorous-based ligands with noble metals has already been extensively realized.³⁰ Phosphines can support a wide range of oxidation states, serving as ligand of intermediate hardness and π -acceptor capability.³⁰ The modularity of the electronic and steric

properties of phosphines also renders them attractive as ligands. Indeed, the impact of electronic and steric effects have been systematized to a great degree using such frameworks as the Tolman parameter and Lever parameter.³⁰ The cone angle of ligated phosphines, for example, have been successful in rationalizing the reactivity of several complexes.³⁰ Accordingly, it is unsurprising that these ligands have been used with first-row transition metal centers, particularly in a context where the increased donicity of these ligands may serve to “ennoble” the base metal.

Early reports of first-row transition metal complexes bearing phosphines and other phosphorous-based ligands indicated that such ligands have successfully facilitated two-electron chemistry at the low-valent metal center in some cases. Misono and coworkers reported the cleavage of dihydrogen with a cobalt phosphine complex to generate a cobalt bis(hydride) complex.³¹ Similarly, Muetterties and coworkers reported a low-valent cobalt triisopropylphosphite that generates a trihydride upon reaction with dihydrogen.³² Notably, these complexes were diamagnetic, consistent with a low-spin configuration, and, by extension, a strong ligand field. Perhaps one of the most notable examples of the utility of a strong ligand field approach are a series of cobalt complexes originally reported by Klein and coworkers.³³ Cobalt(I) derivatives bearing strongly donating alkyl and phosphine ligands were shown to oxidatively add to the C–CN bond of acetonitrile, as well as the C–I bond of methyl iodide to yield the corresponding cobalt(III) bis(methyl) complexes.^{34–36} Later studies with the cobalt(III) bis(methyl) species have shown that it can, in turn, reductively couple ethane to furnish a Co(I) iodide,³⁷ underlying the importance of a strongly donating ligand set to facilitating these multi-electron process (Scheme 1.3).



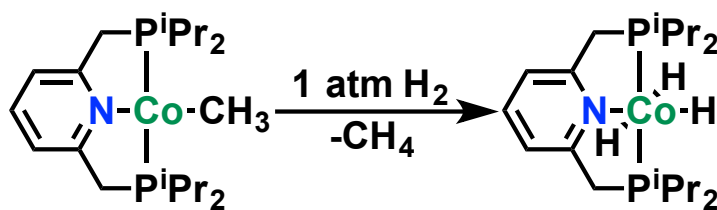
Scheme 1.3 Reductive coupling of ethane from a Co(III) bis(methyl) species

Such examples are not limited to cobalt. Field and coworkers reported an iron complex bearing two 1,2-bis(dimethylphosphino)ethane ligands that is able to activate the C–H bonds of alkenes and arenes,³⁸ alkanes,³⁹ and methane.⁴⁰ Similarly, Jones and coworkers reported catalytic aldimine formation proposed to proceed via oxidative addition of a benzene C–H bond to a low-valent iron complex bearing phosphine and isonitrile ligands.⁴¹ Electron-rich nickel phosphine complexes have proven to be similarly competent towards two-electron reactivity. Nickel(0) complexes have been shown to engage in the oxidative addition of aryl, vinyl, and acyl halide bonds,⁴² as well as the C–CN bond of nitriles⁴³ for example.

More recent examples of two-electron elementary steps occurring at first-row transition metal centers have incorporated some of the insights gleaned from these early studies, typically employing an electron-rich ligand set to more reliably facilitate two-electron pathways at base metals. These examples are replete with the use of pincers-type frameworks and chelates. A recent report by Hartwig using an electron-rich (BINAP)Ni(η^2 -NC-Ph) complex (BINAP = 2,2'-bis(biphenylphosphino)-1,1'-binaphthalene) for the catalytic amination of aryl halides supports a reaction pathway involving a Ni(0)/(II) couple.⁴⁴ Analogously, Smith reported an iron catalyst supported by a chelating bis(carbene) ligand, K(crypt)[Ph₂B(^tBuIm)₂Fe(CO)₂] (^tBuIm = 3-*tert*-butylimidazol-2-ylidene)), that undergoes a reversible intramolecular C–H insertion.⁴⁵ Interestingly, the iron(0) species must undergo a triplet to singlet spin-state change to engage in

this reactivity, again highlighting the importance of ligands that can induce a low-spin electron configuration.

Recent reports by Caulton⁴⁶, Arnold⁴⁷, and Chirik⁴⁸ have also provided evidence for two-electron reactions at cobalt centers. Interestingly, these complexes employ PNP pincer ligands (PNP = bis(phosphino)pyridine), according to this class of ligands a privileged status in many reports of demonstrably non-radical two-electron pathways with first-row transition metals (Scheme 1.4). Reactivity with these complexes has enabled the isolation of several cobalt hydride species^{47,48} and the isolation of a rare, putatively cobalt(V) species.⁴⁶ Compelling evidence of the oxidative addition of C–H bonds and dihydrogen has also been shown with a cobalt(I) PNP complex.⁴⁸ Importantly, these complexes have also been used to great avail in catalytic contexts and studies have proposed that two-electron pathways were likely operative. The Chirik lab have reported protocols for the borylation of C(sp²)–H bonds⁴⁹ and Suzuki cross-coupling of C(sp²)–C(sp²) bonds,⁵⁰ the latter reaction signifying the first example of such a reaction with cobalt. Such impressive reactivity has also been demonstrated with other first-row transition metal centers, including manganese,⁵¹ iron,⁵² and nickel,^{53,54} further attesting to the versatility of this ligand platform.



Scheme 1.4 Oxidative addition of hydrogen to a PNP Co(I) complex

The extension of this reactivity to PCP (PCP = bis(phosphino)aryl) and related pincer complexes has also been demonstrated at non-precious metal centers.⁵⁵ A POCOP cobalt complex

(POCOP = 1,3-bis((phosphino)oxy)benzene) was reported to undergo oxidative addition of methyl iodide to generate the corresponding cobalt(III) iodomethyl complex.⁵⁶ Similarly, the iron POCOP derivative $\text{Fe}\{(\text{Ph}_2\text{POCH}_2)_2\text{MeC}\}(\text{H})(\text{PMe}_3)_2$, prepared by the addition of $\text{FeMe}_2(\text{PMe}_3)_4$ to the disphosphinito PCP ligand $(\text{Ph}_2\text{POCH}_2)_2\text{CH}_2$, is believed to be generated from two C–H activations and a C–C coupling reaction between the methyl ligand and the central carbon atom of the disphosphinito moiety.⁵⁶ A related nickel PCP complex, $({}^{\text{iPr}}\text{PCP})\text{NiMe}$, (${}^{\text{iPr}}\text{PCP}$ = 2,6-bis-((diisopropylphosphino)methyl)phenyl), also undergoes a reductive coupling of the methyl ligand with the anionic carbon of the pincer,⁵⁷ highlighting the unusual pathways fostered by these electron-rich pincer platforms. This reactivity has been leveraged to catalytic effect in a number of systems. Sun reported the catalytic hydrosilylation of aldehydes and ketones with an iron hydrido complex supported by a POCOP pincer ligand.⁵⁸

1.3.2 Complexes bearing NHC carbenes

The recent use of carbene complexes is a particularly interesting development for the study of two-electron processes negotiated by first-row metals. The substitution of *N*-heterocyclic carbenes (NHCs) for phosphines in second- and third-row transition metal systems employed in cross-coupling⁵⁹, hydrogenation⁶⁰, and olefin metathesis⁶¹ reactions has been met with a great degree of success. Such systems maintain the advantages concomitant with the use of PNP and POCOP pincer systems, i.e. the utilization of a sterically bulky, electron-rich planar ligand scaffold, while retaining a greater resiliency towards deleterious ligand oxidation. Such deleterious events have been observed with PCP nickel complexes, for example. The nickel methyl complex reported by Cámpora and coworkers, $({}^{\text{iPr}}\text{PCP})\text{NiMe}$ (PCP = 2,6-bis-((diisopropylphosphino)methyl)phenyl), undergoes a demetalation event and an oxidation of the pincer phosphines to phosphine oxides in addition to reductive coupling of a methyl ligand with

the central carbon of the pincer backbone upon reacting with oxygen.⁵⁷

Importantly, pincers incorporating NHCs have been shown to facilitate impressive catalytic reactivity in many first-row transition metal systems.^{12,62–64} Wang and coworkers reported a nickel pincer NHC complex that is able to cross-couple chloro- and fluoroaromatics.⁶³ Similarly, Chirik reported cobalt and iron bis(carbene) pincer complexes, $(i\text{PrCNC})\text{Fe}(\text{N}_2)_2$ and $(i\text{PrCNC})\text{CoCH}_3$ ($i\text{PrCNC} = 2,6\text{-}(2,6\text{-}i\text{Pr}_2\text{-C}_6\text{H}_3\text{-imidazol-2-ylidene})_2\text{-C}_5\text{H}_3\text{N}$), that catalyze the hydrogenation of trisubstituted olefins, a challenging class of substrates even for precious metal catalysts.⁶⁴ Interestingly, the pyridine backbone of the cobalt complex exhibited redox-activity that aided the catalysis, contributing to the hydride and alkyl migration chemistry of the complex.

In addition to their robustness, NHCs can provide comparable modularity to phosphines. The range of steric and electronic effects for NHCs can often be very useful.⁶⁵ Indeed, NHCs can exhibit higher tunability than phosphines. Whereas phosphine design is largely confined to the selection of the phosphine R groups, a change that profoundly influences both the electronic and steric properties of the phosphine, the imidazol-2-ylidene substructure can be modified in different ways beyond selection of the substituents at the N1 and N3 atoms.⁶⁵ Different R groups can be present at the C4 and C5 carbons of the imidazole. Moreover, the azole subunit can be changed to a triazole, benzimidazole, imidazole, oxazole, etc, conferring a greater degree of control to the experimenter and permitting access to a greater breadth of electronic and steric properties (Figure 1.3). Finally, many carbenes are significantly more electron-rich than phosphine ligands, as assessed by the Tolman electronic parameter, and often bind more strongly to late transition metals than phosphines, possessing higher bond dissociation energies in Ru^{II} and Ni^0 complexes for example.⁶⁶

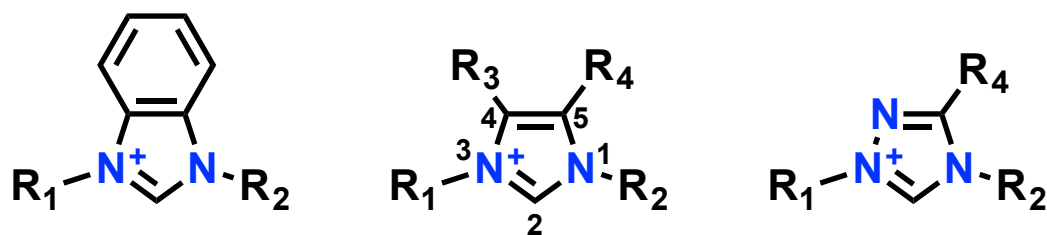


Figure 1.3 Examples of N-heterocyclic carbene substructures

Informed by these properties and pursuant to a strong-field approach for imparting noble metal reactivity onto base metals, we elected to pursue the metalation of a pincer framework reported by Chianese and coworkers (Figure 1.4).⁶⁷ This (^{Ar}CCC) framework (^{Ar}CCC = bis(aryl-benzimidazol-2-ylidene)phenyl) possesses many of the features desirable in the context of a strong-field ligand approach: (1) an anionic carbon linkage to impose the strong ligand field, (2) a benzimidazole to enforce coordination to the C2 carbon of the imidazole, rather than an abnormal carbene coordination, and (3) phenyl substituents that can be selected according to desired solubility and electron donicity. Moreover, the choice of phenyl substituent can provide diagnostic NMR spectroscopic handles useful in establishing the identity or coordination mode of products.

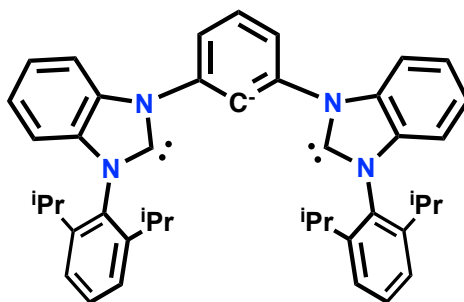


Figure 1.4 (^{DIPP}CCC) ligand

The selection of a pincer framework, as opposed to monodentate ligands or a bidentate chelate, reflects the successes that have been achieved using the pincer architecture.⁶⁸ In addition to the high stability of pincer metal complexes, the rigidity of the tridentate geometry permits

substantive control over increasing the regio- and stereoselectivity of processes occurring at the metal and lends itself to more facile study of mechanistic pathways or the elucidation of relevant intermediates. This well-defined bonding structure is also particularly amenable to rational catalytic design and the tuning of properties relevant to catalytic competency, i.e. stericity, ligand donicity, and the retention of important stereochemical information if needed. Moreover, pincer architectures are especially well-suited for immobilization on solid or dendrimeric supports, enabling the creation of robust recyclable catalysts.⁶⁸ Therefore, the selection of a pincer complex should provide especially important insights into reactivity at the base metal and inform future catalyst design.

Herein, we report the synthesis of a library of cobalt complexes featuring the ^{DIPP}CCC (^{DIPP}CCC = bis(diisopropylphenyl-benzimidazol-2-ylidene)phenyl) pincer ligand variant. The ability of these systems to engage in a Co(I)/(III) redox couple is explored with regard to the cleavage of substrate bonds and is inspired by a desire to activate small molecules and determine the competency of such systems for catalytic reactivity akin to that of noble metals.

1.4 References

1. Osborn, J. A., Jardine, F. H., Young, J. F. & Wilkinson, G. The preparation and properties of tris(triphenylphosphine)halogenorhodium(I) and some reactions thereof including catalytic homogeneous hydrogenation of olefins and acetylenes and their derivatives. *J. Chem. Soc. A Inorganic, Phys. Theor.* 1711–1732 (1966). doi:10.1039/j19660001711
2. Vaska, L. & DiLuzio, J. W. CARBONYL AND HYDRIDO-CARBONYL COMPLEXES OF IRIDIUM BY REACTION WITH ALCOHOLS. HYDRIDO COMPLEXES BY REACTION WITH ACID. *J. Am. Chem. Soc.* **83**, 2784–2785 (1961).
3. Karstedt, B. D. PLATINUM COMPLEXES OF UNSATURATED SILOXANES AND PLATINUM CONTAINING ORGANOPOLYSILOXANES. (1973).
4. Hartwig, J. F. Approaches to catalyst discovery. New carbon≠heteroatom and carbon±carbon bond formation. *Pure Appl. Chem* **71**, 1417–1423 (1999).
5. Wolfe, J. P., Tomori, H., Sadighi, J. P., Yin, J. & Buchwald, S. L. Simple, Efficient Catalyst System for the Palladium-Catalyzed Amination of Aryl Chlorides, Bromides, and Triflates.

- 65**, 1158–1174 (2000).
- Li, C., Chen, D. & Tang, W. Addressing the Challenges in Suzuki–Miyaura Cross-Couplings by Ligand Design. *Synlett* **27**, 2183–2200 (2016).
 - Engle, K. M. & Yu, J.-Q. Developing ligands for palladium(II)-catalyzed C-H functionalization: intimate dialogue between ligand and substrate. *J. Org. Chem.* **78**, 8927–55 (2013).
 - Hirse Korn, K. F., Hulley, E. B., Wolczanski, P. T. & Cundari, T. R. Olefin Substitution in (silox)₃M(olefin) (silox = tBu₃SiO; M = Nb, Ta): The Role of Density of States in Second vs Third Row Transition Metal Reactivity. *J. Am. Chem. Soc.* **130**, 1183–1196 (2008).
 - Volpe, E. C., Wolczanski, P. T. & Lobkovsky, E. B. Aryl-Containing Pyridine-Imine and Azaallyl Chelates of Iron toward Strong Field Coordination Compounds. *Organometallics* **29**, 364–377 (2010).
 - Poli, R. Relationship between One-Electron Transition-Metal Reactivity and Radical Polymerization Processes. *Angew. Chemie Int. Ed.* **45**, 5058–5070 (2006).
 - EPA, U. & Strategies Division, S. Presidential Green Chemistry Challenge: Award Recipients, 1996-2016. (2016). Available at: <https://www.epa.gov/greenchemistry/presidential-green-chemistry-challenge-2016-academic-award>.
 - Yu, R. P. *et al.* High-Activity Iron Catalysts for the Hydrogenation of Hindered, Unfunctionalized Alkenes. *ACS Catal.* **2**, 1760–1764 (2012).
 - Tondreau, A. M. *et al.* Iron catalysts for selective anti-Markovnikov alkene hydrosilylation using tertiary silanes. *Science* **335**, 567–70 (2012).
 - Hojilla Atienza, C. C., Milsmann, C., Lobkovsky, E. & Chirik, P. J. Synthesis, electronic structure, and ethylene polymerization activity of bis(imino)pyridine cobalt alkyl cations. *Angew. Chem. Int. Ed. Engl.* **50**, 8143–7 (2011).
 - Wong, J. L. *et al.* Disulfide reductive elimination from an iron(III) complex. *Chem. Sci.* **4**, 1906 (2013).
 - Heyduk, A. F., Zarkesh, R. a & Nguyen, A. I. Designing catalysts for nitrene transfer using early transition metals and redox-active ligands. *Inorg. Chem.* **50**, 9849–63 (2011).
 - Chaudhuri, P., Hess, M., Flörke, U. & Wieghardt, K. From Structural Models of Galactose Oxidase to Homogeneous Catalysis : Efficient Aerobic Oxidation of Alcohols. **37**, 2217–2220 (2000).
 - Wang, K. & Stiefel, E. I. Toward Separation and Purification of Olefins Using Dithiolene Complexes : An Electrochemical Approach. **291**, 106–109 (2001).
 - Smith, A. L., Hardcastle, K. I. & Soper, J. D. Redox-Active Ligand-Mediated Oxidative Addition and Reductive Elimination at Square Planar Cobalt(III): Multielectron Reactions

- for Cross-Coupling. *J. Am. Chem. Soc.* **132**, 14358–14360 (2010).
20. Bart, S. C., Lobkovsky, E. & Chirik, P. J. Preparation and molecular and electronic structures of iron(0) dinitrogen and silane complexes and their application to catalytic hydrogenation and hydrosilation. *J. Am. Chem. Soc.* **126**, 13794–807 (2004).
 21. Bouwkamp, M. W., Bowman, A. C., Lobkovsky, E. & Chirik, P. J. Iron-Catalyzed [$2\pi + 2\pi$] Cycloaddition of r, ω -Dienes : The Importance of Redox-Active Supporting Ligands. **128**, 13340–13341 (2006).
 22. Bart, S. C., Lobkovsky, E., Bill, E. & Chirik, P. J. Synthesis and Hydrogenation of Bis (imino) pyridine Iron Imides. **128**, 5302–5303 (2006).
 23. Kaim, W. & Schwederski, B. Non-innocent ligands in bioinorganic chemistry—An overview. *Coord. Chem. Rev.* **254**, 1580–1588 (2010).
 24. Salanouve, E. *et al.* Tandem C–H Activation/Arylation Catalyzed by Low-Valent Iron Complexes with Bisiminopyridine Ligands. *Chem. - A Eur. J.* **20**, 4754–4761 (2014).
 25. Zhu, D., Thapa, I., Korobkov, I., Gambarotta, S. & Budzelaar, P. H. M. Redox-Active Ligands and Organic Radical Chemistry. *Inorg. Chem.* **50**, 9879–9887 (2011).
 26. Jones, G. D. *et al.* Ligand Redox Effects in the Synthesis, Electronic Structure, and Reactivity of an Alkyl–Alkyl Cross-Coupling Catalyst. **128**, 13175–13183 (2006).
 27. Tennyson, A. G., Lynch, V. M. & Bielawski, C. W. Arrested Catalysis: Controlling Kumada Coupling Activity via a Redox-Active N-Heterocyclic Carbene. *J. Am. Chem. Soc.* **132**, 9420–9429 (2010).
 28. Jacquet, J., Desage-El Murr, M. & Fensterbank, L. Metal-Promoted Coupling Reactions Implying Ligand-Based Redox Changes. *ChemCatChem* **8**, 3310–3316 (2016).
 29. Myers, T. W., Yee, G. M. & Berben, L. A. Redox-Induced Carbon-Carbon Bond Formation by Using Noninnocent Ligands. *Eur. J. Inorg. Chem.* **2013**, 3831–3835 (2013).
 30. Crabtree, R. H. *The Organometallic Chemistry of the Transition Metals*. (John Wiley & Sons, Inc., 2009).
 31. Misono, A., Uchida, Y., Saito, T. & Song, K. M. Tris(triphenylphosphine) cobalt dihydride. A molecular-nitrogen fixing complex. *Chem. Commun.* 419–420 (1967).
 32. Rakowski, M. C. & Muetterties, E. L. Low valent cobalt triisopropyl phosphite complexes. Characterization of a catalyst for the hydrogenation of α, β -unsaturated ketones. *J. Am. Chem. Soc.* **99**, 739–743 (1977).
 33. Klein, H.-F. & Karsch, H. H. Methylkobaltverbindungen mit nicht chelatisierenden Liganden, I. Methyltetrakis(trimethylphosphin)kobalt und seine Derivate. *Chem. Ber.* **108**, 944–955 (1975).
 34. Xu, H., Williard, P. G. & Bernskoetter, W. H. C–CN Bond Activation of Acetonitrile using

- Cobalt(I). *Organometallics* **31**, 1588–1590 (2012).
35. Hammer, R. & Klein, H.-F. The Tetrakis(trimethylphosphine)cobalt Anion. *Zeitschrift für Naturforsch. B* **32**, 138–143 (1977).
 36. Klein, H.-F. Trimethylphosphane Complexes of Nickel, Cobalt, and Iron—Model Compounds for Homogeneous Catalysis. *Angew. Chemie Int. Ed. English* **19**, 362–375 (1980).
 37. Xu, H. & Bernskoetter, W. H. Mechanistic considerations for C-C bond reductive coupling at a cobalt(III) center. **133**, 14956–14959 (2011).
 38. Baker, M. V. & Field, L. D. Reaction of sp² carbon-hydrogen bonds in unactivated alkenes with bis(diphosphine) complexes of iron. *J. Am. Chem. Soc.* **108**, 7433–7434 (1986).
 39. Baker, M. V. & Field, L. D. Reaction of carbon-hydrogen bonds in alkanes with bis(diphosphine) complexes of iron. *J. Am. Chem. Soc.* **109**, 2825–2826 (1987).
 40. Field, L. D. *et al.* Methane activation by an iron phosphine complex in liquid xenon solution. *J. Chem. Soc. Chem. Commun.* **85**, 1339 (1991).
 41. Jones, W. D., Foster, G. P. & Putinas, J. M. The catalytic activation and functionalization of carbon-hydrogen bonds. Aldimine formation by the insertion of isonitriles into aromatic carbon-hydrogen bonds. *J. Am. Chem. Soc.* **109**, 5047–5048 (1987).
 42. Fahey, D. R. & Mahan, J. E. Oxidative additions of aryl, vinyl, and acyl halides to triethylphosphinenickel(0) complexes. *J. Am. Chem. Soc.* **99**, 2501–2508 (1977).
 43. Favero, G. & Morvillo, A. Mechanism of oxidative addition of benzonitriles to DI(1,4-bis(diethylphosphino)butane)nickel(0). *J. Organomet. Chem.* **260**, 363–368 (1984).
 44. Ge, S., Green, R. A. & Hartwig, J. F. Controlling First-Row Catalysts: Amination of Aryl and Heteroaryl Chlorides and Bromides with Primary Aliphatic Amines Catalyzed by a BINAP-Ligated Single-Component Ni(0) Complex. **136**, 1617–1627 (2015).
 45. Hickey, A. K. *et al.* Two-state reactivity in C–H activation by a four-coordinate iron(0) complex. *Chem. Commun.* **53**, 1245–1248 (2017).
 46. Ingleson, M., Fan, H., Pink, M., Tomaszewski, J. & Caulton, K. G. Three-Coordinate Co(I) Provides Access to Unsaturated Dihydrido-Co(III) and Seven-Coordinate Co(V). *J. Am. Chem. Soc.* **128**, 1804–1805 (2006).
 47. Rozenel, S. S., Padilla, R., Camp, C. & Arnold, J. Unusual activation of H₂ by reduced cobalt complexes supported by a PNP pincer ligand. *Chem. Commun. (Camb)*. **50**, 2612–4 (2014).
 48. Semproni, S. P., Hojilla Atienza, C. C. & Chirik, P. J. Oxidative addition and C–H activation chemistry with a PNP pincer-ligated cobalt complex. *Chem. Sci.* **5**, 1956–1960 (2014).
 49. Obligacion, J. V., Semproni, S. P., Pappas, I. & Chirik, P. J. Cobalt-Catalyzed C(sp²)-H Borylation: Mechanistic Insights Inspire Catalyst Design. *J. Am. Chem. Soc.* **138**, 10645–

- 10653 (2016).
50. Neely, J. M., Bezdek, M. J. & Chirik, P. J. Insight into Transmetalation Enables Cobalt-Catalyzed Suzuki–Miyaura Cross Coupling. *ACS Cent. Sci.* **2**, 935–942 (2016).
 51. Mastalir, M., Glatz, M., Pittenauer, E., Allmaier, G. & Kirchner, K. Sustainable Synthesis of Quinolines and Pyrimidines Catalyzed by Manganese PNP Pincer Complexes. *J. Am. Chem. Soc.* **138**, 15543–15546 (2016).
 52. Rezayee, N. M., Samblanet, D. C. & Sanford, M. S. Iron-Catalyzed Hydrogenation of Amides to Alcohols and Amines. *ACS Catal.* **6**, 6377–6383 (2016).
 53. Zhao, H., Li, X., Zhang, S. & Sun, H. Synthesis and Characterization of Iron, Cobalt, and Nickel [PNP] Pincer Amido Complexes by N-H Activation. *Zeitschrift für Anorg. und Allg. Chemie* **641**, 2435–2439 (2015).
 54. Mastalir, M. & Kirchner, K. A triazine-based Ni(II) PNP pincer complex as catalyst for Kumada–Corriu and Negishi cross-coupling reactions. *Monatshefte für Chemie - Chem. Mon.* **148**, 105–109 (2017).
 55. Murugesan, S. & Kirchner, K. Non-precious metal complexes with an anionic PCP pincer architecture. *Dalt. Trans.* **45**, 416–439 (2016).
 56. Xu, G., Sun, H. & Li, X. Activation of sp^3 Carbon–Hydrogen Bonds by Cobalt and Iron Complexes and Subsequent C–C Bond Formation. *Organometallics* **28**, 6090–6095 (2009).
 57. Martínez-Prieto, L. M. *et al.* Synthesis and Reactivity of Nickel and Palladium Fluoride Complexes with PCP Pincer Ligands. NMR-Based Assessment of Electron-Donating Properties of Fluoride and Other Monoanionic Ligands. *Organometallics* **31**, 1425–1438 (2012).
 58. Huang, S., Zhao, H., Li, X., Wang, L. & Sun, H. Synthesis of [POCOP]-pincer iron and cobalt complexes via C_{sp^3} -H activation and catalytic application of iron hydride in hydrosilylation reactions. *RSC Adv.* **5**, 15660–15667 (2015).
 59. Grasa, G. a. *et al.* Suzuki–Miyaura cross-coupling reactions mediated by palladium/imidazolium salt systems. *Organometallics* **21**, 2866–2873 (2002).
 60. Strassner, T. *The Role of NHC Ligands in Oxidation Catalysis*. (Springer-Verlag Berlin Heidelberg, 2007).
 61. Weskamp, T., Schattenmann, W. C., Spiegler, M. & Herrmann, W. A. A Novel Class of Ruthenium Catalysts for Olefin Metathesis. *Angew. Chemie Int. Ed.* **37**, 2490–2493 (1998).
 62. Sun, Y., Li, X. & Sun, H. [CNN]-pincer nickel(ii) complexes of N-heterocyclic carbene (NHC): synthesis and catalysis of the Kumada reaction of unactivated C–Cl bonds. *Dalt. Trans.* **43**, 9410 (2014).
 63. Guo, W.-J. & Wang, Z.-X. Cross-Coupling of ArX with ArMgBr Catalyzed by N-Heterocyclic Carbene-Based Nickel Complexes. *J. Org. Chem.* **78**, 1054–1061 (2013).

64. Yu, R. P. *et al.* Catalytic hydrogenation activity and electronic structure determination of bis(arylimidazol-2-ylidene)pyridine cobalt alkyl and hydride complexes. *J. Am. Chem. Soc.* **135**, 13168–84 (2013).
65. Crabtree, R. H. Abnormal, mesoionic and remote N-heterocyclic carbene complexes. *Coord. Chem. Rev.* **257**, 755–766 (2013).
66. Dröge, T. & Glorius, F. The Measure of All Rings-N-Heterocyclic Carbenes. *Angew. Chemie Int. Ed.* **49**, 6940–6952 (2010).
67. Chianese, A. R., Mo, A., Lampland, N. L., Swartz, R. L. & Bremer, P. T. Iridium Complexes of CCC-Pincer N-Heterocyclic Carbene Ligands: Synthesis and Catalytic C–H Functionalization. *Organometallics* **29**, 3019–3026 (2010).
68. Szabó, K. J. Pincer Complexes as Catalysts in Organic Chemistry. *Top Organomet Chem* **40**, 203–242 (2013).

Chapter 2

Synthesis and characterization of cobalt CCC bis(carbene) pincer complexes†

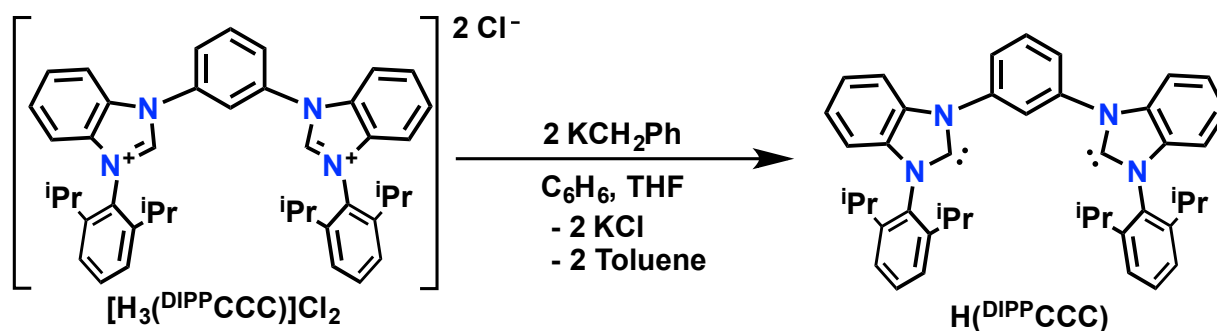
2.1 Metalation of the (^{DIPP}CCC) platform

Seeking to promote two-electron reactivity at base metals through the application of a strong-field approach, we turned to the metalation of the ^{DIPP}CCC pincer (^{DIPP}CCC = bis(diisopropylphenyl-benzimidazol-2-ylidene)phenyl) previously reported by Chianese and coworkers.¹ Initial attempts to metalate the platform by reacting the benzimidazolium salt precursor with Co(N(SiMe₃)₂)₂py in dichloromethane solvent led to intractable mixtures. Consequently, we explored alternative routes to metalated derivatives. Traditional metalation pathways for monoanionic pincer platforms on cobalt have been reported in the literature, citing the importance of lithiation of the aryl ring for the installation of the anionic Co–C_{aryl} bond as in the case of [(POCOP)CoI] (POCOP = κ³-C₆H₃-1,3-[OP(^tBu)₂]₂).² Given the parallels between the POCOP and CCC pincer framework, we sought to isolate the bis(carbene) and subsequently investigate the viability of a lithiation route to the targeted cobalt complexes.

Initial attempts to isolate the bis(carbene) via deprotonation of [H₃(^{DIPP}CCC)]Cl₂ with 2.1 equivalents of lithium hexamethyldisilazide proved challenging given the difficulty of separating the hexamethyldisilane product from the targeted carbene, prompting an examination of alternate bases to achieve the deprotonation. Gratifyingly, a modification of the ligand procedure involving the addition of benzyl potassium instead of lithium hexamethyldisilazide was found to be especially successful (Scheme 2.1). The formation of toluene byproduct, as opposed to the less

† Portions of this chapter are reproduced from the following publication with permission from the authors. Ibrahim, A.D.; Tokmic, K.; Brennan, M.R.; Kim, D.; Matson, E.M.; Bertke, J. A.; Nilges, M. J.; Fout, A.R. *Dalton Trans.* **2016**, 45 (24), 9805-9811.

tractable hexamethyldisilazane, rendered this reaction especially amenable to purification and established this as the synthetically preferred route to the bis(carbene) ligand. Moreover, the dissipation of the orange color of the benzyl potassium in the reaction mixture provided a useful means with which to monitor the progress of the reaction, with a transition to a clear, light yellow solution indicative of the reaction's completion.



Scheme 2.1 Preparation of the bis(carbene) $H(DIPPCCC)$

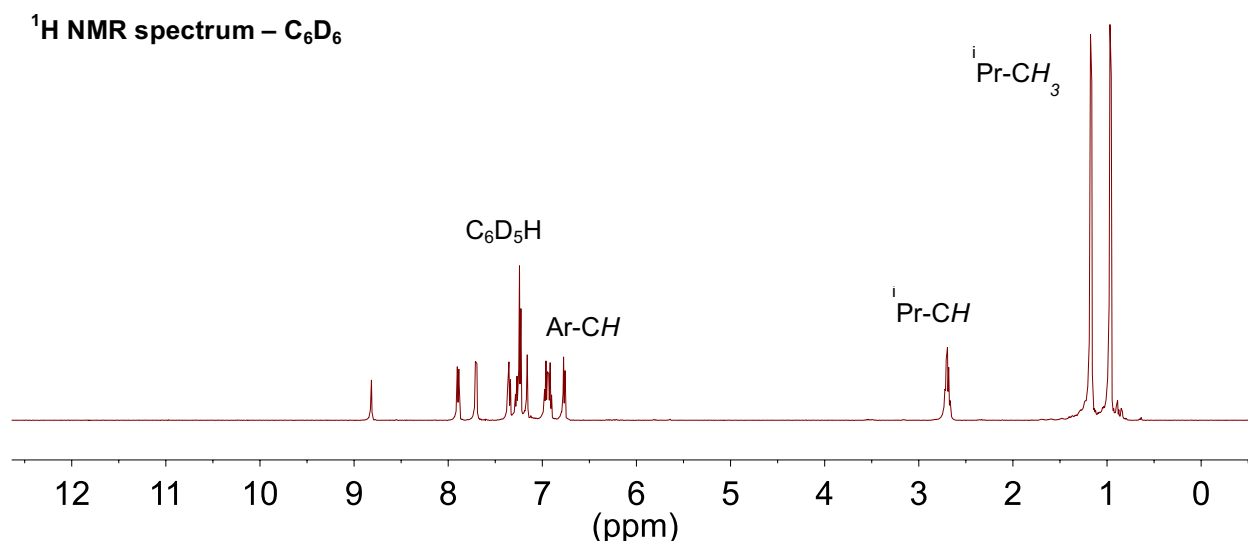


Figure 2.1 ^1H NMR spectrum of $H(DIPPCCC)$ in C_6D_6

An analysis of the bis(carbene) product $H(DIPPCCC)$ by ^1H and ^{13}C NMR spectroscopies, in addition to CHN elemental analysis, allowed for a definitive assignment of the free carbene. A loss of the downfield resonance at 12.45 ppm in the ^1H NMR spectrum is consistent with a

deprotonation of the benzimidazolium salt (Figure 2.1). Similarly, the ^{13}C NMR spectrum possessed a new resonance at 231.27 ppm, assigned to the carbene carbons of the ligand.

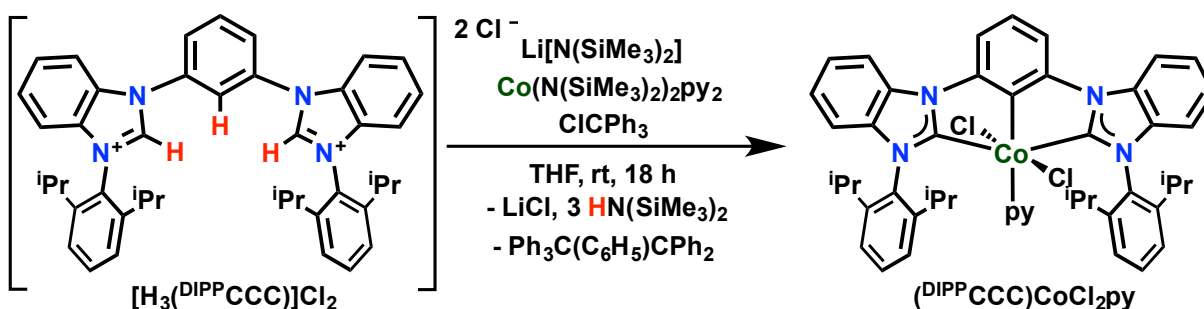
Addition of an equivalent of $^n\text{BuLi}$ to the free carbene, $\text{H}^{(\text{DIPP})\text{CCC}}$,³ resulted in the undesired activation of the sterically unencumbered C–H bond *ortho* to the NHC moiety, suggesting that lithiation would not be a plausible route for accessing the desired cobalt complexes. As a result, we explored alternative routes to the desired metalated derivatives.

2.2 Synthesis of $(^{\text{DIPP}}\text{CCC})\text{Co}^{\text{III}}\text{Cl}_2\text{py}$

Initial attempts at metalation of the CCC ligand platform with cobalt focused on the preparation and subsequent reaction of the *in situ* generated bis(carbene) ligand with CoCl_2 , pyridine, and an equivalent of oxidant to generate a $(^{\text{DIPP}}\text{CCC})\text{Co}^{\text{III}}\text{Cl}_2\text{py}$ derivative. While such attempts proved to be successful, low yields (< 50%) of the target complexes following workup deemed this route not synthetically useful.

We next investigated the use of metal hexamethyldisilazides as an alternative route to the desired cobalt derivative. The sequential addition of $\text{LiN}(\text{SiMe}_3)_2$, $\text{Co}(\text{N}(\text{SiMe}_3)_2)_2(\text{py})_2$,⁴ and an equivalent of ClCPh_3 as an oxidant to the benzimidazolium salt of the CCC platform, $[\text{H}_3(^{\text{DIPP}}\text{CCC})]\text{Cl}_2$, in THF, followed by stirring of the mixture at room temperature overnight, resulted in the formation of a green solution (Scheme 2.2). Following workup, the product, $(^{\text{DIPP}}\text{CCC})\text{CoCl}_2\text{py}$ (**1**) was isolated as a bright green powder in good yield, 80%. Characterization of **1** by ^1H NMR spectroscopy revealed a diamagnetic spectrum with 14 resonances, consistent with the formation of a low-spin, Co^{III} product, assigned as the desired **1** (Figure 2.2). Two doublets integrating to 12H each were located at 0.68 and 0.98 ppm, corresponding to the ^iPr methyl moieties of the flanking aryl substituents. The presence of one septet integrating to 4H

corresponds to the methine protons of the ⁱPr moieties, signifying a symmetric coordination of the ligand platform. Additional resonances integrating to 22H between 6.41 and 8.83 ppm were assigned to the aryl backbone of the pincer ligand and the bound pyridine. The corresponding signals in the ¹³C{¹H} NMR spectrum at 195.29 and 156.39 ppm were assigned to the C_{NHC} and C_{Ar} carbons, respectively, and were significantly shifted from those of the free carbene, H(^{DIPP}CCC) (231.27 ppm (C_{NHC}), 147.30 ppm (C_{Ar})). These values compare favorably with the previously reported (^{DIPP}CCC)NiCl complex (185.89 ppm(C_{NHC}); 150.88 ppm(C_{Ar})).



Scheme 2.2 Preparation of (^{DIPP}CCC)CoCl₂py

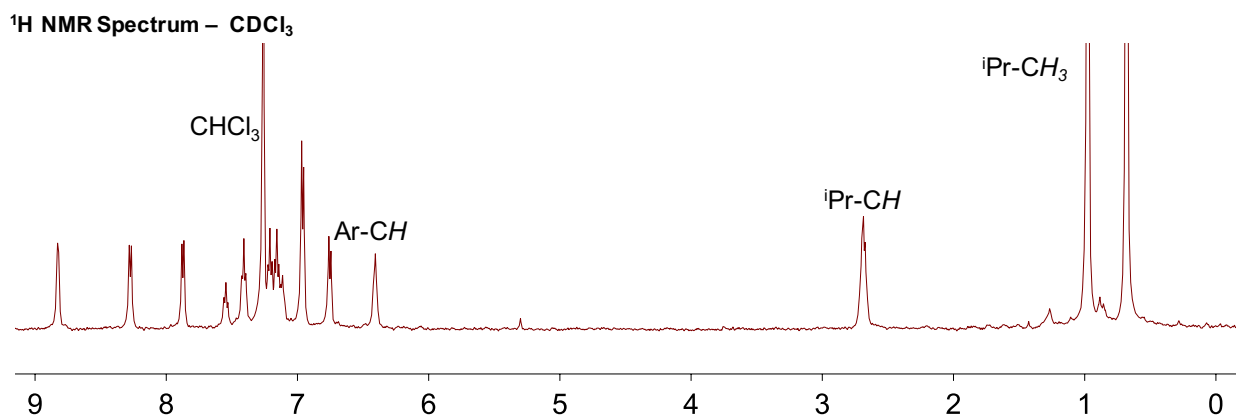


Figure 2.2 ¹H NMR spectrum of (^{DIPP}CCC)CoCl₂py in CDCl₃

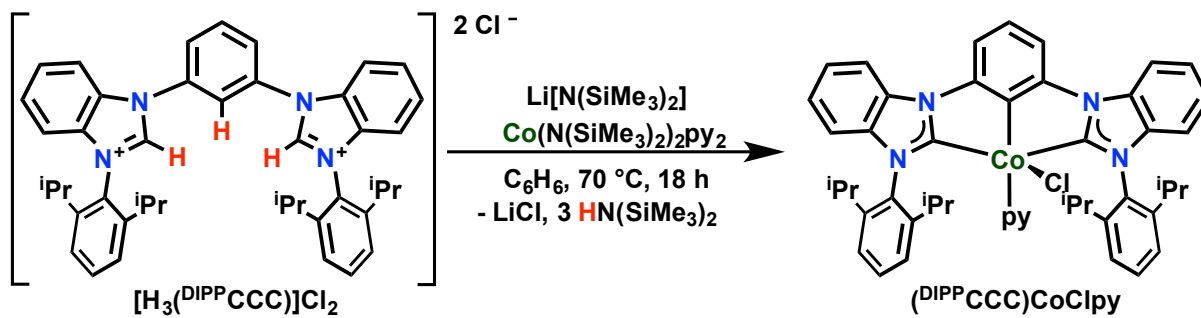
Further characterization of **1** by single-crystal X-ray diffraction studies established the identity

of the compound. Green crystals of the complex suitable for analysis were obtained via slow evaporation of a concentrated benzene solution, confirming the formation of the desired octahedral Co^{III} product (Figure 2.6, Tables 2.1 & 2.2). The two $\text{Co}-\text{C}_{\text{NHC}}$ bond lengths of 1.981(2) and 2.000(2) Å of **1** are within the range reported for $\text{Co}^{\text{III}}-\text{C}_{\text{NHC}}$ bonds, 1.815 Å – 2.012 Å.⁵⁻⁷ Likewise, the $\text{Co}-\text{C}_{\text{Ar}}$ bond length of 1.880(2) Å for **1** is within the range of $\text{Co}^{\text{III}}-\text{C}_{\text{Ar}}$ bonds, which range from 1.845 – 2.057 Å,⁷⁻⁹ but is shorter than the bond length for the analogous Co^{III} species, $(\text{PCP}^{\text{Me-}i\text{Pr}})\text{CoCl}_2$ ($\text{PCP} = N,N'$ -bis(diisopropylphosphino)- N,N' -dimethyl-1,2-diaminobenzene),¹⁰ reported by Kirchner and coworkers (1.937(1) Å). This is likely due to the increased rigidity of the CCC ligand backbone compared to the PCP system. The $\text{Co}-\text{Cl}$ bond lengths, 2.2787(6) and 2.3175(6) Å, also fall within the regime of recently reported Co^{III} complexes featuring an anionic $\text{Co}-\text{C}_{\text{Ar}}$ linkage, 2.229 – 2.429 Å.^{7,11,12} Finally, the $\text{C}_{\text{Ar}}-\text{Co}-\text{N}_{\text{py}}$ and $\text{C}_{\text{Ar}}-\text{Co}-\text{Cl}$ bond angles of 179.26(9) and 89.23(7)°, respectively, signify a nearly idealized octahedral geometry at cobalt.

Strongly-donating monoanionic pincer ligands featuring a $\text{Co}-\text{C}_{\text{aryl}}$ linkage are uncommon in the literature. Van Koten's report of a $[\text{C}_6\text{H}_3(\text{CH}_2\text{NMe}_2)_2]\text{CoClpy}$ species signifies one of the first cobalt pincer complexes containing an ECE ligand (E = donor groups).¹³ More recently, Nishiyama and coworkers reported the synthesis of NCN-Co complexes containing bis(oxazoliny)phenyl (phebox) as auxiliary ligands.⁹ Similarly, the work of Li,¹⁴ Heinekey,² Wass,¹⁵ and Kirchner¹⁰ has been instrumental in establishing facile synthetic protocols to cobalt complexes featuring monoanionic PCP pincer ligands. Nevertheless, due to the difficulty in metalating these ligands with first-row transition metals, such compounds remain largely underexplored.

2.3 Synthesis of (^{DIPP}CCC)Co^{II}Clpy

Interested in accessing different oxidation states of cobalt with the CCC platform, we next turned our attention to the preparation of a one-electron-reduced Co^{II} derivative. Reasoning that withholding an equivalent of oxidant should provide the target complex, we employed a similar synthetic protocol to the preparation of **1** but without the use of an oxidant. Heating a mixture of LiN(SiMe₃)₂, Co(N(SiMe₃)₂)₂py₂⁴ with the benzimidazolium salt of the [H₃(^{DIPP}CCC)]Cl₂ platform in benzene resulted in the formation of an orange solution (Scheme 2.3). Following workup, the product, (^{DIPP}CCC)CoClpy (**2**) was isolated as an orange powder in 75% yield. Characterization of **2** by ¹H NMR spectroscopy was consistent with the formation of a new paramagnetic species with resonances ranging from -10 to 16 ppm.



Scheme 2.3 Synthesis of (^{DIPP}CCC)CoClpy

Interestingly, extension of this protocol to the mesityl variant of the ligand platform was unsuccessful and another route to the Co^{II} species was required. In contrast to the broad resonances observed in the paramagnetic ¹H NMR spectrum for **2**, the mesityl analogue is NMR silent.

2.4 EPR spectroscopy

The X-band EPR spectrum of **2** obtained from a 1:1 toluene:THF glass at 77 K is depicted in Figure 2.3. The EPR parameters for **2** ($g_x = 2.259$, $g_y = 2.215$, and $g_z = 1.995$; $A_{Co}(x,y,z) = 9$

MHz, 7 MHz, 266 MHz) are consistent with a low-spin $d^7 S = 1/2$ compound.¹⁶ While superhyperfine interactions to the ^{14}N nuclei ($A_N(x,y,z) = 24 \text{ MHz}, 27 \text{ MHz}, 31 \text{ MHz}$) were observed, such interactions were weakly resolved. Moreover, no resolved superhyperfine coupling to the ^{35}Cl and ^{37}Cl nuclei was discernable.

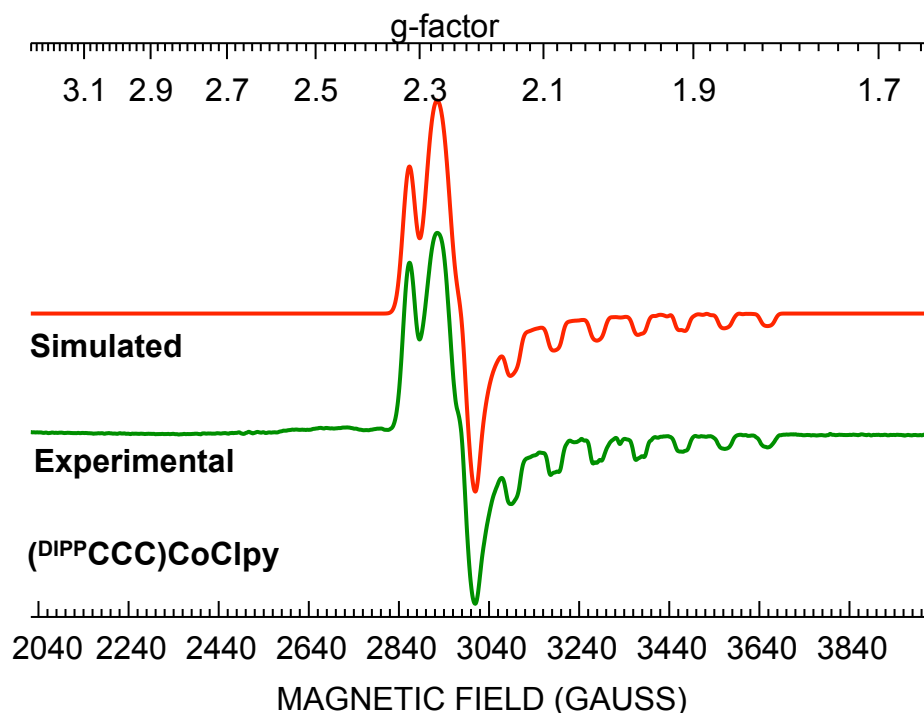


Figure 2.3 EPR spectra of $(^{\text{DIPP}}\text{CCC})\text{CoCl}_2\text{py}$ recorded in toluene:THF (1:1) glass at 77 K. EPR parameters for $(^{\text{DIPP}}\text{CCC})\text{CoCl}_2\text{py}$ (2.5E+3 GAIN; 2.00 G MODAMP; 20.00 dB POWER; NU= 9.2903 GHz)

Gratifyingly, these results were consistent with the anticipated effects of pincer ligation. Given the highly donating nature of the CCC ligand platform, we expected a strong ligand field and, by extension, a low-spin configuration upon complexation of the cobalt metal center with the pincer. A low-spin Co^{II} derivative is indicative that the electron configuration of the metalated derivatives is not exclusively the consequence of a favorable d-electron count and geometry, as in the case of the $d^6 \text{Co}^{\text{III}}$ octahedral complex.

2.5 Crystallographic characterization of (^{DIPP}CCC)Co^{II}Clpy

To unambiguously identify the structure of complex **2**, orange crystals suitable for X-ray diffraction were grown by slow evaporation from a concentrated solution in benzene at room temperature. Crystallographic characterization of **2** confirmed the formation of the target complexes, revealing a square pyramidal geometry ($\tau = 0.26$)¹⁷ about a Co^{II} center with a chloride occupying the apical position (Figure 2.6, Tables 2.1 & 2.2). The two Co–C_{NHC} bond lengths of 1.963(4) and 1.948(4) Å for (^{DIPP}CCC)CoClpy are similar to typical values reported for Co^{II}–C_{NHC} bonds (1.845 – 2.127 Å). In contrast, the Co–C_{Ar} bond length of 1.871(3) Å for **2** is noticeably shorter than typical Co^{II}–C_{Ar} bonds reported in the literature (1.9020 - 2.0570 Å)^{18,19,7} and shorter than those observed in the [Co(PCP^{Me}-*i*Pr)] complexes recently reported by Kirchner and coworkers (1.919 to 1.953 Å)¹⁰ or the ^RPOCOP^RCoI complex reported by Heinekey (1.924(4) Å).² The Co–Cl bond length of 2.4465(9) Å for **2** also differ considerably from the value reported for the (^{iPr}CNC)CoCl complex (2.201 Å), as well as the bond lengths in the [Co(PCP^{Me}-*i*Pr)] and [Co(PCP-*t*Bu)] complexes (2.234(1) – 2.3103(4) Å) and 2.260(1) Å, respectively.¹⁰ Furthermore, the pyridine ligand of **2** lies in the basal position with a Co–N₅ bond length of 2.025(3) Å, in contrast to the apical position of the pyridine ligand observed in the analogous PCP system (Co–N: 2.1417(8) Å).¹⁰ Finally, the C_{Ar}–Co–N₅ and Cl–Co–N₅ angles in **2** (175.65(14)° and 93.66(9)°, respectively) are distorted from an idealized square pyramidal geometry but similar to those reported for (PCP^{Me}-*i*Pr)CopyCl (166.89(3)° and 96.28(3)°).¹⁰

2.6 Cyclic voltammetry

Seeking to investigate the accessibility of a Co^I derivative of the ^{DIPP}CCC ligand platform, we studied the electrochemical properties of **2** using cyclic voltammetry (Figure 2.4). The study

was carried out in a 1 mM solution of **2** in acetonitrile with 0.1 M [NBu₄][PF₆] as electrolyte. At a scan rate of 100 mV/s, a single reversible redox event assigned to the Co^{II}/Co^I redox couple was observed in the window between -1 and -2 V with an E_{1/2} at -1.46 V vs Fc/Fc⁺. This suggested that the Co^{II} species may be amenable to chemical reduction.

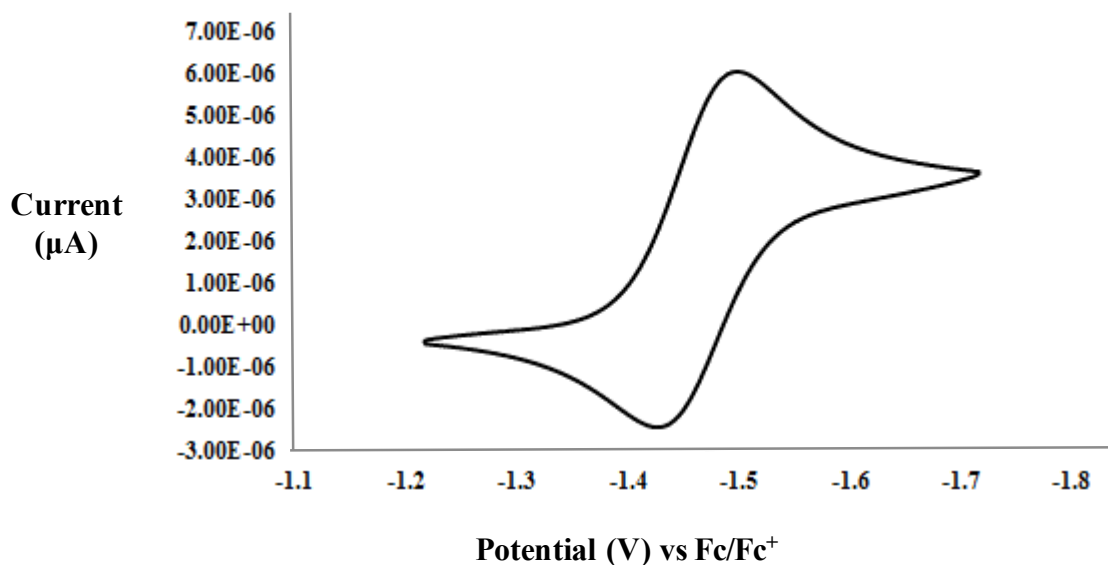
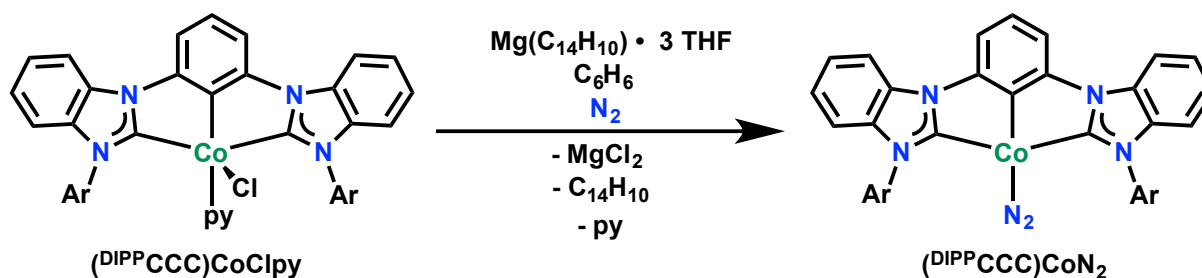


Figure 2.4 Cyclic voltammogram of 1mM solution of (^{DIPP}CCC)CoCl₂py in acetonitrile with 0.1 M [NBu₄][PF₆]

2.7 Synthesis of (^{DIPP}CCC)Co^IN₂

Encouraged by these results, and interested in the synthesis of low-valent complexes featuring the ^{DIPP}CCC ligand platform, we investigated the chemical reduction of **2**. This goal was readily accomplished by the addition of an equivalent of 9,10-Dihydro-9,10-anthracendiyl-tris(THF)magnesium as a solid to a frozen solution of **2** in benzene (Scheme 2.4). Workup of the dark brown reaction mixture afforded a brown powder in good yields (77%). Characterization of the product by ¹H and ¹³C NMR spectroscopies confirmed the formation of a new diamagnetic

species, consistent with the predicted low-spin Co^I product, $(^{\text{DIPP}}\text{CCC})\text{CoN}_2$, **3**. The presence of 11 resonances in the ^1H NMR spectrum, shifted from those of **1**, indicated the loss of the pyridine ligand and is consistent with a C_2 symmetric ligand environment (Figure 2.5). Resonances located at 0.88 and 1.27 ppm and integrating to 12H each were assigned to the methyls of the ^iPr moiety, while a septet at 2.71 ppm integrating to 4H was assigned to the methine protons of the ^iPr groups. The presence of 15 resonances in ^{13}C NMR spectrum are also consistent with the proposed formulation. The complex was additionally characterized by IR spectroscopy, revealing an intense feature at 2063 cm^{-1} , assigned to the vibrational mode of a bound dinitrogen molecule, shifted from that of free N_2 (2331 cm^{-1}).²⁰ The presence of this N_2 ligand suggests formation of a monomeric species due to the steric bulk of the flanking aryl substituents.



Scheme 2.4 Reduction of $(^{\text{DIPP}}\text{CCC})\text{CoClpy}$

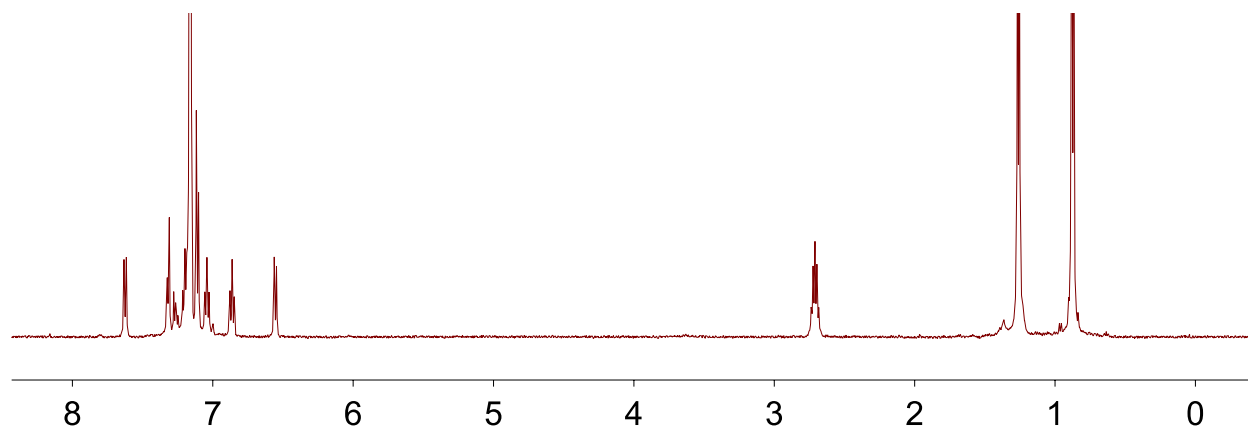


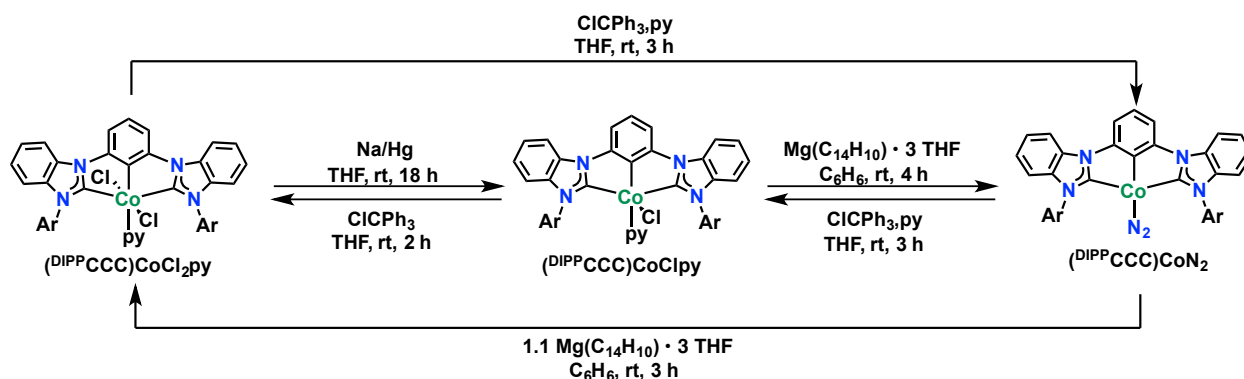
Figure 2.5 ^1H NMR spectrum of $(^{\text{DIPP}}\text{CCC})\text{CoN}_2$ in C_6D_6

Due to the limited amount of structural data on four-coordinate Co^{I} compounds featuring a terminal dinitrogen ligand, complex **3** was further characterized by X-ray crystallography. Red-brown crystals were grown by slow evaporation from benzene at room temperature. Crystallographic characterization of the complex provided definitive evidence of a square planar geometry about the metal, with an N_2 molecule bound *trans* to the $\text{Co}-\text{C}_{\text{aryl}}$ bond (Figure 2.6, Tables 2.1 & 2.2). The $\text{Co}-\text{C}_{\text{NHC}}$ bond lengths of 1.911(3) and 1.899(3) Å and the $\text{Co}-\text{C}_{\text{aryl}}$ bond length of 1.872(3) Å are shorter than those reported for complex **1**, perhaps due to greater electron density in the $\text{Co}-\text{C}$ bonds and coordinative unsaturation about the cobalt metal center. An N_2 bond length of 1.111(3) Å indicates a largely unactivated dinitrogen ligand (d_{N_2} : 1.09 Å). Indeed, a comparison to structurally analogous cobalt dinitrogen complexes reveals that the bond distance of the dinitrogen ligand typically falls within the regime of 1.011 – 1.122 Å,^{31–34} signifying that a lack of activation of the dinitrogen ligand is not uncommon with low-valent cobalt compounds.

Expectedly, given that **3** is a 16-electron complex, the addition of an equivalent of triphenylphosphine to $(^{\text{DIPP}}\text{CCC})\text{CoN}_2$, **3**, resulted in an immediate color change to deep red, affording the 18-electron $(^{\text{DIPP}}\text{CCC})\text{CoN}_2(\text{PPh}_3)$ (**3-PPh₃**) in excellent yields (89%). This compound possessed no resonances in the ^{31}P NMR spectrum likely attributed to coupling of the phosphorous ligand to the ^{59}Co nucleus ($I = 7/2$, 100% abundance). However, the additional aryl resonances in the ^1H NMR spectrum compared to **3** are in agreement with the binding of a triphenylphosphine ligand.

As depicted in Scheme 2.5, the interconversion of all of these compounds is readily achieved. Conversion of the Co^{I} derivative **3** to the Co^{II} , **2**, was accomplished by the addition of one equivalent of ClCPh_3 as the oxidant. An additional equivalent of ClCPh_3 to **2** furnished the Co^{III} analogue, although this was accompanied by the formation of small amounts of impurities

that could readily be overcome through the previously described synthetic pathways.



Scheme 2.5 Interconversion between Co^{I} , Co^{II} , Co^{III} derivatives of the CCC pincer

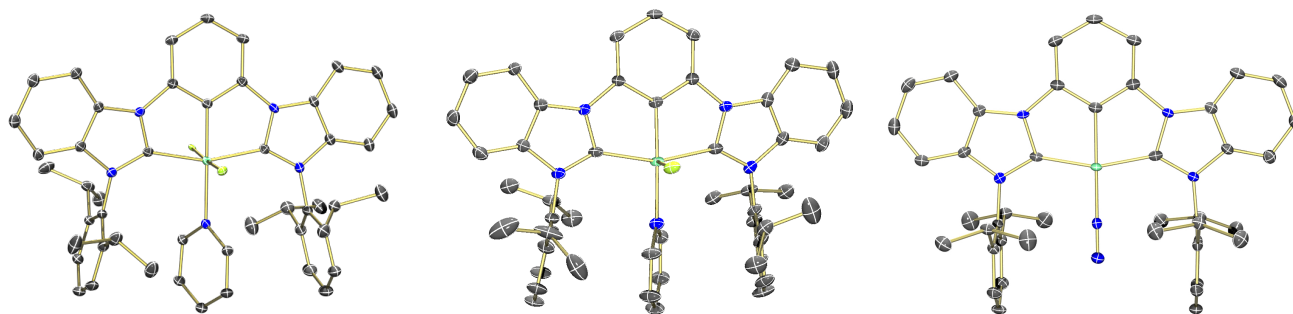


Figure 2.6 Crystal structures of complexes 1, 2, and 3

2.8 Conclusions

In conclusion, a series of cobalt pincer complexes featuring the electron-rich, monoanionic bis(carbene) ($^{\text{DIPPP}}\text{CCC}$) were synthesized. The $\text{Co}^{\text{I-III}}$ derivatives have been prepared in good yields, including the room temperature synthesis of a Co^{III} derivative from the benzimidazolium salt precursor of the ($^{\text{DIPPP}}\text{CCC}$) ligand framework. In contrast to traditional routes that make use of lithiation and subsequent addition of cobalt halide compounds, this room temperature synthesis utilizes Co^{II} sources featuring equivalents of internal base for aryl C–H bond cleavage to generate the metal derivative. A suite of characterization techniques was used to identify and study these

complexes, including NMR spectroscopy and X-ray crystallography. Such complexes provide an interesting platform from which to study two-electron processes on base metals, particularly given the extensively characterized nature of the different oxidation states of cobalt with the ligand platform.

2.9 Experimental section

General Considerations. All manipulations of air- and moisture-sensitive compounds were carried out in the absence of water and dioxygen in an MBraun inert atmosphere drybox under a dinitrogen atmosphere except where specified otherwise. All glassware was oven dried for a minimum of 8 h and cooled in an evacuated antechamber prior to use in the drybox. Solvents for sensitive manipulations were dried and deoxygenated on a Glass Contour System (SG Water USA, Nashua, NH) and stored over 4 Å molecular sieves purchased from Strem following a literature procedure prior to use.²⁶ Chloroform-*d*, and benzene-*d*₆ were purchased from Cambridge Isotope Labs and were degassed and stored over 4 Å molecular sieves prior to use. Lithium hexamethyldisilazide was purchased from Sigma-Aldrich and recrystallized from toluene under an inert atmosphere prior to use. Celite® 545 (J. T. Baker) was dried in a Schlenk flask for 24 h under dynamic vacuum while heating to at least 150°C prior to use in a glovebox. DPEPhos (>99%) and CoCl₂ (99% anhydrous) were purchased from stream and used as received. PdCl₂ was purchased from Pressure Chemicals. [Co(N(SiMe₃)₂)₂]₂•THF^{27,28} and Pd(PPh₃)₄²⁹ were prepared by literature procedures. NMR Spectra were recorded at room temperature on a Varian spectrometer operating at 500 MHz (¹H NMR) and 126 MHz (¹³C NMR) (U500, VXR500, UI500NB) and referenced to the residual CHCl₃ and C₆D₅H resonance (δ in parts per million). Solid-state infrared spectra were recorded using a PerkinElmer Frontier FT-IR spectrophotometer equipped with a KRS5 thallium bromide/iodide universal attenuated total reflectance accessory.

Elemental analyses were performed by the University of Illinois at Urbana–Champaign School of Chemical Sciences Microanalysis Laboratory in Urbana, IL. Electrospray ionization mass spectrometry (ESI) was recorded on a Water Q-TOF Ultima ESI instrument. Cyclic voltammetry studies were collected on CH Instruments 1410C potentiostat. EPR samples were prepared in an MBraun glovebox. The sample concentration is approximately 10mM in tetrahydrofuran/toluene (1:1) mixture. EPR spectra were recorded on a Varian E-line 12” Century series X-band CW spectrometer and the spectra were simulated using the program SIMPOW6.^{30,31} EPR parameters for **2a** (2.5E+3 GAIN; 2.00G MODAMP; 20.00dB POWER; NU= 9.2903GHz).

Modified Ligand Procedure

Preparation of N-(2-bromophenyl)-2,6-diisopropylaniline (L1). A 20 mL scintillation vial charged with Pd(PPh₃)₄ (0.454 g, 0.39 mmol) and DPEPhos (0.317 g, 0.589 mmol) was stirred at 80°C for 20 minutes in toluene (20 mL). The DPEPhos/Pd(PPh₃)₄ solution was then filtered through a pad of celite into a 150 mL Schlenk bomb and 2-bromoiodobenzene (6.696 g, 23.7 mmol), 2,6-diisopropylaniline (2.784 g, 15.70 mmol) and sodium *tert*-butoxide (6.074 g, 63.20 mmol) were added and the mixture was diluted toluene to a final volume of approximately 80 mL. After stirring the mixture at 100°C for 36 h, the suspension was allowed to cool to ambient temperature and then filtered through a plug of silica, eluting with 250 mL of Et₂O. The filtrate was concentrated to an oil under reduced pressure and loaded on a silica gel column. The product was separated using hexanes as the eluent; yielding a white solid after removal of the solvent under reduced pressure (4.80 g, 14.44 mmol, 92%). The ¹H and ¹³C NMR spectra match those of the reported compound.³²

Preparation of N¹,N^{1'}-(1,3-phenylene)bis(N²-(2,6-diisopropylphenyl)benzene-1,2-diamine) (L2). A 20 mL scintillation vial charged with Pd(PPh₃)₄ (1.692 mg, 1.464 mmol) and DPEPhos

(1.176 g, 2.184 mmol) were stirred at 80°C for 20 minutes in toluene (20 mL). The DPEPhos/Pd(PPh₃)₄ solution was then filtered through a pad of celite into a 250 mL Schlenk bomb and **L1** (3.044 g, 9.161 mmol), 1,3-diaminobenzene (0.393 g, 3.634 mmol) and sodium *tert*-butoxide (1.7563 g, 18.28 mmol) were added and the mixture was diluted with *ca.* 120 mL of toluene. After stirring the mixture at 100°C for 24 h, the suspension was allowed to cool to ambient temperature and then filtered through a plug of silica, eluting with 500 mL of Et₂O. The solvent was removed under reduced pressure and the residue adsorbed on 30 g of dry silica and loaded onto a silica gel column. The product is separated with a stepwise gradient of 2-5% ethyl acetate/hexanes, yielding an off-white solid after the removal of solvent (1.931 g, 3.16 mmol, 87%). The ¹H and ¹³C NMR spectra match those of the reported compound.¹

Preparation of 1,1'-(1,3-phenylene)bis(3-(2,6-diisopropylphenyl)-1H-benzo[d]imidazole-3-ium) chloride [H₃(^{DIPP}CCC)]Cl₂. Compound **L2** (2.00 g, 3.274 mmol) was suspended in 20 mL triethyl orthoformate and heated to reflux at 80°C under an N₂ atmosphere. Concentrated hydrochloric acid (37% w/w, 808 mg of solution, 8.20 mmol) was added dropwise and the color of the suspension turned off-white. After stirring the mixture for 4 h, the volatiles were removed under reduced pressure and a beige solid was collected. The solid was triturated with Et₂O (approx. 5 x 10 mL) until washes were colorless and dried under vacuum at 70°C overnight (2.142 g, 3.045 mmol, 93%). The ¹H and ¹³C NMR spectra match those of the reported compound.¹

Preparation of H(^{DIPP}CCC). A 20 mL scintillation vial was charged with the benzimidazolium salt H₃(^{DIPP}CCC)Cl₂ (0.075 g, 0.107 mmol) and approximately 2 mL of benzene. The resulting slurry was frozen at -35 °C. To this frozen mixture, a thawing mixture of KCH₂Ph (0.0291 g, 0.223 mmol) in approximately 2 mL of benzene was added. An additional 2 mL of benzene were used to rinse and complete this transfer. After stirring for 10 min, *ca.* 2 mL of THF was added to

the reaction mixture, resulting in a rapid dissipation of the orange color. When the solution turned clear, solvents were removed under reduced pressure and the solid residue was dissolved in benzene and filtered over Celite to remove KCl. Removal of volatiles under reduced pressure led to the isolation of a yellow-white solid. Washing with hexanes (2×2 mL) left a white powder, which was dried in vacuo to afford $\text{H}(\text{DIPPCCC})$ as the pure product (0.042 g, 0.067 mmol, 62%). Anal. Calcd for $\text{C}_{44}\text{H}_{46}\text{N}_4$: C, 83.77; H, 7.35; N, 8.88. Found: C, 83.10; H, 7.28; N, 8.88. ^1H NMR (C_6D_6 , 500 MHz): δ 8.82 (t, $J = 2.2$ Hz, 1H, Ar-CH), 7.89 (dd, $J = 7.9, 2.1$ Hz, 2H), 7.70 (d, $J = 7.8$ Hz, 2H), 7.35 (t, $J = 7.8$ Hz, 2H), 7.28 (d, $J = 7.8$ Hz, 1H), 7.24 (d, $J = 7.4$ Hz, 4H), 6.94 (m, 4H), 6.77 (d, $J = 7.7$ Hz, 2H), 2.70 (sept, $J = 6.9$ Hz, 4H, ^iPr -CH), 1.17 (d, $J = 6.8$ Hz, 12H, ^iPr -CH₃), 0.96 (d, $J = 6.8$ Hz, 12H, ^iPr -CH₃). ^{13}C NMR (C_6D_6 , 126 MHz): δ 231.27, 147.30, 142.59, 138.36, 135.70, 134.06, 130.12, 129.64, 124.21, 123.04, 122.98, 122.90, 121.77, 111.74, 111.36, 28.88, 24.79, 23.53.

Synthesis of Metal Complexes

Synthesis of $(\text{DIPPCCC})\text{CoCl}_2\text{py}$ (1). A 20 mL scintillation vial charged with $[\text{H}_3(\text{DIPPCCC})]\text{Cl}_2$ (0.0585 g, 0.08321 mmol) in *ca.* 5 mL of THF, a solution of lithium hexamethyldisilazide (0.0135 g, 0.0801 mmol) were stirred at ambient temperature for 5 min. Dropwise addition of a THF (*ca.* 3 mL) a solution of $[\text{Co}(\text{N}(\text{SiMe}_3)_2)_2] \cdot \text{THF}$ (0.0376 g, 0.0832 mmol) and 5 drops of anhydrous pyridine were then added, followed by a THF (*ca.* 3 mL) solution of trityl chloride (0.0232 g, 0.832 mmol). After stirring the mixture for 18 h, the volatiles were removed under reduce pressure and the green solid was washed with hexanes (2×10 mL), dissolved in DCM (10 mL), filtered over a plug of Celite and the solvent was removed under reduced pressure to give a green solid (0.0558g, 0.0666 mmol, 80%). Crystals suitable for X-ray diffraction were grown by slow

evaporation from benzene. ^1H NMR (CDCl_3 , 25 °C) δ 8.82 (d, $J = 4$ Hz, 2H), 8.27 (d, $J = 8.0$ Hz, 2H), 7.87 (d, $J = 8.0$ Hz, 2H), 7.55 (t, $J = 7.8$ Hz, 1H), 7.41 (t, $J = 7.5$ Hz, 2H), 7.20 (t, $J = 7.8$ Hz, 2H), 7.16 (t, $J = 7.8$ Hz, 2H), 7.09 – 7.13 (m, 1H), 6.96 (d, $J = 7.5$ Hz, 4H), 6.75 (d, $J = 8.0$ Hz, 2H), 6.41 (s, 2H), 2.69 (hept, $J = 6.5$ Hz, 4H), 0.98 (d, $J = 6.0$ Hz, 12H), 0.68 (d, $J = 6.5$ Hz, 12H). ^{13}C NMR (CDCl_3): δ 195.3, 156.4, 153.6, 148.7, 147.5, 138.6, 138.6, 134.6, 133.0, 132.2, 130.2, 124.6, 124.1, 123.8, 122.2, 122.1, 112.8, 112.1, 110.3, 27.8, 26.2, 22.8. HRMS (ESI), calc. for $\text{C}_{44}\text{H}_{45}\text{CoN}_4$ ($\text{M} - \text{Cl} - \text{C}_5\text{H}_5\text{N}$) $^+$: 723.2665; found 723.2668.

Alternative Synthesis of 1. A solution of trityl chloride (0.052 g, 0.187 mmol) in approximately 2 mL of THF was prepared and added to a solution of **2** (0.150 g, 0.187 mmol) in ca. 4 mL of THF at room temperature. Additional solvent (2 mL) was used to rinse and complete the transfer and the reaction mixture was stirred for 1 h. The solvent was removed under reduced pressure to afford a solid bright green residue. Trituration with diethyl ether (2 mL X 2) and subsequent evacuation of solvent under reduced pressure afforded a green solid (0.132 g, 0.157 mmol, 84%).

Synthesis of ($^{\text{DIPP}}\text{CCC}$)CoClpy (2**).** A 20 mL scintillation vial was charged with $\text{Co}(\text{N}(\text{SiMe}_3)_2)_2 \cdot \text{THF}$ (0.128 g, 0.283 mmol), $\text{LiN}(\text{SiMe}_3)_2$ (0.048 g, 0.287 mmol), and approximately 4 mL of C_6H_6 . Subsequent addition of anhydrous pyridine (30 drops) to this dark green solution resulted in an immediate color change to dark blue and the mixture was stirred for approximately 5 min. Upon completion of the stirring period, the solution was added to a 15 mL high-pressure vessel containing the benzimidazolium salt, $[\text{H}_3(^{\text{DIPP}}\text{CCC})]\text{Cl}_2$ (0.200 g, 0.284 mmol). The vessel was sealed, taken outside of the glovebox, and heated in an oil bath at 70 °C overnight. Following the conclusion of the heating period, the vessel was brought into a glove box and filtered over a frit layered with Celite. Benzene was added to the solid until the washes became

colorless and the filtrate was subsequently evacuated of all solvent under reduced pressure to afford a bright orange solid. The solid was stirred in a 4:1 mixture of hexanes (8 mL) and diethyl ether (2 mL) for 15 min and filtered over a frit. Subsequent washes with ether (ca. 5 mL) and hexanes (10 mL) followed by drying under reduced pressure yielded the pure solid (0.171 g, 0.213 mmol, 75%). Crystals suitable for X-ray diffraction were grown by slow evaporation from benzene. Analysis for $C_{49}H_{50}ClN_5LiCl$: Calcd. C, 69.59; H, 5.96; N, 8.28. Found C, 70.01; H, 6.15; N, 8.28. 1H NMR (500 MHz, C_6D_6) δ 18.62, 13.29, 11.67, 10.78, 8.47, 7.96, 7.72, 7.55, 7.32, 7.00, 6.86, 4.18, 1.14, -8.80. HRMS (ESI), calc. for $C_{44}H_{45}CoN_4$ (M - Cl - py) $^+$: 688.2980; found 688.2976.

Synthesis of (^{DIPP}CCC)CoN $_2$ (3). A 20 mL scintillation vial was charged with **2** (0.350 g, 0.436 mmol) and approximately 4 mL of benzene. The resulting solution was frozen at -35 °C and Mg($C_{14}H_{10}$)•3THF (0.182 g, 0.435 mmol) was added as a solid. The reaction mixture took on a dark brown color and was stirred to room temperature for 4 h. Following the completion of the stirring period, the mixture was filtered over a frit. Removal of solvent from the filtrate under reduced pressure afforded a solid brown residue that was stirred in hexanes (20 mL) for 15 min and subsequently filtered. The collected solid was washed with ca. 40 mL hexanes to remove anthracene and dried under reduced pressure (0.240 g, 0.335 mmol, 77%). Crystals suitable for X-ray diffraction were grown by slow evaporation from benzene. 1H NMR (500 MHz, C_6D_6) δ 7.63 (d, J = 7.5 Hz, 2H), 7.32 (d, J = 7.0 Hz, 2H), 7.29 – 7.23 (m, 2H), 7.20 (t, J = 7.5 Hz, 3H), 7.11 (d, J = 7.5 Hz, 4H), 7.04 (t, J = 7.5 Hz, 2H), 6.86 (t, J = 7.5 Hz, 2H), 6.55 (d, J = 8.0 Hz, 2H), 2.71 (sept, J = 6.8 Hz, 4H), 1.26 (d, J = 6.5 Hz, 12H), 0.87 (d, J = 6.5 Hz, 12H). ^{13}C NMR (500 MHz, C_6D_6) δ 149.9, 147.0, 139.1, 133.9, 131.4, 124.5, 123.7, 123.5, 122.5, 110.5, 110.3, 107.2, 28.8,

24.7, 24.1. HRMS (ESI), calc. for $C_{44}H_{45}CoN_4$ ($M - N_2$)⁺: 688.2976; found 688.2973. IR: 2063 cm^{-1} (N_2).

Synthesis of (^{DIPP}CCC)CoN₂(PPh₃) (3-PPh₃). A 20 mL scintillation vial was charged with **3** (0.040 g, 0.056 mmol), PPh₃ (0.015g, 0.056 mmol) and benzene (*ca.* 2 mL). Immediately upon addition, the solution turned dark red and the benzene was removed after 5 min of stirring under reduced pressure to furnish a red solid (0.049 g, 0.050 mmol, 89%). NMR data (in benzene-*d*₆, 25 °C): ¹H δ = 7.76 (d, J = 8.0 Hz, 2H), 7.39 (d, J = 7.5 Hz, 2H), 7.23 (t, J = 7.5 Hz, 2H), 7.03 (t, J = 7.5 Hz, 2H), 6.98-6.73 (m, 10H), 6.53 (d, J = 8 Hz, 2H), 3.05-2.41 (broad, 4H), 1.04-0.60 (broad, 24H). ¹³C δ = 144.0, 141.1, 137.3, 135.9, 132.1, 129.8, 128.6, 124.4, 121.8, 121.0, 119.6, 110.8, 109.9, 105.8, 28.8, 25.2, 23.7. IR: 2117 cm^{-1} (N_2). HRMS (ESI), calc. for $C_{44}H_{45}CoN_4$ ($M - P(C_6H_5)_3 N_2$): 689.3054; found 689.3037.

Table 2.1 Crystallographic Parameters for complexes **1**, **2**, and **3**

	(^{DIPP} CCC)CoCl ₂ py (1) cd99da	(^{DIPP} CCC)CoClpy (2) cm49f	(^{DIPP} CCC)CoN ₂ (3) cd06h
Empirical Formula	C ₅₅ H ₅₆ Cl ₂ Co N ₅	C ₄₉ H ₅₀ Cl Co N ₅	C ₄₇ H ₄₈ Co N ₆
Formula Weight	916.88	803.32	755.84
Temperature	105(2) K	173(2) K	100(2) K
Wavelength	0.71073 Å	0.71073 Å	0.71073 Å
Crystal system	Monoclinic	Monoclinic	Triclinic
Space group	P 2 ₁ /c	C 2 ₁ /c	P-1
Unit Cell Dimensions	a = 14.7605(5) Å b = 17.6571(6) Å c = 17.9623(3) Å α = 90° β = 91.1198(13)° γ = 90°	a = 36.876(3) Å b = 15.1289(11) Å c = 22.0454(17) Å α = 90° β = 121.969(8)° γ = 90°	a = 10.9123(19) Å b = 13.358(2) Å c = 15.720(3) Å α = 65.272(7)° β = 78.937(8)° γ = 69.194(8)°
Volume	4654.5(3) Å ³	10433.6(14) Å ³	1943.0(6) Å ³
Z	4	8	2
Reflections collected	122537	30721	7133
Independent reflections	10300	9540	7133
Goodness-of-fit on F ²	1.023	0.979	1.087
Final R indices [I > σ(I)]	R1 = 0.0500 wR2 = 0.1416	R1 = 0.0577 wR2 = 0.1612	R1 = 0.0481 wR2 = 0.1106

Table 2.2 Selected bond lengths and angles for complexes **1**, **2**, and **3**

	(^{DIPP} CCC)CoCl ₂ Py (1)	(^{DIPP} CCC)CoClPy (2)	(^{DIPP} CCC)Co(N ₂) (3)
Bond Distances (Å)			
Co – C1	1.981(2)	1.963(4)	1.911(3)
Co – C13	1.880(2)	1.871(3)	1.872(2)
Co – C20	2.000(2)	1.948(4)	1.899(3)
Co – Cl1	2.2787(6)	2.4465(9)	N/A
Co – Cl2	2.3175(6)	N/A	N/A
Co – N	2.098(2)	2.025(3)	1.802(2)
N – N	N/A	N/A	1.111(3)
Bond Angles (°)			
C13-Co-N5	179.26(9)	175.65(14)	178.73(12)
C1-Co-C13	79.90(10)	80.04(15)	79.76(11)
C13-Co-C20	79.82(10)	80.73(15)	79.95(12)
C1-Co-C20	159.69(10)	159.88(14)	159.54(11)
C1-Co-Cl	176.93(2)	N/A	N/A

2.10 References

1. Chianese, A. R., Mo, A., Lampland, N. L., Swartz, R. L. & Bremer, P. T. Iridium Complexes of CCC-Pincer N-Heterocyclic Carbene Ligands: Synthesis and Catalytic C–H Functionalization. *Organometallics* **29**, 3019–3026 (2010).
2. Hebden, T. J. *et al.* Preparation of a Dihydrogen Complex of Cobalt. *Angew. Chemie* **123**, 1913–1916 (2011).
3. Matson, E. M. *et al.* Nickel(II) Pincer Carbene Complexes: Oxidative Addition of an Aryl C–H Bond to Form a Ni(II) Hydride. *Organometallics* **34**, 399–407 (2015).
4. Panda, A., Stender, M., Olmstead, M. M., Klavins, P. & Power, P. P. Reactions of $M\{N(SiMe_3)_2\}_2$ (M=Mn, Fe or Co) with pyridine and 4,4'-bipyridyl: structural and magnetic studies. *Polyhedron* **22**, 67–73 (2003).
5. Xi, Z., Liu, B., Lu, C. & Chen, W. Cobalt(III) complexes bearing bidentate, tridentate, and tetradentate N-heterocyclic carbenes: synthesis, X-ray structures and catalytic activities. *Dalton Trans.* 7008–14 (2009). doi:10.1039/b906242d
6. Scepaniak, J. J., Margarit, C. G., Bontchev, R. P. & Smith, J. M. Cobalt azide complexes with a tris(carbene)borate ligand scaffold. *Acta Crystallogr. Sect. C Cryst. Struct. Commun.* **69**, 968–971 (2013).
7. Allen, F. H. The Cambridge Structural Database: a quarter of a million crystal structures and rising. *Acta Crystallogr. Sect. B Struct. Sci.* **58**, 380–388 (2002).
8. Hicks, J. & Jones, C. Extremely bulky amido first row transition metal(II) halide complexes: potential precursors to low coordinate metal-metal bonded systems. *Inorg. Chem.* **52**, 3900–7 (2013).
9. Hosokawa, S., Ito, J. & Nishiyama, H. NCN-Pincer Cobalt Complexes Containing Bis(oxazoliny)phenyl Ligands. *Organometallics* **32**, 3980–3985 (2013).
10. Murugesan, S. *et al.* Synthesis and Reactivity of Four- and Five-Coordinate Low-Spin Cobalt(II) PCP Pincer Complexes and Some Nickel(II) Analogues. *Organometallics* **33**, 6132–6140 (2014).
11. Zheng, T. & Sun, H. Dichlorido[2,3,5,6-tetrafluoro-4-(trifluoromethyl)phenyl- κ C 1]bis(trimethylphosphine- κ P)cobalt(III). *Acta Crystallogr. Sect. E Struct. Reports Online* **66**, m574–m574 (2010).
12. Robitzer, M. *et al.* Transmetalation of Aryl Units from Gold(I) to Cobalt(III): A Clean Route to the Synthesis of Anion Cobaltoreceptors. *Organometallics* **24**, 1756–1761 (2005).
13. Van der Zeijden, A. A. H. & Van Koten, G. Monoarylcobalt(II) compounds stabilized by bis ortho chelation. *Inorg. Chem.* **25**, 4723–4725 (1986).
14. Zhu, G., Li, X., Xu, G., Wang, L. & Sun, H. A new PC(sp³)P ligand and its coordination chemistry with low-valent iron, cobalt and nickel complexes. *Dalton Trans.* **43**, 8595–8

- (2014).
15. Kent, M. A. *et al.* Cobalt PCP Pincer Complexes via an Unexpected Sequence of Ortho Metalations. *Organometallics* **33**, 5686–5692 (2014).
 16. Morton, J. R., Preston, K. F., Page, Y. Le & Krusic, P. J. Electron paramagnetic resonance spectra of the Fe₂(CO)₈ radical trapped in single crystals of PPN⁺FeCo(CO)₈. *J. Chem. Soc. Faraday Trans. 1 Phys. Chem. Condens. Phases* **85**, 4019–4030 (1989).
 17. Addison, A. W., Rao, T. N., Reedijk, J., van Rijn, J. & Verschoor, G. C. Synthesis, structure, and spectroscopic properties of copper(II) compounds containing nitrogen/sulphur donor ligands; the crystal and molecular structure of aqua[1,7-bis(N-methylbenzimidazol-2-yl)-2,6-dithiaheptane]copper(II) perchlorate. *J. Chem. Soc. Dalt. Trans.* 1349–1356 (1984). doi:10.1039/dt9840001349
 18. Theopold, K. H., Silvestre, J., Byrne, E. K. & Richeson, D. S. Homoleptic mesityl complexes of cobalt(II). Synthesis, crystal structure, and theoretical description of bis(μ-mesityl)dimesityldicobalt. *Organometallics* **8**, 2001–2009 (1989).
 19. Li, J., Li, X., Wang, L., Hu, Q. & Sun, H. C-Cl bond activation and catalytic hydrodechlorination of hexachlorobenzene by cobalt and nickel complexes with sodium formate as a reducing agent. *Dalton Trans.* **43**, 6660–6 (2014).
 20. Dugan, T. R., Macleod, K. C., Brennessel, W. W. & Holland, P. L. Cobalt-Magnesium and Iron-Magnesium Complexes with Weakened Dinitrogen Bridges. *Eur. J. Inorg. Chem.* 3891–3897 (2013). doi:10.1002/ejic.201300187
 21. Yu, R. P. *et al.* Catalytic hydrogenation activity and electronic structure determination of bis(arylimidazol-2-ylidene)pyridine cobalt alkyl and hydride complexes. *J. Am. Chem. Soc.* **135**, 13168–84 (2013).
 22. Lin, T. & Peters, J. C. Boryl-Mediated Reversible H₂ Activation at Cobalt: Catalytic Hydrogenation, Dehydrogenation, and Transfer Hydrogenation. **135**, 15310–15313 (2013).
 23. Rozenel, S. S., Padilla, R. & Arnold, J. Chemistry of reduced monomeric and dimeric cobalt complexes supported by a PNP pincer ligand. *Inorg. Chem.* **52**, 11544–11550 (2013).
 24. Bowman, A. C. *et al.* Synthesis and molecular and electronic structures of reduced bis(imino)pyridine cobalt dinitrogen complexes: ligand versus metal reduction. *J. Am. Chem. Soc.* **132**, 1676–84 (2010).
 25. Mo, Z., Chen, D., Leng, X. & Deng, L. Intramolecular C(sp³)-H Bond Activation Reactions of Low-Valent Cobalt Complexes with Coordination Unsaturation. *Organometallics* **31**, 7040–7043 (2012).
 26. Pangborn, A. B., Giardello, M. A., Grubbs, R. H., Rosen, R. K. & Timmers, F. J. Safe and Convenient Procedure for Solvent Purification. *Organometallics* **15**, 1518–1520 (1996).
 27. Eichhöfer, A., Lan, Y., Mereacre, V., Bodenstein, T. & Weigend, F. Slow Magnetic Relaxation in Trigonal-Planar Mononuclear Fe(II) and Co(II) Bis(trimethylsilyl)amido

- Complexes—A Comparative Study. *Inorg. Chem.* **53**, 1962–1974 (2014).
28. Bürger, H. & Wannagat, U. Silylamido-Derivate von Eisen und Kobalt. *Monatshefte für Chemie und verwandte Teile anderer Wissenschaften* **94**, 1007–1012 (1963).
 29. Coulson, D. R., Satek, L. C. & Grim, S. O. in 121–124 (John Wiley & Sons, Inc., 2007). doi:10.1002/9780470132449.ch23
 30. Nilges, M. J., Matteson, K. & Belford, R. L. SIMPOW6: a software package for simulation of ESP powder-type spectra.
 31. Hemmings, M. A. & Berlinger, L. *ESR Spectroscopy in Membrane Biophysics, Biological Magnetic Resonance*. (Springer, 2007).
 32. Chianese, A. R., Bremer, P. T., Wong, C. & Reynes, R. J. Rigid, Sterically Diverse N-Heterocyclic Carbene-Pyridine Chelates: Synthesis, Mild Palladation, and Palladium-Catalyzed Allylic Substitution. *Organometallics* **28**, 5244–5252 (2009).

Chapter 3

Catalytic hydrosilylation with (^{DIPP}CCC)CoN₂: substrate scope and mechanistic insights†

3.1 Introduction

The catalytic hydrosilylation of alkenes is a formidable tool for the synthesis of organosilicon reagents, a class of compounds widely employed in the production of consumer goods and commodity chemicals.¹⁻³ Nevertheless, the high cost, irretrievability, and, at times, orthogonal reactivity of precious metal catalysts have inspired efforts to develop alternative platforms that feature a broad substrate scope and earth-abundant metals such as cobalt, iron, or nickel.⁴ In addition to the metal center, the silane featured in the catalysis is of great importance – as tertiary silanes are more difficult to use and hydrosiloxanes are of particular interest industrially.⁵ Hydrosilylation featuring earth-abundant catalysts has garnered a significant amount of attention from several research groups, but improvements to functional group tolerance with tertiary silanes within these systems is still a formidable endeavor.

Earth-abundant hydrosilylation catalysts featuring iron have been investigated by Chirik,^{6,7} Huang,⁸ Thomas,⁹ Ritter¹⁰ and others.¹¹ Likewise, nickel-catalyzed hydrosilylation has experienced a resurgence of interest.¹²⁻¹⁴ Recent reports from the labs of Holland,¹⁵ Hu,¹⁶ Nagashima,¹¹ and Chirik¹⁷ have provided powerful new catalysts that address some of the known hydrosilylation limitations. The Co^I β -diketiminato complexes reported by Holland and coworkers were shown to facilitate the chemoselective hydrosilylation of alkenes in the presence of a variety of functional groups.¹⁵ However, the hydrosilylation of substrates

† Portions of this chapter are reproduced from the following publication with permission from the authors. Ibrahim, A.D.; Entsminger, S.W.; Zhu, L.; Fout, A. R. *ACS Catal.* **2016**, *6* (6), 3589–3593.

featuring ketone or protic functionalities, such as hydroxyls or NH_x groups, was absent.¹⁵ Similarly, Hu reports a highly chemoselective $[(^{\text{Me}}\text{N}_2\text{N})\text{NiOMe}]$ pincer complex for the hydrosilylation of alkenes in the presence of traditionally challenging functionalities such as esters, ketones, primary amines, and even formyl functionalities.¹⁶ However, hydrosilylation with tertiary silanes proceeded in low yields ($\sim 30\%$) and substrates featuring hydroxyl groups were not tolerated.¹⁶ The report by Nagashima features the use of tertiary hydrosiloxanes¹¹ with an ill-defined cobalt or iron catalyst and Chirik reports an expanded substrate scope with a cobalt system,¹⁷ but the functional group tolerance of both examples could be broadened.

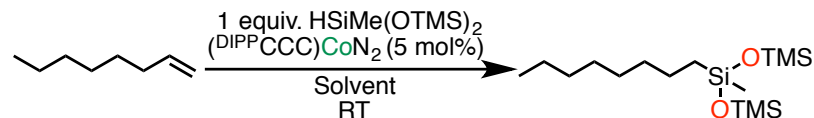
Interested in exploring the competency of low-valent cobalt complexes, we probed the competency of $(^{\text{DIPP}}\text{CCC})\text{CoN}_2$ (**1**) ($^{\text{DIPP}}\text{CCC}$ = bis(diisopropylphenyl-benzimidazol-2-ylidene)phenyl)¹⁸ toward catalysis. Our initial endeavors focused on the hydrosilylation of alkenes. Our addition into this well-established research area^{11,15,19–21} is to improve functional group tolerance with tertiary silanes and hydrosiloxanes. Herein, we report a highly chemoselective Co^{I} catalyst for the hydrosilylation of terminal alkenes that is amenable to the use of both secondary and tertiary silanes in high yields. In addition to substrates containing ketone, ester, and amine functionalities, we demonstrate the selective 1,2-hydrosilylation of alkenes in the presence of aldehyde, alcohol, and nitrile groups, as well as conjugated dienes.

3.2 Results and discussion

Initial hydrosilylation experiments utilized 1-octene as a model substrate to optimize catalyst loading and solvent choice (Table 3.1). In all cases, the anti-Markovnikov product was exclusively observed at room temperature. An addition of a drop of Hg to the reaction did not inhibit reactivity, suggesting that catalysis is likely homogeneous and not supported by colloids or nanoparticles of cobalt metal. As depicted in Table 3.2, various silanes were compared at room

temperature under optimized conditions (5 mol% catalyst loading in benzene). The reaction was amenable to the use of secondary (Entry 2) and tertiary silanes, with low conversion for Et₃SiH

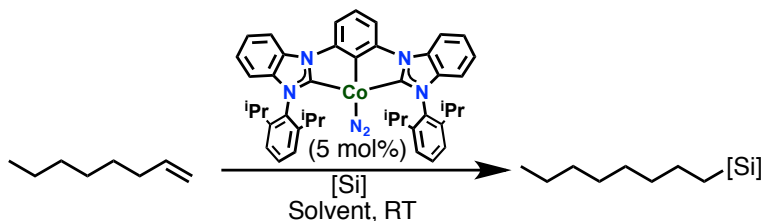
Table 3.1 Optimization of catalytic loading and solvent choice



Entry	% of cat.	Solvent	Time	GC-Yield
1	5 mol %	Benzene	1 h	41%
2	5 mol %	THF	1 h	24%
3	5 mol %	1,4-dioxane	1 h	32%
4	5 mol %	MeCN	1 h	< 1%
5	2.5 mol %	Benzene	1 h	5%
6	1 mol %	Benzene	1 h	1%
7	1 mol %	Neat	1 h	11%

(Entry 3) but good yields with Me₂PhSiH (Entry 4) and hydrosiloxanes such as MD'M (Entry 5) (MD'M = 1,1,1,3,5,5,5-heptamethyltrisiloxane) and trimethoxysilane (Entry 6). Running the

Table 3.2 Hydrosilylation of 1-octene



Entry	[Si]	Solvent	Time	GC-Yield
1	Ph ₃ SiH	Benzene	1 h	< 5%
2	Ph ₂ SiH ₂	Benzene	1 h	88%
3	Et ₃ SiH	Benzene	21 h	< 35%
4	PhMe ₂ SiH	Benzene	1 h	82%
5	MD'M	Benzene	1 h	41%
6	(OMe) ₃ SiH	Benzene	1 h	94%*

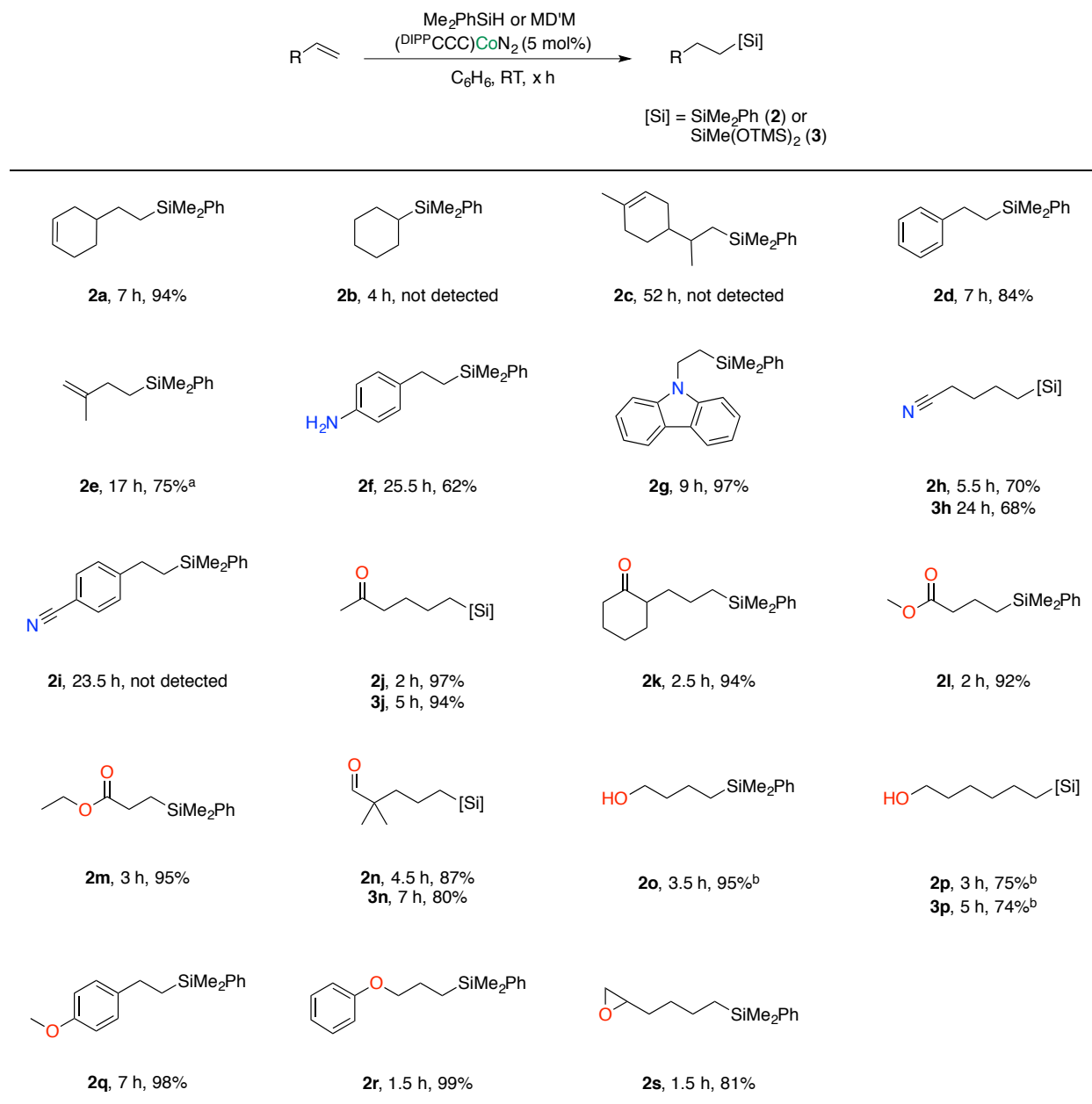
* = NMR yield

reactions in neat silane did result in the desired hydrosilylated product but was impeded by catalyst solubility. All reactions were run in duplicate and yields were analyzed by gas chromatography and mass spectrometry.

Encouraged by these results, we sought to extend the substrate scope of the catalytic reaction sequence using both Me_2PhSiH and MD'M (Table 3.3). Terminal alkenes bearing a wide variety of functional groups were investigated. In the presence of more than one olefinic bond, the less hindered double bond is selectively hydrosilylated (**2a**). Unfortunately, cyclic alkenes, such as cyclohexene (**2b**), and substrates such as limonene (**2c**), which feature a 1,1-disubstituted olefin, are not reactive towards hydrosilylation.

We postulated that such steric constraints can be leveraged to selectively hydrosilylate more challenging substrates. Given the significant challenges associated with the 1,2-hydrosilylation of conjugated dienes, we turned our attention to isoprene, an industrially relevant feedstock used in the production of natural rubber.²² We reasoned that the steric constraints afforded by the disubstituted alkene and conferred by our sterically encumbered catalyst would favor hydrosilylation at the less hindered terminal olefinic bond. In line with our hypothesis, hydrosilylation of isoprene proceeded with 1,2-selectivity (**2e**). As expected, the analogous reaction with 2.4 equiv of 1,3-butadiene, which possesses equally accessible double bonds, furnished the 1,4-hydrosilylation product, as detected in the ^1H NMR spectrum. These results corroborated the importance of sterics in modulating catalytic selectivity. Selective 1,4-hydrosilylation of dienes has been reported with a number of catalysts, attributed to the thermodynamic favorability of π -allyl intermediates.²³ However, very few examples of selective 1,2-hydrosilylation have been reported, and **2e** signifies a rare example where steric control leads

Table 3.3 Substrate scope



Isolated yields are an avg. of duplicate runs. All reactions performed on 0.56 mmol scale with a 1:1 mol mixture of alkene and silane in 3 mL of benzene unless otherwise noted. ^a Heated at 70 °C and with 2 equiv of isoprene. ^b Solvent was 1,4 dioxane.

to selectivity with a well-defined cobalt catalyst.^{23–25}

Primary amines (**2f**), tertiary amines (**2g**), and nitriles (**2h,3h**) were also tolerated. Extending this protocol to 4-vinylaniline was successful, resulting in alkene-selective hydrosilylation to give 4-(2-(dimethyl(phenyl)silyl)ethyl)aniline (**2f**) in moderate yield (62%).

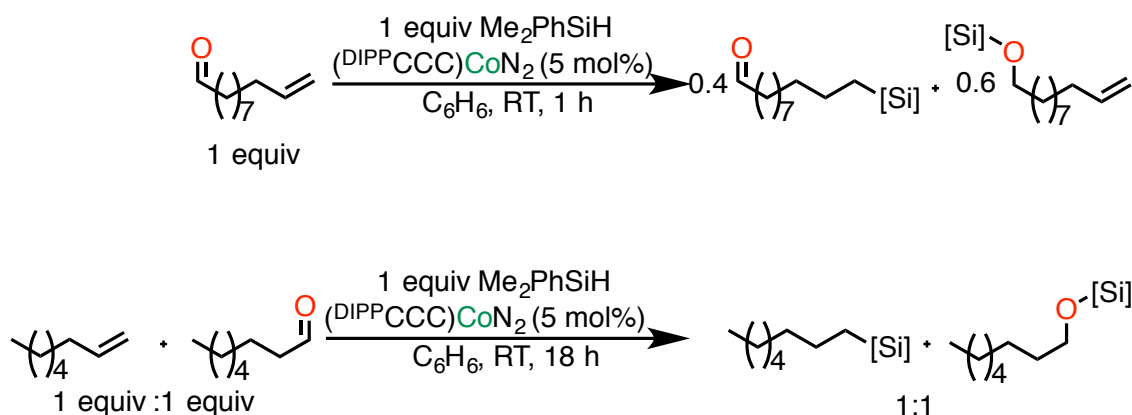
Although 4-cyanostyrene was not productive towards the formation of the desired organosilicon product (**2i**), 4-pentenenitrile was amenable to hydrosilylation with both Me₂PhSiH (**2h**) and MD'M (**3h**). Such reactivity has been observed with precious metal catalysts^{26,27} but has not been reported with cobalt.

Encouraged by these results, we next turned our attention to the hydrosilylation of alkene substrates bearing carbonyl functionalities. Utilizing Me₂PhSiH and 5-hexen-2-one as a model ketone-bearing substrate, the corresponding organosilicon product 6-(dimethyl(phenyl)silyl)hexan-2-one (**2j**) was isolated in 97% yield. Extending the protocol to MD'M and Ph₂SiH₂ furnished the corresponding organosilicon in 94% (**3j**) and 86% isolated yield, respectively. In all cases, no hydrosilylation of the ketone functional group was detected and the anti-Markovnikov product was exclusively formed (**2j-k**). Esters (**2l-m**) and even a formyl-containing substrate, 2,2-dimethyl-4-pentenal (**2n**), were tolerated with the latter also resulting in a high yielding product with the more challenging MD'M silane (**3n**). As of the publication of this manuscript, this signifies only the first cobalt system that is tolerant of formyl functionality.¹⁶

An investigation into the origin of this formyl group tolerance suggests that the observed selectivity is not solely attributable to steric considerations. Hydrosilylation of 10-undecenal, a substrate bearing a more sterically accessible aldehyde group, furnished two major products in a 1.4:1 ratio favoring hydrosilylation of the aldehyde over the alkene (Scheme 3.1). A competition experiment, between 1-octene and octanal, however, initially favors hydrosilylation of the alkene (1.6:1) but gradually converges to a 1:1 ratio over the course of 18 hours.

We next explored the hydrosilylation of substrates containing unprotected alcohols, a challenging functional group for iron and nickel catalysts.^{8,16} In the presence of 5 mol% of catalyst, 3-buten-1-ol was reacted with Me₂PhSiH to afford 4-(dimethyl(phenyl)silyl)butan-1-ol in 95%

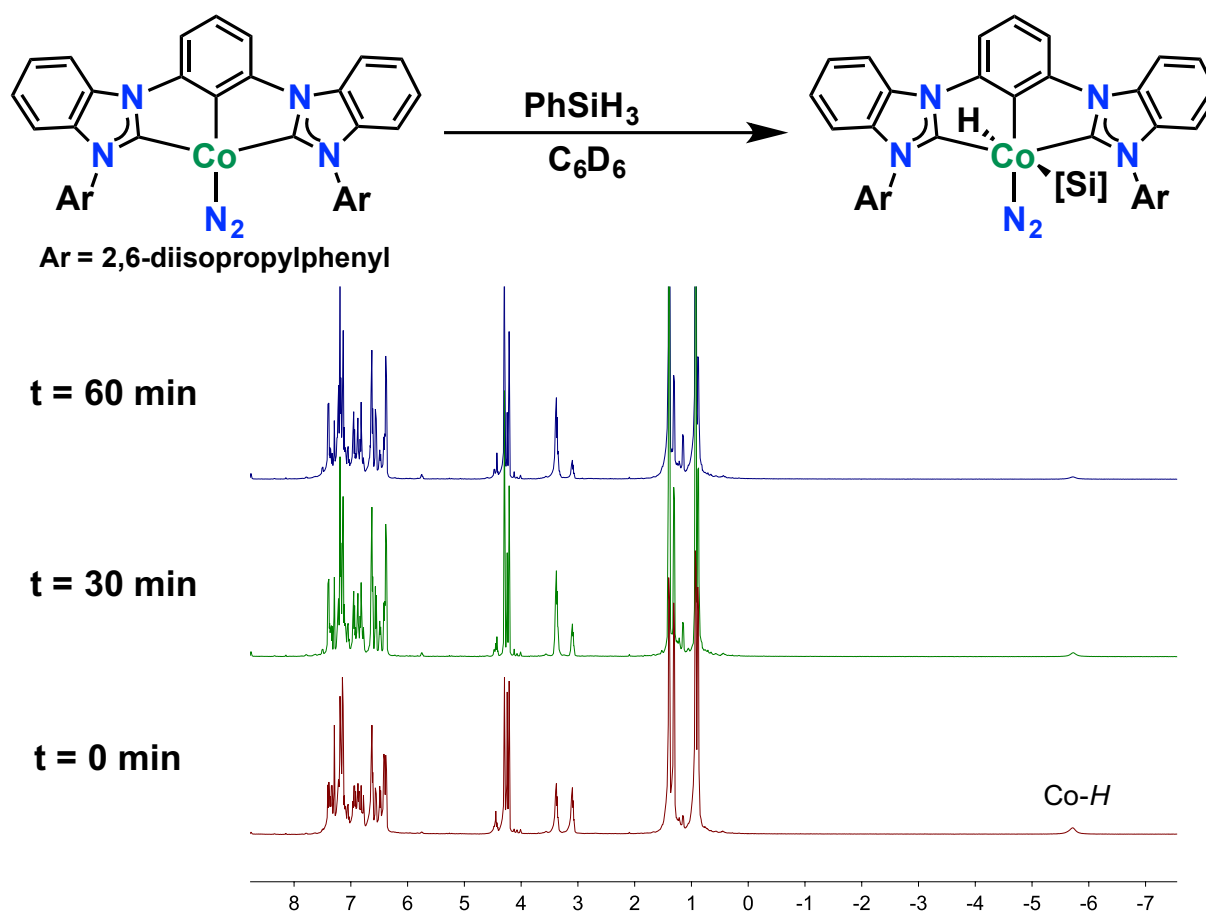
yield (**2o**). The hydrosilylation of 5-hexen-1-ol with Me₂PhSiH (**2p**) and MD'M (**3p**) proceeded in similar fashion in 1,4-dioxane. Although tolerated with certain Pt and Rh catalysts,^{28,29} to the best of our knowledge alcohols have not been previously reported with cobalt hydrosilylation catalysts. Further elaboration of the catalyst's ability to tolerate oxygen-containing substrates led us to investigate the hydrosilylation of substrates bearing methoxy, allyl ether, and epoxide moieties (**2q-s**). Gratifyingly, hydrosilylation of these substrates proceeded in excellent yields. Undesirable isomerization products or cleavage of the epoxide were not observed.



Scheme 3.1 Hydrosilylation of aldehydes versus alkenes

Interested in gaining insights into the mechanism of hydrosilylation, we next investigated the stoichiometric reactivity of the (DIPPPCCC)CoN₂ catalyst towards silanes. We hypothesized that treatment of the Co^I complex with silane would result in oxidative addition of a Si–H bond to the metal center, similar to what has been observed in recent reports by Arnold³⁰ and Chirik³¹ with low-valent, electron-rich cobalt complexes. Such a species could then proceed along a Chalk-Harrod reaction profile to hydrosilylate unsaturated carbon-carbon bonds.³² Monitoring of the reaction of PhSiH₃ with (DIPPPCCC)CoN₂ by ¹H NMR spectroscopy suggested that such a hypothesis was plausible (Scheme 3.2). The presence of a broad upfield resonance at -5.76 ppm

and decreased symmetry in the ^1H NMR spectrum, particularly in the resonances attributed to the ^iPr groups of the ligand framework, were consistent with the possibility of an oxidative addition of a Si–H bond onto the metal center. However, rapid thermal decomposition of this species to a new compound precluded further characterization and therefore the possibility of an η^2 -bound Si–H bond could not be ruled out. The observation of intermediates following addition of Me_2PhSiH was similarly limited, as no product formation was observed on the ^1H NMR time scale in both the stoichiometric addition and in the presence of excess silane.



Scheme 3.2 Reaction of cobalt catalyst with PhSiH_3 monitored by ^1H NMR spectroscopy

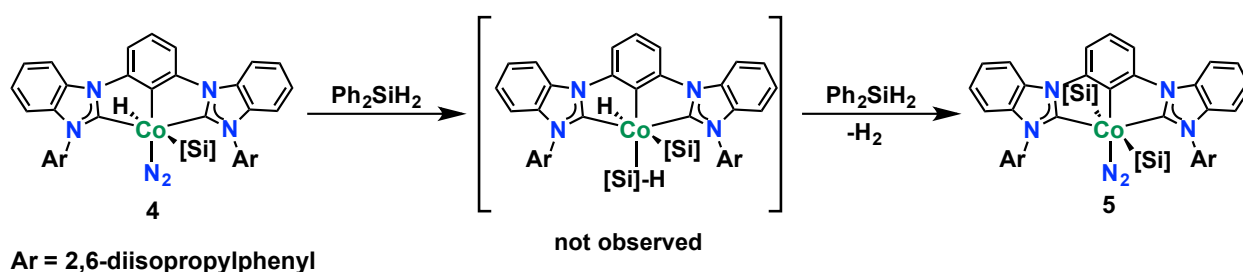
Interestingly, addition of Ph_2SiH_2 to the catalyst resulted in the formation of a more

thermally robust compound amenable to characterization. Analogous to the reaction with PhSiH_3 , addition of Ph_2SiH_2 to the Co^{I} catalyst rapidly resulted in the formation of a new diamagnetic compound, **4**, with an upfield resonance at -7.08 ppm, as well as decreased symmetry of the ligand framework in the ^1H NMR spectrum. Two septets at 3.42 and 2.21 ppm, attributed to the methine protons of the ^iPr groups of the ligand framework, and four doublets at 1.50, 1.11, 0.94, and 0.63 ppm, assigned to the methyls of the ^iPr groups, are consistent with a C_s -symmetric compound. The presence of a downfield resonance at 5.52 ppm in the ^1H NMR spectrum was assigned to the proton of a bound silyl ligand.

Additional characterization with ^1H -coupled ^{29}Si NMR spectroscopy was undertaken to establish the solution-state structure of **4**. The presence of a resonance at 8.28 ppm in the ^{29}Si NMR was assigned to a silyl ligand bound to the cobalt center. From this peak a $^1J_{\text{SiH}}$ coupling constant of 165 Hz and a smaller, weakly-resolved $^2J_{\text{SiH}}$ coupling constant of ~ 13 Hz were measured. The value of the latter coupling constant is below the 20 Hz J_{SiH} coupling value threshold associated with η^2 -bound Si-H bonds³³ and is consistent with cleavage of the Si-H bond by the cobalt metal center. This was further corroborated by a two-dimensional ^1H - ^{29}Si HMBC experiment, where the resonance centered at 8.28 ppm in the ^{29}Si NMR exhibits a cross-peak with the hydride, and a one-dimensional NOE experiment (Figures 3.5 and 3.3), allowing for the assignment of **4** as the Co^{III} silyl-hydride compound, $(^{\text{DIPP}}\text{CCC})\text{Co}(\text{SiHPh}_2)(\text{H})(\text{N}_2)$. Complex **4** is catalytically relevant as the addition of 1-octene furnished the hydrosilylated compound and regenerated the $(^{\text{DIPP}}\text{CCC})\text{CoN}_2$ starting material.

Cooling a concentrated reaction mixture of $(^{\text{DIPP}}\text{CCC})\text{CoN}_2$ and Ph_2SiH_2 in diethyl ether to -35 °C yielded yellow crystals suitable for single crystal X-ray diffraction. Surprisingly, an

octahedral Co^{III} bis(silyl) compound, $(^{\text{DIPP}}\text{CCC})\text{Co}(\text{SiHPh}_2)_2(\text{N}_2)$ (**5**), a minor decomposition product noted in ^1H NMR spectra of **4** was obtained. Subsequent attempts to independently synthesize **5** were unsuccessful, accompanied in all cases by the concomitant formation of **4**, which prohibited the effective characterization of the Co^{III} bis(silyl) species. This off-cycle decomposition product (**5**) supports cleavage of the Si–H bond, as formation of **5** is likely the result of a σ -bond metathesis with **4** and an η^2 -bound silane (Scheme 3.3).



Scheme 3.3 Proposed mechanism for formation of **5**

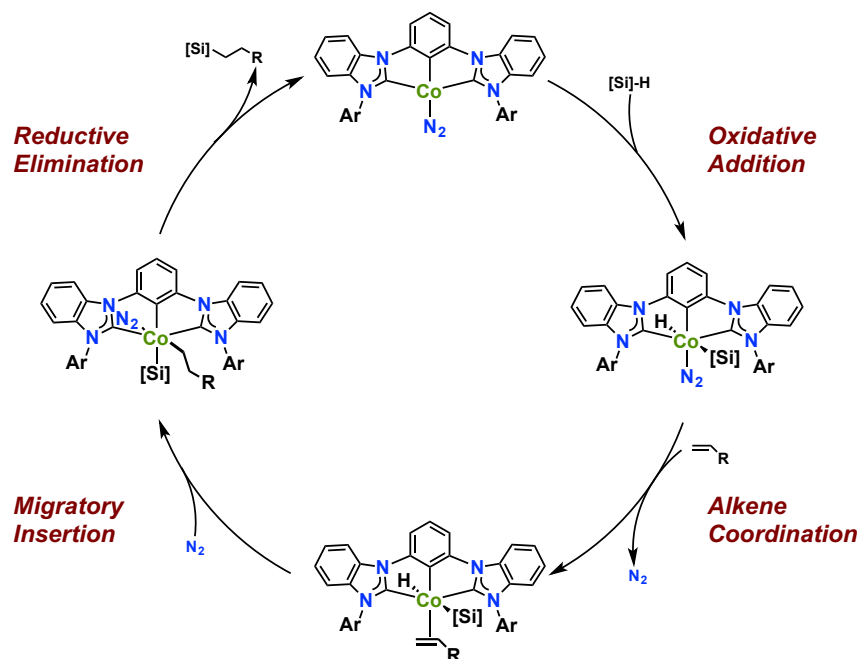


Figure 3.1 Proposed catalytic mechanism for hydrosilylation with $(^{\text{DIPP}}\text{CCC})\text{CoN}_2$

This series of experiments has led to the proposal of a Chalk-Harrod type mechanism (Figure 3.1)

whereby oxidative addition of the silane is followed by coordination of the alkene. Subsequent migratory insertion of the hydride or silyl ligand into the alkene, followed by reductive elimination, furnishes the hydrosilylated product and regenerates the Co^{I} catalyst.

3.3 Conclusions

In conclusion, we have developed a highly selective Co^{I} system for the hydrosilylation of alkenes. This hydrosilylation, proposed to proceed through a Chalk-Harrod type mechanism, furnishes the anti-Markovnikov product exclusively in all observed cases and is tolerant of a wide range of challenging functionalities, including unprotected alcohols, ketones, and dienes. The hydrosilylation of a substrate bearing formyl functionality and an alkene bearing nitrile functionality have also been shown to proceed selectively at the alkene.

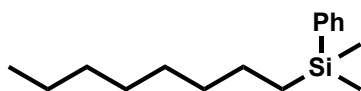
3.4 Experimental section

General Considerations. All manipulations of air- and moisture-sensitive compounds were carried out in the absence of water and dioxygen in an MBraun inert atmosphere drybox under a dinitrogen atmosphere except where specified otherwise. All glassware was oven dried for a minimum of 8 h and cooled in an evacuated antechamber prior to use in the drybox. Solvents for sensitive manipulations were dried and deoxygenated on a Glass Contour System (SG Water USA, Nashua, NH) and stored over 4 Å molecular sieves purchased from Strem following drying via a literature procedure prior to use.³⁴ Chloroform- d_1 and benzene- d_6 were purchased from Cambridge Isotope Labs and were degassed and stored over 4 Å molecular sieves prior to use. Celite® 545 (J. T. Baker) was dried in a Schlenk flask for 24 h under dynamic vacuum while heating to at least 150 °C prior to use in a glovebox. NMR Spectra were recorded at room temperature on a Varian spectrometer operating at 600 MHz, 500 MHz, or 400 MHz (^1H NMR) 126 MHz or 101 MHz (^{13}C

NMR), and 119 MHz (^{29}Si NMR) (UI600, U500, VXR500, UI500NB, U400) and referenced to the residual CHCl_3 and $\text{C}_6\text{D}_5\text{H}$ resonance (δ in parts per million, and J in Hz). Infrared spectra were recorded using a PerkinElmer Frontier FT-IR spectrophotometer equipped with a KRS5 thallium bromide/iodide universal attenuated total reflectance accessory. Electrospray ionization mass spectrometry (ESI) was recorded on a Waters Q-TOF Ultima ESI instrument. Electron ionization mass spectrometry (EI) was recorded on a Waters 70-VSE EI instrument. Diphenylsilane and 1,1,13,5,5,5-heptamethyltrisiloxane were purchased from Oakwood Chemical. Dimethylphenylsilane and allyl phenyl ether were purchased from Alfa Aesar. 4-pentenitrile and 1,3-butadiene (15% in toluene) were purchased from TCI Chemicals, and the remainder of the alkene substrates, as well as trimethoxysilane, was purchased from Sigma-Aldrich. All liquids were dried over 4 Å molecular sieves prior to use.

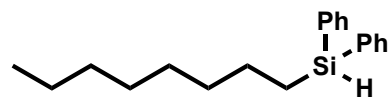
General Hydrosilylation Procedure. A 20 mL scintillation vial is charged with olefin (0.558 mmol) and silane (0.558 mmol) inside a glove box. Using the selected solvent, the resulting mixture is then transferred to a vial containing the catalyst ($^{\text{DIPP}}\text{CCC})\text{CoN}_2$ (**1**) (0.020 g, 0.02790 mmol), which was prepared according to literature procedure.¹⁸ A final rinse and transfer with the selected solvent, for a total solvent volume of ca. 3 mL, completes the setup and the reaction is stirred at room temperature for the allotted time. Upon completion, the vial is taken out of the glove box and the crude reaction is concentrated under reduced pressure and loaded onto a silica gel column. Elution, followed by the removal of solvent under reduced pressure, affords the target compound.

Characterization Data.



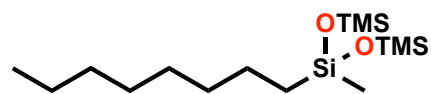
Dimethyl(octyl)(phenyl)silane. A modified form of the general procedure, whereby purification was conducted inside

the glovebox, was followed using 1-octene (0.558 mmol), dimethylphenylsilane (0.558 mmol), and benzene (3 mL). After 2 h, the crude reaction was purified by flash chromatography with hexanes to afford dimethyl(octyl)(phenyl)silane as a colorless oil (0.125 g, 0.502 mmol, 90%). ^1H NMR (500 MHz, CDCl_3) δ 7.57-7.52 (m, 2H), 7.40-7.36 (m, 3H), 1.38-1.23 (m, 12H), 0.91 (t, $J = 6.9$ Hz, 3H), 0.80-0.74 (m, 2H), 0.28 (s, 6H). ^{13}C NMR (126 MHz, CDCl_3) δ 139.9, 133.7, 128.9, 127.8, 33.8, 32.1, 29.4, 24.0, 22.8, 15.9, 14.3, -2.8. HRMS (EI), calc. for $\text{C}_{15}\text{H}_{25}\text{Si}$ ($\text{M} - \text{CH}_3$) $^+$: 233.1726; found 233.1719.



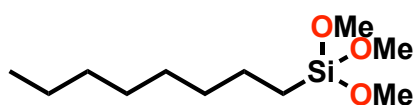
Octyldiphenylsilane. A modified form of the general procedure, whereby purification was conducted inside the

glovebox, was followed using 1-octene (0.558 mmol), diphenylsilane (0.558 mmol), and benzene (3 mL). After 2 h, the crude reaction was purified by flash chromatography with hexanes to afford octyldiphenylsilane as a colorless oil (0.147 g, 0.497 mmol, 89%). ^1H NMR (500 MHz, CDCl_3) δ 7.62-7.56 (m, 4H), 7.45-7.35 (m, 6H), 4.88 (t, $J = 3.7$ Hz, 1H), 1.53-1.45 (m, 2H), 1.43-1.36 (m, 2H), 1.32-1.24 (m, 8H), 1.20-1.15 (m, 2H), 0.90 (t, $J = 6.8$ Hz, 3H). ^1H NMR (500 MHz, C_6D_6) δ 7.64 – 7.54 (m, 4H), 7.22 – 7.15 (m, 6H), 5.13 (t, $J = 3.7$ Hz, 1H), 1.55 – 1.44 (m, 2H), 1.37 – 1.22 (m, 10H), 1.15 – 1.07 (m, 2H), 0.89 (t, $J = 7.1$ Hz, 3H). ^{13}C NMR (101 MHz, CDCl_3) δ 135.3, 134.9, 129.6, 128.1, 33.3, 32.1, 29.4, 24.6, 22.8, 14.3, 12.3. HRMS (EI), calc. for $\text{C}_{20}\text{H}_{27}\text{Si}$ ($\text{M} - \text{H}$) $^+$: 295.18821; found 295.18864.

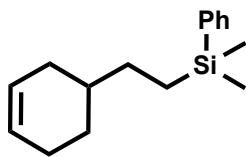


1,1,1,3,5,5,5-heptomethyl-3-octyltrisiloxane. A modified form of the general procedure, whereby purification was

conducted inside the glovebox, was followed using 1-octene (0.558 mmol), 1,1,1,3,5,5,5-heptamethyltrisiloxane (0.558 mmol), and benzene (3 mL). After 2 h, the crude reaction was purified by flash chromatography with hexanes to afford 1,1,1,3,5,5,5-heptamethyl-3-octyltrisiloxane as a colorless oil (0.164 g, 0.491 mmol, 88%). ^1H NMR (400 MHz, CDCl_3) δ 1.35-1.23 (m, 12H), 0.88 (t, $J = 6.9$ Hz, 3H), 0.47-0.43 (m, 2H), 0.09 (s, 18H), -0.01 (s, 3H). ^{13}C NMR (101 MHz, CDCl_3) δ 33.4, 32.1, 29.5, 29.5, 23.3, 22.9, 17.8, 14.3, 2.0, -0.1. HRMS (EI), calc. for $\text{C}_{15}\text{H}_{38}\text{O}_2\text{Si}_3$ (M^+): 334.21797; found 334.21797.



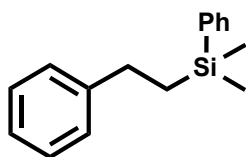
Trimethoxy(octyl)silane. Inside a drybox, a mixture of 1-octene (0.140 mmol), trimethoxysilane (0.140 mmol), and mesitylene internal standard (0.140 mmol) were taken up in C_6D_6 and added to a tared vial containing **1** (0.007 mmol) for a total volume of 3 mL. After 1 h of stirring at room temperature, an NMR aliquot was taken indicating 94% conversion to product. ^1H NMR spectroscopy data match literature values.³⁵



(2-(cyclohex-3-en-1-yl)ethyl)dimethyl(phenyl)silane (2a).

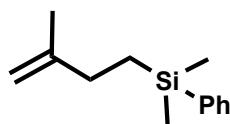
A modified form of the general procedure, whereby purification was conducted inside the glovebox, was followed using 4-vinyl-1-cyclohexene (0.558 mmol), dimethylphenylsilane (0.558 mmol), and benzene (3 mL). After 7 h, the crude reaction was purified by flash chromatography with hexanes to afford **2a** as a colorless oil (0.128 g, 0.525 mmol, 94%). ^1H NMR (500 MHz, CDCl_3) δ 7.57-7.53 (m, 2H), 7.40-7.37 (m, 3H), 5.70-5.67 (m, 2H), 2.15 (d, $J = 16.4$ Hz, 1H), 2.09-2.01 (m, 2H), 1.82-1.74 (m,

1H), 1.69-1.58 (m, 1H), 1.53-1.43 (m, 1H), 1.36-1.28 (m, 2H), 1.26-1.14 (m, 1H), 0.84-0.77 (m, 2H), 0.31 (s, 6H). ¹³C NMR (126 MHz, CDCl₃) δ 139.7, 133.7, 128.9, 127.9, 127.2, 126.8, 36.7, 31.8, 30.7, 28.7, 25.5, 12.8, -2.9. HRMS (EI), calc. for C₁₆H₂₃Si (M – H)⁺: 243.15691; found 243.15629.



dimethyl(phenethyl)(phenyl)silane (2d). The general procedure was followed using styrene (0.558 mmol), dimethylphenylsilane (0.558 mmol), and benzene (3 mL).

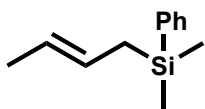
After 7 h, the crude reaction was purified by flash chromatography with hexanes to afford **2d** as a colorless oil (0.113 g, 0.469 mmol, 84%). ¹H NMR (500 MHz, CDCl₃) δ 7.56-7.51 (m, 2H), 7.39-7.34 (m, 3H), 7.28-7.23 (m, 2H), 7.20-7.15 (m, 3H), 2.69-2.60 (m, 2H), 1.19-1.08 (m, 2H), 0.30 (s, 6H). ¹³C NMR (126 MHz, CDCl₃) δ 145.1, 139.2, 133.7, 129.1, 128.4, 127.9, 127.9, 125.7, 30.1, 17.9, -2.9. HRMS (EI), calc. for C₁₅H₁₇Si (M – CH₃)⁺: 225.1100; found 225.1097.



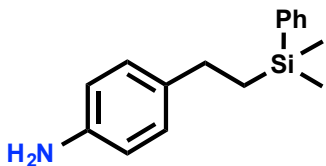
dimethyl(3-methylbut-3-en-1-yl)(phenyl)silane (2e). A modified procedure was followed using isoprene (1.116 mmol), dimethylphenylsilane (0.558 mmol), and benzene (3

mL). The reaction was conducted in a high pressure vessel and sealed following addition of the silane and olefin mixture to the catalyst. The sealed vessel was then taken outside of the glove box and heated to 70 °C for 17 h. The crude reaction was purified by flash chromatography with hexanes to afford **2e** as a colorless oil (0.086 g, 0.419 mmol, 75%). ¹H NMR (500 MHz, CDCl₃) δ 7.60 – 7.54 (m, 2H), 7.43 – 7.38 (m, 3H), 4.74 (s, 1H), 4.72 (s, 1H), 2.10 – 2.02 (m, 2H), 1.76

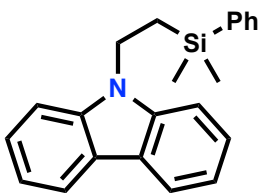
(s, 3H), 1.00 – 0.92 (m, 2H), 0.33 (s, 6H). ^{13}C NMR (126 MHz, CDCl_3) δ 148.5, 139.4, 133.7, 129.0, 127.9, 108.6, 32.0, 22.4, 13.9, -3.0. HRMS (EI), calc. for $\text{C}_{13}\text{H}_{20}\text{Si}$ (M^+): 204.1334; found 204.1331. IR: 1649 cm^{-1} (C=C).



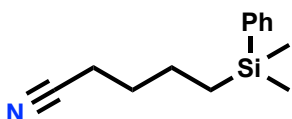
(E)-1-Dimethyl(phenyl)silylbut-2-ene. Inside a drybox, a mixture of 1,3-butadiene (0.335 mmol) and dimethylphenylsilane (0.140 mmol) were taken up in toluene and added to a tared vial containing **1** (0.007 mmol) for a total volume of 3 mL. After 1 h, the stirring was stopped, the vial was taken outside of the drybox, and volatiles were removed under reduced pressure. The residue was taken up in hexanes and filtered over a pipette filter containing silica. The filtrate was pumped down under vacuum to yield a clear oil. ^1H NMR spectroscopy data of the oil match literature values for the title compound.³⁶



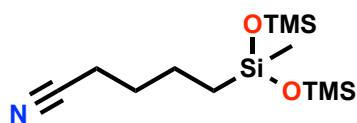
4-(2-(dimethyl(phenyl)silyl)ethyl)aniline (2f). The general procedure was followed using 4-vinylaniline (0.558 mmol), dimethylphenylsilane (0.558 mmol), and benzene (3 mL). After 25.5 h, the crude reaction was purified by flash chromatography using a solvent gradient with ethyl acetate/hexanes (v/v = 1:20 to v/v = 1:2) to afford **2f** as a light brown oil (0.088 g, 0.346 mmol, 62%). ^1H NMR (500 MHz, CDCl_3) δ 7.58-7.50 (m, 2H), 7.40-7.35 (m, 3H), 6.98 (d, J = 8.3 Hz, 2H), 6.62 (d, J = 8.3 Hz, 2H), 3.53 (s, 2H), 2.63-2.48 (m, 2H), 1.15-1.01 (m, 2H), 0.29 (s, 6H). ^{13}C NMR (126 MHz, CDCl_3) δ 144.1, 139.4, 135.3, 133.7, 129.0, 128.6, 127.9, 115.4, 29.1, 18.0, -2.9. HRMS (ES), calc. for $\text{C}_{16}\text{H}_{22}\text{NSi}$ ($\text{M} + \text{H}^+$): 256.1522; found 256.1524. IR: 3365 cm^{-1} , 3457 cm^{-1} (NH_2).



9-(2-(dimethyl(phenyl)silyl)ethyl)-9H-carbazole (2g). The general procedure was followed using 9-vinylcarbazole (0.558 mmol), dimethylphenylsilane (0.558 mmol), and benzene (3 mL). After 9 h, the crude reaction was purified by flash chromatography with ethyl acetate/hexanes (v/v = 1:50) to afford **2g** as a white solid (0.178 g, 0.541 mmol, 97%). ¹H NMR (400 MHz, CDCl₃) δ 8.15 (d, *J* = 7.6 Hz, 2H), 7.68 – 7.62 (m, 2H), 7.54 – 7.46 (m, 5H), 7.33 – 7.27 (m, 4H), 4.33-4.37 (m, 2H), 1.51 – 1.38 (m, 2H), 0.45 (s, 6H). ¹³C NMR (101 MHz, CDCl₃) δ 139.8, 137.9, 133.7, 129.5, 128.2, 125.6, 123.1, 120.5, 118.8, 108.6, 38.9, 16.2, -3.0. HRMS (ES), calc. for C₂₂H₂₃NSi (M⁺): 329.1600; found 329.1598.



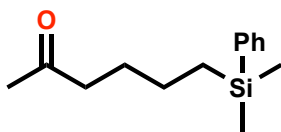
5-(dimethyl(phenyl)silyl)pentanenitrile (2h). The general procedure was followed using 4-pentenenitrile (0.558 mmol), dimethylphenylsilane (0.558 mmol), and benzene (3 mL). After 5.5 h, the crude reaction was purified by flash chromatography with ethyl acetate/hexanes (v/v = 1:20) to afford **2h** as a colorless oil (0.085 g, 0.391 mmol, 70%). ¹H NMR (500 MHz, CDCl₃) δ 7.53 – 7.48 (m, 2H), 7.39 – 7.34 (m, 3H), 2.31 (t, *J* = 7.2 Hz, 2H), 1.67 (tt, *J* = 7.3 Hz, 2H), 1.52 – 1.42 (m, 2H), 0.83 – 0.73 (m, 2H), 0.29 (s, 6H). ¹³C NMR (126 MHz, CDCl₃) δ 138.9, 133.6, 129.1, 128.0, 119.9, 29.0, 23.3, 16.9, 15.3, 13.3, -3.0. HRMS (EI), calc. for C₁₃H₁₉NSi (M⁺): 217.12868; found 217.12881. IR: 2246 cm⁻¹ (CN), 1725 cm⁻¹ (C=O) (aldehyde impurity ~4% by ¹H NMR spectroscopy).



5-(1,1,1,3,5,5,5-heptamethyltrisiloxan-3-yl)pentanenitrile

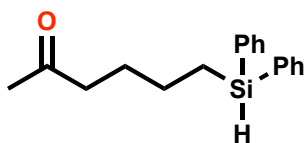
(3h). The general procedure was followed using 4-pentenenitrile (0.558 mmol), 1,1,1,3,5,5,5-

heptamethyltrisiloxane (0.558 mmol), and benzene (3 mL). After 24 h, the crude reaction was purified by flash chromatography with ethyl acetate/hexanes (v/v = 1:20) to afford **3h** as a pale yellow oil (0.125 g, 0.413 mmol, 68%). ¹H NMR (500 MHz, Chloroform-*d*) δ 2.33 (t, *J* = 7.2 Hz, 2H), 1.67 (tt, *J* = 7.3 Hz, 2H), 1.53 – 1.42 (m, 2H), 0.50 – 0.43 (m, 2H), 0.09 (s, 18H), 0.01 (s, 3H). ¹³C NMR (126 MHz, CDCl₃) δ 119.9, 28.6, 22.5, 16.9, 2.0, 1.8, -0.2. HRMS (EI), calc. for C₁₂H₂₉O₂NSi₃ (M)⁺: 303.1506; found 303.1499. IR: 2248 cm⁻¹ (w) (CN)



6-(dimethyl(phenyl)silyl)hexan-2-one (2j). The general procedure was followed using 5-hexen-2-one (0.558 mmol),

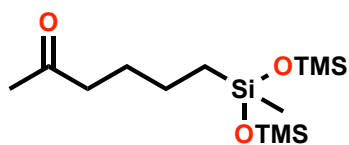
dimethylphenylsilane (0.558 mmol), and benzene (3 mL). After 2 h, the crude reaction was purified by flash chromatography with ethyl acetate/hexanes (v/v = 1:20) to afford **2j** as a colorless oil (0.127 g, 0.541 mmol, 97%). ¹H NMR (500 MHz, CDCl₃) δ 7.52-7.48 (m, 2H), 7.38-7.33 (m, 3H), 2.39 (t, *J* = 7.5 Hz, 2H), 2.11 (s, 3H), 1.59 (tt, *J* = 7.5 Hz, 2H), 1.38-1.26 (m, 2H), 0.77-0.73 (m, 2H), 0.26 (s, 6H). ¹³C NMR (126 MHz, CDCl₃) δ 209.4, 139.5, 133.7, 129.0, 127.9, 43.6, 30.0, 27.8, 23.7, 15.8, -3.0. HRMS (ES), calc. for C₁₄H₂₂O₂SiNa (M + Na)⁺: 257.1338; found 257.1337. IR: 1715 cm⁻¹ (C=O).



6-(diphenylsilyl)hexan-2-one (2j-Ph₂). The general

procedure was followed using 5-hexen-2-one (0.558 mmol), dimethylphenylsilane (0.558 mmol), and benzene (3 mL). After 2 h, the crude reaction was

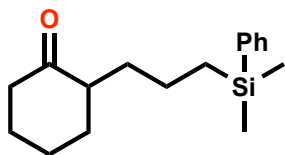
purified by flash chromatography with ethyl acetate/hexanes (v/v = 1:10) to afford **2j-Ph₂** as a colorless oil (0.136 g, 0.480 mmol, 86%). ¹H NMR (500 MHz, CDCl₃) δ 7.59-7.53 (m, 4H), 7.43-7.34 (m, 6H), 4.86 (t, *J* = 3.5 Hz, 1H), 2.40 (t, *J* = 7.4 Hz, 2H), 2.10 (s, 3H), 1.66 (tt, *J* = 7.6, 2H), 1.50-1.43 (m, *J* = 9.5, 6.6 Hz, 2H), 1.18-1.14 (m, 2H). ¹³C NMR (126 MHz, CDCl₃) δ 209.2, 135.2, 134.4, 129.7, 128.1, 43.5, 30.0, 27.4, 24.2, 12.2. HRMS (EI), calc. for C₁₈H₂₁OSi (M - H)⁺: 281.1362; found 281.1357. IR: 1714 cm⁻¹ (C=O), 2113 cm⁻¹ (Si-H).



6-(1,1,1,3,5,5,5-heptamethyltrisiloxan-3-yl) hexan-2-one

(3j). The general procedure was followed using 5-hexen-2-one (0.558 mmol), 1,1,1,3,5,5,5-heptamethyltrisiloxane (0.558

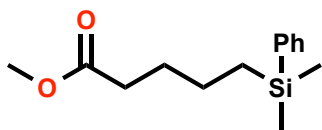
mmol), and benzene (3 mL). After 5 h, the crude reaction was purified by flash chromatography with ethyl acetate/hexanes (v/v = 1:20) to afford **3j** as a pale yellow oil (0.168 g, 0.525 mmol, 94%). ¹H NMR (500 MHz, Chloroform-*d*) δ 2.40 (t, *J* = 7.5 Hz, 2H), 2.12 (s, 3H), 1.58 (tt, *J* = 7.5 Hz, 2H), 1.36-1.26 (m, 2H), 0.49-0.41 (m, 2H), 0.07 (s, 18H), -0.02 (s, 3H). ¹³C NMR (126 MHz, CDCl₃) δ 209.4, 43.7, 30.0, 27.5, 22.9, 17.6, 2.0, -0.2. HRMS (ES), calc. for C₁₃H₃₂O₃Si₃Na (M + Na)⁺: 343.1557; found 343.1545. IR: 1719 cm⁻¹ (C=O).



2-(3-(dimethyl(phenyl)silyl)propyl)cyclohexan-1-one (2k).

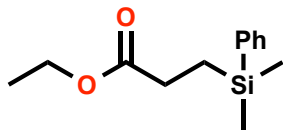
The general procedure was followed using 2-allylcyclohexanone (0.558 mmol), dimethylphenylsilane (0.558 mmol), and benzene (3 mL). After 2.5 h, the crude reaction was purified by flash chromatography with ethyl acetate/hexanes (v/v = 1:20) to afford **2k** as a pale yellow oil (0.144 g, 0.525 mmol, 94%). ¹H NMR (500 MHz, CDCl₃) δ 7.52-7.47 (m, 2H), 7.37-7.32 (m, 3H), 2.39-

2.34 (m, 1H), 2.31-2.21 (m, 2H), 2.09-1.96 (m, 2H), 1.89-1.76 (m, 2H), 1.73-1.53 (m, 2H), 1.41-1.26 (m, 3H), 1.24-1.17 (m, 1H), 0.82-0.66 (m, 2H), 0.25 (s, 6H). ^{13}C NMR (126 MHz, CDCl_3) δ 213.7, 139.7, 133.7, 128.9, 127.8, 50.6, 42.1, 34.0, 33.4, 28.2, 25.0, 21.7, 16.0, -2.9. HRMS (ES), calc. for $\text{C}_{17}\text{H}_{26}\text{ONaSi}$ ($\text{M} + \text{Na}$) $^+$: 297.1651; found 297.1649. IR: 1709 cm^{-1} (C=O).



methyl 5-(dimethyl(phenyl)silyl)pentanoate (2l). The general procedure was followed using methyl 4-pentenoate (0.558 mmol), dimethylphenylsilane (0.558 mmol), and benzene (3

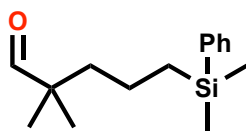
mL). After 2 h, the crude reaction was purified by flash chromatography with ethyl acetate/hexanes (v/v = 1:20) to afford **2l** as a colorless oil (0.129 g, 0.513 mmol, 92%). ^1H NMR (500 MHz, CDCl_3) δ 7.52-7.48 (m, 2H), 7.37-7.33 (m, 3H), 3.65 (s, 3H), 2.29 (t, $J = 7.5$ Hz, 2H), 1.65 (tt, $J = 7.4$ Hz, 2H), 1.40-1.30 (m, 2H), 0.80-0.72 (m, 2H), 0.26 (s, 6H). ^{13}C NMR (126 MHz, CDCl_3) δ 174.4, 139.4, 133.7, 129.0, 127.9, 51.6, 33.9, 28.8, 23.7, 15.6, -2.9. HRMS (EI), calc. for $\text{C}_{13}\text{H}_{19}\text{O}_2\text{Si}$ ($\text{M} - \text{CH}_3$) $^+$: 235.1154; found 235.1153. IR: 1738 cm^{-1} (C=O).



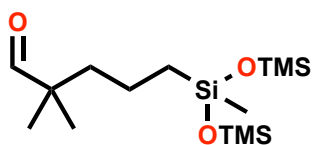
ethyl 3-(dimethyl(phenyl)silyl)propanoate (2m). The general procedure was followed using ethyl acrylate (0.558

mmol), dimethylphenylsilane (0.558 mmol), and benzene (3 mL). After 3 h, the crude reaction was purified by flash chromatography with ethyl acetate/hexanes (v/v = 1:10) to afford **2m** as a pale yellow oil (0.125 g, 0.530 mmol, 95%). ^1H NMR (400 MHz, CDCl_3) δ 7.58 – 7.44 (m, 2H), 7.41 – 7.31 (m, 3H), 4.08 (q, $J = 7.1$ Hz, 2H), 2.37 – 2.15 (m, 2H), 1.23 (t, $J = 7.1$ Hz, 3H), 1.13 – 1.05 (m, 2H), 0.29 (s, 6H). ^{13}C NMR (101 MHz, CDCl_3) δ 175.1, 138.3, 133.7, 129.2, 128.0, 60.5, 29.0, 14.4, 11.0, -3.2. HRMS (ES), calc. for $\text{C}_{13}\text{H}_{20}\text{O}_2\text{NaSi}$ ($\text{M} + \text{Na}$) $^+$: 259.1130; found 259.1126. IR:

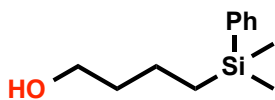
1733 cm^{-1} (C=O).



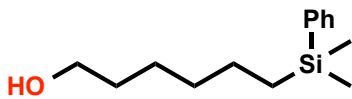
5-(dimethyl(phenyl)silyl)-2,2-dimethylpentanal (2n). The general procedure was followed using 2,2-dimethyl-4-pentenal (0.558 mmol), dimethylphenylsilane (0.558 mmol), and benzene (3 mL). After 4.5 h, the crude reaction was purified by flash chromatography with ethyl acetate/hexanes (v/v = 1:20) to afford **2n** as a pale yellow oil (0.121 g, 0.485 mmol, 87%). ^1H NMR (400 MHz, CDCl_3) δ 9.42 (s, 1H), 7.62-7.45 (m, 3H), 7.44-7.30 (m, 5H), 1.57-1.41 (m, 3H), 1.34-1.17 (m, 3H), 1.02 (s, 6H), 0.80-0.67 (m, 3H), 0.26 (s, 6H). ^{13}C NMR (101 MHz, CDCl_3) δ 206.6, 139.3, 133.6, 129.0, 127.9, 46.2, 41.5, 21.4, 18.9, 16.6, -2.9. HRMS (EI), calc. for $\text{C}_{15}\text{H}_{23}\text{OSi}$ ($\text{M} - \text{H}$) $^+$: 247.15183; found 247.15175. IR: 1727 cm^{-1} (C=O).



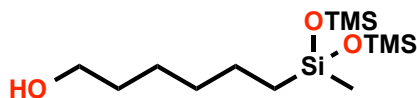
5-(1,1,1,3,5,5,5-heptamethyltrisiloxan-3-yl)-2,2-dimethylpentanal (3n). The general procedure was followed using 2,2-dimethyl-4-pentenal (0.558 mmol), 1,1,1,3,5,5,5-heptamethyltrisiloxane (0.558 mmol), and benzene (3 mL). After 7 h, the crude reaction was purified by flash chromatography with ethyl acetate/hexanes (v/v = 1:20) to afford **3n** as a colorless oil (0.149 g, 0.446 mmol, 80%). ^1H NMR (500 MHz, Chloroform-*d*) δ 9.44 (s, 1H), 1.53 – 1.42 (m, 2H), 1.29 – 1.16 (m, 5H), 1.03 (s, 6H), 0.47 – 0.38 (m, 2H), 0.07 (s, 18H), -0.02 (s, 3H). ^{13}C NMR (126 MHz, CDCl_3) δ 206.56, 46.17, 41.18, 21.41, 18.14, 2.01, -0.07. HRMS (ES), calc. for $\text{C}_{14}\text{H}_{34}\text{O}_3\text{Si}_3\text{Na}$ ($\text{M} + \text{Na}$) $^+$: 357.1713; found 357.1706. IR: 1730 cm^{-1} (C=O).



4-(dimethyl(phenyl)silyl)butan-1-ol (2o). The general procedure was followed using 3-buten-1-ol (0.558 mmol), dimethylphenylsilane (0.558 mmol), and 1,4-dioxane (3 mL). After 3.33 h, the crude reaction was purified by flash chromatography with a solvent gradient of ethyl acetate/hexanes (v/v = 1:10 to v/v = 1:2) to afford **2o** as a pale yellow oil (0.110 g, 0.530 mmol, 95%). ¹H NMR (500 MHz, CDCl₃) δ 7.54-7.48 (m, 2H), 7.38 – 7.33 (m, 3H), 3.62 (t, *J* = 6.4 Hz, 2H), 1.59 (tt, *J* = 6.9 Hz, 2H), 1.46-1.35 (m, 2H), 1.22 (s, 1H), 0.82 – 0.72 (m, 2H), 0.27 (s, 6H). ¹³C NMR (126 MHz, CDCl₃) δ 139.5, 133.7, 129.0, 127.9, 62.8, 36.7, 20.3, 15.7, -2.9. HRMS (ES), calc. for C₁₂H₂₀ONaSi (M + Na)⁺: 231.1181; found 231.1181. IR: 3328 cm⁻¹ (O–H).

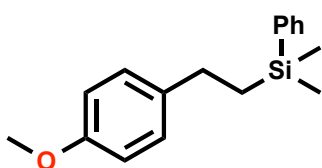


6-(dimethyl(phenyl)silyl)hexan-1-ol (2p). The general procedure was followed using 5-hexen-1-ol (0.558 mmol), dimethylphenylsilane (0.558 mmol), and 1,4-dioxane (3 mL). After 3 h, the crude reaction was purified by flash chromatography with ethyl acetate/hexanes (v/v = 1:10) to afford **2p** as a colorless oil (0.099 g, 0.419 mmol, 75%). ¹H NMR (500 MHz, CDCl₃) δ 7.57-7.49 (m, 2H), 7.40-7.34 (m, 3H), 3.67-3.56 (m, 2H), 1.58-1.52 (m, 2H), 1.52-1.49 (m, 1H), 1.35 (s, 7H), 0.81-0.74 (m, 2H), 0.28 (s, 6H). ¹³C NMR (126 MHz, CDCl₃) δ 139.7, 133.7, 128.9, 127.8, 63.1, 33.4, 32.8, 25.5, 23.9, 15.8, -2.9. HRMS (EI), calc. for C₁₃H₂₁OSi (M – CH₃)⁺: 221.1362; found 221.1354. IR: 3323 cm⁻¹ (O–H).

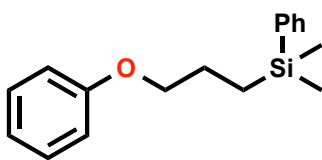


6-(1,1,1,3,5,5,5-heptamethyltrisiloxan-3-yl)hexan-1-ol (3p). The general procedure was followed using 5-hexen-1-ol (0.558 mmol), 1,1,1,3,5,5,5-heptamethyltrisiloxane (0.558 mmol), and 1,4-dioxane (3 mL). After 5 h, the

crude reaction was purified by flash chromatography with ethyl acetate/hexanes (v/v = 1:10) to afford **3p** as a pale yellow oil (0.133 g, 0.413 mmol, 74%). ^1H NMR (500 MHz, CDCl_3) δ 3.63 (t, $J = 6.7$ Hz, 2H), 1.61-1.52 (m, 2H), 1.38-1.30 (m, 7H), 0.49-0.41 (m, 2H), 0.08 (s, 18H), -0.01 (s, 3H). ^{13}C NMR (126 MHz, CDCl_3) δ 63.2, 33.2, 32.9, 25.6, 23.2, 17.7, 2.0, -0.1. HRMS (ES), calc. for $\text{C}_{13}\text{H}_{34}\text{O}_3\text{Si}_3\text{Na}$ ($\text{M} + \text{Na}$) $^+$: 345.1714; found 345.1722. IR: 3341 cm^{-1} (O-H).

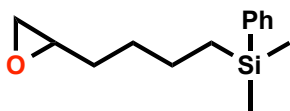


(4-methoxyphenethyl)dimethyl(phenyl)silane (2q). The general procedure was followed using 4-vinylanisole (0.558 mmol), dimethylphenylsilane (0.558 mmol), and benzene (3 mL). After 7 h, the crude reaction was purified by flash chromatography with ethyl acetate/hexanes (v/v = 3:40) to afford **2q** as a colorless oil (0.148 g, 0.547 mmol, 98%). ^1H NMR (500 MHz, CDCl_3) δ 7.65 – 7.58 (m, 2H), 7.49 – 7.40 (m, 3H), 7.20 – 7.13 (m, 2H), 6.92 – 6.85 (m, 2H), 3.84 (s, 3H), 2.73 – 2.62 (m, 2H), 1.25 – 1.14 (m, 2H), 0.36 (s, 6H). ^{13}C NMR (126 MHz, CDCl_3) δ 157.7, 139.2, 137.2, 133.7, 129.0, 128.7, 127.9, 113.8, 55.4, 29.2, 18.1, -2.9. HRMS (EI), calc. for $\text{C}_{17}\text{H}_{22}\text{OSi}$ (M^+) $^+$: 270.1440; found 270.1438.



dimethyl(3-phenoxypropyl)(phenyl)silane (2r). The general procedure was followed using allyl phenyl ether (0.558 mmol), dimethylphenylsilane (0.558 mmol), and benzene (3 mL). After 1.5 h, the crude reaction was purified by flash chromatography with ethyl acetate/hexanes (v/v = 1:20) to afford **2r** as a colorless oil (0.149 g, 0.552 mmol, 99%). ^1H NMR (500 MHz, CDCl_3) δ 7.61 – 7.54 (m, 2H), 7.43 – 7.36 (m, 3H), 7.34 – 7.27 (m, 2H), 6.99 – 6.93 (m, 1H), 6.93 – 6.87 (m, 2H), 3.94 (t, $J = 6.8$ Hz, 2H), 1.90 – 1.80 (m, 2H), 0.96 – 0.87 (m, 2H), 0.35 (s, 6H).

^{13}C NMR (126 MHz, CDCl_3) δ 159.2, 139.1, 133.7, 129.5, 129.1, 127.9, 120.6, 114.6, 70.5, 24.0, 11.9, -3.0. HRMS (ES), calc. for $\text{C}_{17}\text{H}_{22}\text{ONaSi}$ ($\text{M} + \text{Na}$) $^+$: 293.1338; found 293.1344.



dimethyl(4-(oxiran-2-yl)butyl)(phenyl)silane (2s). The

general procedure was followed using 1,2-epoxy-5-hexene (0.558 mmol), dimethylphenylsilane (0.558 mmol), and benzene (3 mL). After 1.5 h, the crude reaction was purified by flash chromatography with ethyl acetate/hexanes ($v/v = 1:20$) to afford **2s** as a pale yellow oil (0.106 g, 0.452 mmol, 81%). ^1H NMR (500 MHz, CDCl_3) δ 7.56 – 7.48 (m, 2H), 7.39 – 7.33 (m, 3H), 2.90-2.85 (m, 1H), 2.73 (t, $J = 4.19$ Hz, 1H), 2.45-2.42 (m, 1H), 1.58 – 1.33 (m, 6H), 0.82 – 0.70 (m, 2H), 0.27 (s, 6H). ^{13}C NMR (126 MHz, CDCl_3) δ 139.6, 133.7, 128.9, 127.9, 52.5, 47.3, 32.3, 29.9, 23.9, 15.8, -2.9. HRMS (ES), calc. for $\text{C}_{14}\text{H}_{22}\text{ONaSi}$ ($\text{M} + \text{Na}$) $^+$: 257.1338; found 257.1335.

^1H NMR monitoring of the reaction of **1** with PhSiH_3

To a frozen solution of the catalyst ($^{\text{DIPP}}\text{CCC})\text{CoN}_2$ (**1**) (0.020 g, 0.0705 mmol) in 0.5 mL of C_6D_6 , was added PhSiH_3 (0.009 g, 0.106 mmol). The reaction was monitored in a screw-top NMR tube following thawing by ^1H NMR spectroscopy.

Synthesis of ($^{\text{DIPP}}\text{CCC})\text{Co}(\text{SiHPh}_2)(\text{H})(\text{N}_2)$ (4**).** A 20 mL scintillation vial was charged with diphenylsilane and taken up in ca. 0.5 mL of deuterated benzene. The resulting dark brown solution was added to a J. Young NMR tube bearing the catalyst **1** (0.020 g, 0.0705 mmol) and analyzed by ^1H and ^{29}Si NMR spectroscopy. ^1H NMR (600 MHz, C_6D_6) δ 7.44 (d, $J = 7.8$ Hz), 7.31 (s, 1H), 7.03 (d, $J = 4.4$ Hz), 7.00 (d, $J = 7.8$ Hz), 6.80 (m), 6.73 (t, $J = 7.2$ Hz), 6.48 (d, $J = 8.0$ Hz), 5.52

(s), 3.42 (sept, $J = 6.7$ Hz), 2.21 (sept, $J = 6.7$ Hz), 1.50 (d, $J = 6.7$ Hz), 1.11 (d, $J = 6.8$ Hz), 0.94 (d, $J = 6.8$ Hz), 0.63 (d, $J = 6.8$ Hz), -7.08 (s, 1H). T_1 (min, 293 K, 500 MHz) of resonance at -7.08 ppm: 148 ms. ^{29}Si NMR (600 MHz, C_6D_6) δ 8.28. IR: 2280 cm^{-1} , 2268 cm^{-1} .

^1H NMR of unreacted **1**² (500 MHz, C_6D_6) δ 7.63 (d, $J = 7.5$ Hz), 7.32 (d, $J = 7.0$ Hz), 7.29 – 7.23 (m), 7.20 (t, $J = 7.5$ Hz), 7.11 (d, $J = 7.5$ Hz), 7.04 (t, $J = 7.5$ Hz), 6.86 (t, $J = 7.5$ Hz), 6.55 (d, $J = 8.0$ Hz), 2.71 (sept, $J = 6.8$ Hz), 1.26 (d, $J = 6.5$ Hz), 0.87 (d, $J = 6.5$ Hz).

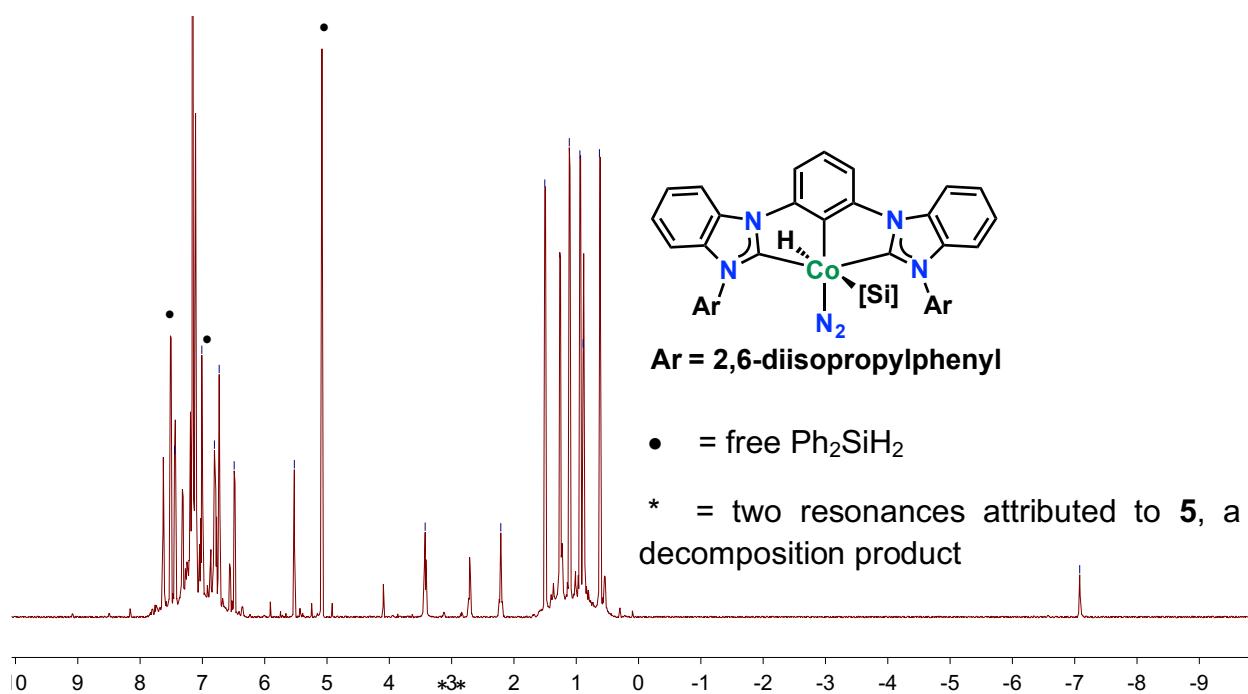


Figure 3.2 ^1H NMR spectrum of **4** in C_6D_6

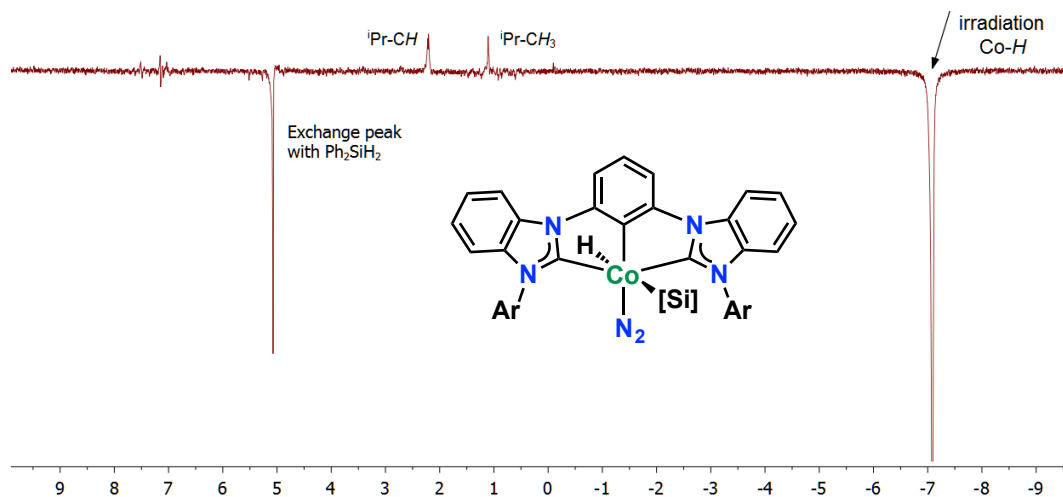


Figure 3.3 NOE ^1H NMR spectrum of **4**

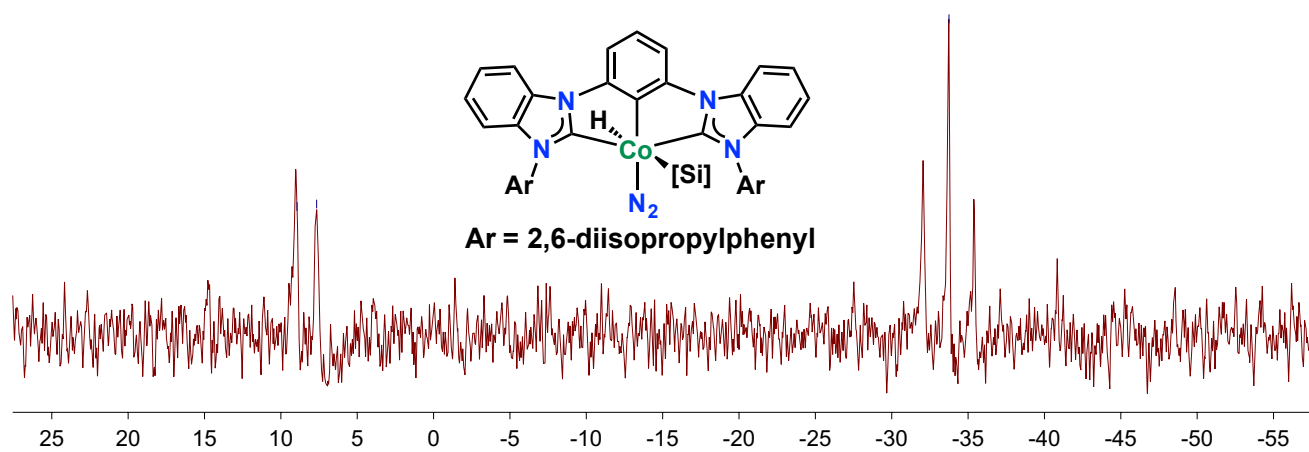


Figure 3.4 ^1H -coupled ^{29}Si NMR spectrum of **4**

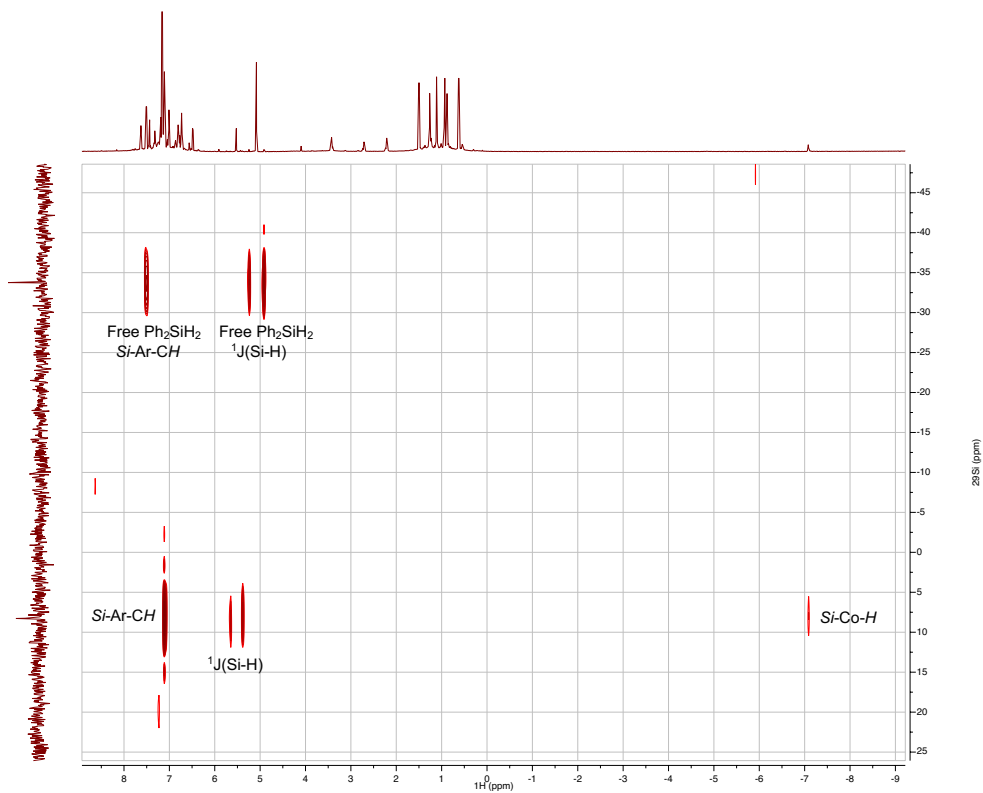


Figure 3.5 $^{29}\text{Si} - ^1\text{H}$ HMBC NMR spectrum of **4**

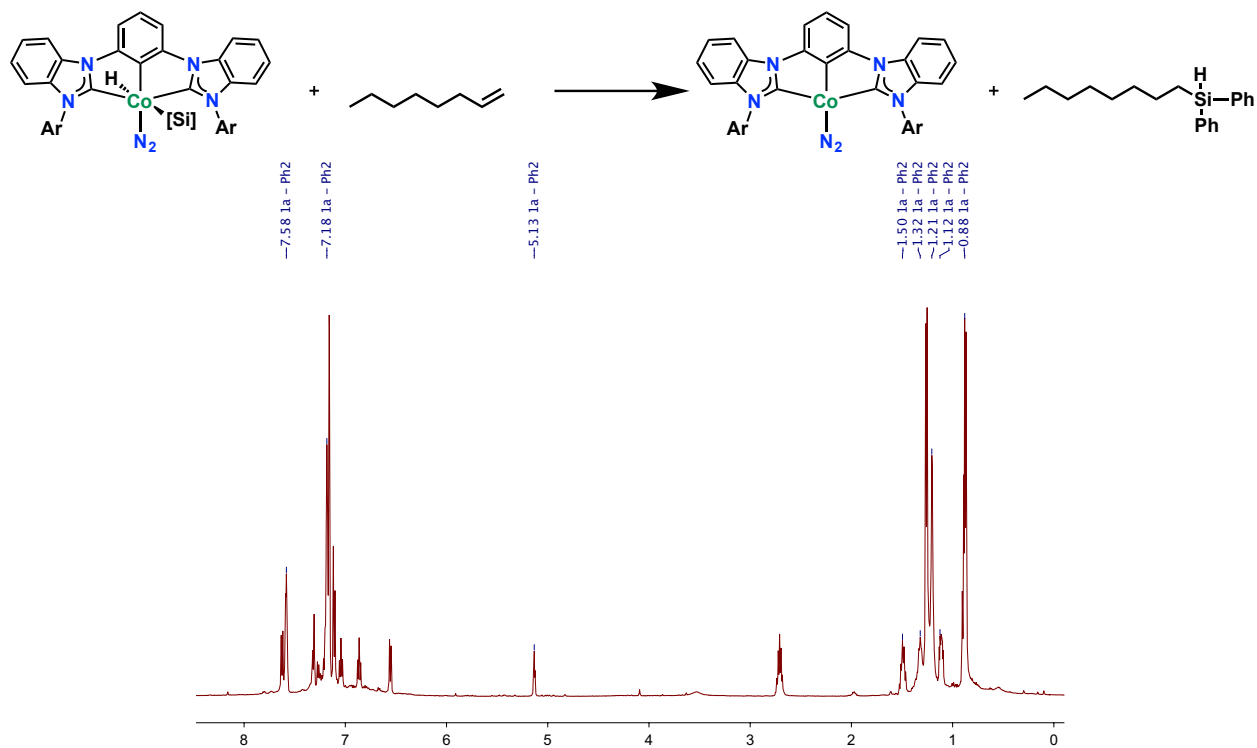


Figure 3.6 ^1H NMR spectrum of the reaction of **4** with 1-octene

Synthesis of (^{DIPP}CCC)Co(SiHPh₂)₂(N₂) (5). A 20 mL scintillation vial was charged with Ph₂SiH₂ (0.013 g, 0.0705 mmol) and transferred to a separate vial containing **1**² (0.025 g, 0.0349 mmol) using C₆H₆ (ca. 3 mL). The resulting red-purple reaction mixture was stirred at room temperature for 1 h. Following completion of the stir time, the solvent was removed under reduced pressure and the remaining solid residue was dissolved in diethyl ether before being filtered over a plug of Celite. Additional solvent was added to the plug as needed until the washes were virtually colorless. The filtrate was, in turn, cooled at -35 °C at least overnight to yield crystalline material suitable for X-ray diffraction. The mother liquor was then decanted and the remaining yellow material was dried *in vacuo* prior to analysis by ¹H NMR spectroscopy in C₆D₆ solvent. Both compounds **1** and **4** (NMR data listed below) are present in the material. HRMS (ES), calc. for C₆₈H₆₈CoN₄Si₂ (M – N₂)⁺: 1054.4236; found 1054.4253.

¹H NMR of **4** (600 MHz, C₆D₆) δ 7.44 (d, *J* = 7.8 Hz), 7.31 (s, 1H), 7.03 (d, *J* = 4.4 Hz), 7.00 (d, *J* = 7.8 Hz), 6.80 (m), 6.73 (t, *J* = 7.2 Hz), 6.48 (d, *J* = 8.0 Hz), 5.52 (s), 3.42 (sept, *J* = 6.7 Hz), 2.21 (sept, *J* = 6.7 Hz), 1.50 (d, *J* = 6.7 Hz), 1.11 (d, *J* = 6.8 Hz), 0.94 (d, *J* = 6.8 Hz), 0.63 (d, *J* = 6.8 Hz), -7.08 (s, 1H).

¹H NMR of unreacted **1**² (500 MHz, C₆D₆) δ 7.63 (d, *J* = 7.5 Hz), 7.32 (d, *J* = 7.0 Hz), 7.29 – 7.23 (m), 7.20 (t, *J* = 7.5 Hz), 7.11 (d, *J* = 7.5 Hz), 7.04 (t, *J* = 7.5 Hz), 6.86 (t, *J* = 7.5 Hz), 6.55 (d, *J* = 8.0 Hz), 2.71 (sept, *J* = 6.8 Hz), 1.26 (d, *J* = 6.5 Hz), 0.87 (d, *J* = 6.5 Hz).

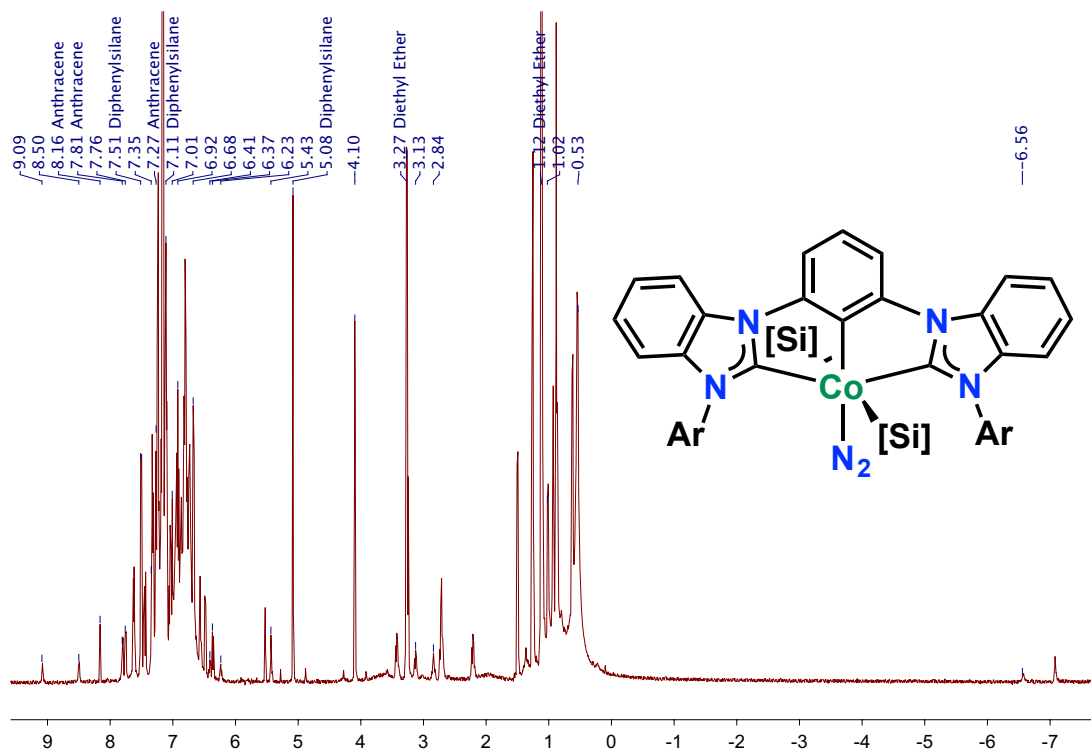


Figure 3.7 ^1H NMR spectrum of **5**

Table 3.4 Crystallographic Parameters for complex **5**

	(^{DIPP} CCC)Co(SiHPh ₂) ₂ (N ₂) (5)
Empirical formula	C ₇₆ H ₈₇ CoN ₆ O ₂ Si ₂
Formula weight	1231.62
Temperature (K)	100.15
Wavelength (Å)	0.71073
Crystal system	monoclinic
Space group	P2 ₁
Unit Cell Dimensions	
a (Å)	12.1686(4)
b (Å)	15.7163(5)
c (Å)	17.6104(6)
α (°)	90
β (°)	100.7617(11)
γ (°)	90
Volume (Å ³)	3308.67(19)
Z	2
Reflections collected	73761
Independent reflections	14756 [R _{int} = 0.0346]
Goodness-of-fit on F ²	1.041
Final R indexes [I >= 2σ (I)]	R ₁ = 0.0276, wR ₂ = 0.0708
Final R indexes [all data]	R ₁ = 0.0295, wR ₂ = 0.0737

Table 3.5 Select bond distances and bond angles for **5**

	(^{DIPP} CCC)Co(SiHPh ₂) ₂ (N ₂)
Bond Distances	
Co – Si1	2.3507(7)
Co – Si2	2.3467(7)
Co – C1	1.940(2)
Co – C20	1.948(2)
Co – C13	1.866(2)
Co – N5	1.8401(19)
N5 – N6	1.102(3)
Bond Angles (°)	
C1-Co-C20	160.19(9)
C13-Co-N5	179.62(10)
Si1-Co-Si2	166.26(2)

3.5 References

1. Marciniak, B. *Hydrosilylation: A Comprehensive Review on Recent Advances*. (Springer, 2009).
2. Tamao, K., Ishida, N., Tanaka, T. & Kumada, M. Silafunctional compounds in organic synthesis. Part 20. Hydrogen peroxide oxidation of the silicon-carbon bond in organoalkoxysilanes. *Organometallics* **2**, 1694–1696 (1983).
3. Fleming, I., Henning, R. & Plaut, H. The phenyldimethylsilyl group as a masked form of the hydroxy group. *J. Chem. Soc. Chem. Commun.* 29–31 (1984).
4. *Catalysis without Precious Metals*. (Wiley-VCH Verlag GmbH & Co. KGaA, 2010). doi:10.1002/9783527631582
5. Noda, D., Tahara, A., Sunada, Y. & Nagashima, H. Non-Precious-Metal Catalytic Systems Involving Iron or Cobalt Carboxylates and Alkyl Isocyanides for Hydrosilylation of Alkenes with Hydrosiloxanes. *J. Am. Chem. Soc.* **138**, 2480–2483 (2016).
6. Tondreau, A. M. *et al.* Iron catalysts for selective anti-Markovnikov alkene hydrosilylation using tertiary silanes. *Science* **335**, 567–70 (2012).
7. Bart, S. C., Lobkovsky, E. & Chirik, P. J. Preparation and molecular and electronic structures of iron(0) dinitrogen and silane complexes and their application to catalytic hydrogenation and hydrosilation. *J. Am. Chem. Soc.* **126**, 13794–807 (2004).
8. Peng, D. *et al.* Phosphinite-iminopyridine iron catalysts for chemoselective alkene hydrosilylation. *J. Am. Chem. Soc.* **135**, 19154–19166 (2013).
9. Greenhalgh, M. D., Frank, D. J. & Thomas, S. P. Iron-Catalysed Chemo-, Regio-, and Stereoselective Hydrosilylation of Alkenes and Alkynes using a Bench-Stable Iron(II) Pre-Catalyst. *Adv. Synth. Catal.* **356**, 584–590 (2014).
10. Wu, J. Y., Stanzl, B. N. & Ritter, T. A strategy for the synthesis of well-defined iron catalysts and application to regioselective diene hydrosilylation. *J. Am. Chem. Soc.* **132**, 13214–13216 (2010).
11. Noda, D., Tahara, A., Sunada, Y. & Nagashima, H. Non-Precious-Metal Catalytic Systems Involving Iron or Cobalt Carboxylates and Alkyl Isocyanides for Hydrosilylation of Alkenes with Hydrosiloxanes. *J. Am. Chem. Soc.* jacs.5b11311 (2016). doi:10.1021/jacs.5b11311
12. Kuznetsov, A. & Gevorgyan, V. General and Practical One-Pot Synthesis of Dihydrobenzosiloles from Styrenes. *Org. Lett.* **14**, 914–917 (2012).
13. Steiman, T. J. & Uyeda, C. Reversible substrate activation and catalysis at an intact metal-metal bond using a redox-active supporting ligand. *J. Am. Chem. Soc.* **137**, 6104–6110 (2015).
14. Lipschutz, M. I. & Tilley, T. D. Synthesis and reactivity of a conveniently prepared two-

- coordinate bis(amido) nickel(II) complex. *Chem. Commun. (Camb)*. **48**, 7146–8 (2012).
15. Chen, C. *et al.* Rapid, Regioconvergent, Solvent-Free Alkene Hydrosilylation with a Cobalt Catalyst. *J. Am. Chem. Soc.* **137**, 13244–13247 (2015).
 16. Buslov, I., Becoue, J., Mazza, S., Montandon-Clerc, M. & Hu, X. Chemoselective Alkene Hydrosilylation Catalyzed by Nickel Pincer Complexes. *Angew. Chemie* **54**, 14523–14526 (2015).
 17. Schuster, C. H., Diao, T., Pappas, I. & Chirik, P. J. Bench-Stable, Substrate-Activated Cobalt Carboxylate Pre-Catalysts for Alkene Hydrosilylation with Tertiary Silanes. *ACS Catal.* **6**, 2632–2636 (2016).
 18. Ibrahim, A. D. *et al.* Monoanionic bis(carbene) pincer complexes featuring cobalt(I–III) oxidation states. *Dalt. Trans.* **45**, 9805–9811 (2016).
 19. Brookhart, M. & Grant, B. E. Mechanism of a cobalt(III)-catalyzed olefin hydrosilation reaction: direct evidence for a silyl migration pathway. *J. Am. Chem. Soc.* **115**, 2151–2156 (1993).
 20. Sun, J. & Deng, L. Cobalt Complex-Catalyzed Hydrosilylation of Alkenes and Alkynes. *ACS Catal.* **6**, 290–300 (2016).
 21. Hilt, G., Lüers, S. & Schmidt, F. Cobalt(I)-Catalyzed Diels-Alder, 1,4-Hydrovinylation and 1,4-Hydrosilylation Reactions of Non-Activated Starting Materials on a Large Scale. *Synthesis (Stuttg)*. **2004**, 634–638 (2004).
 22. Ratcha, A. *et al.* Polyisoprene modified poly(alkyl acrylate) foam as oil sorbent material. *J. Appl. Polym. Sci.* **132**, 42688 (2015).
 23. Parker, S. E., Börgel, J. & Ritter, T. 1,2-selective hydrosilylation of conjugated dienes. *J. Am. Chem. Soc.* **136**, 4857–4860 (2014).
 24. Swisher, J. V. & Zullig, C. Stereochemistry of methyldichlorosilane additions to pentadienes. *J. Org. Chem.* **38**, 3353–3357 (1973).
 25. United States Patent Application: 0140330024. Available at: <http://appft1.uspto.gov/netacgi/nph-Parser?Sect1=PTO1&Sect2=HITOFF&d=PG01&p=1&u=/netahtml/PTO/srchnum.html&r=1&f=G&l=50&s1='20140330024'.PGNR.&OS=DN/20140330024&RS=DN/20140330024>. (Accessed: 14th April 2016)
 26. Huckaba, A. J., Hollis, T. K. & Reilly, S. W. Homobimetallic Rhodium NHC Complexes as Versatile Catalysts for Hydrosilylation of a Multitude of Substrates in the Presence of Ambient Air. *Organometallics* **32**, 6248–6256 (2013).
 27. Sabourault, N., Mignani, G., Wagner, A. & Mioskowski, C. Platinum Oxide (PtO₂): A Potent Hydrosilylation Catalyst. *Org. Lett.* **4**, 2117–2119 (2002).
 28. Mark, I. E. *et al.* Highly Active and Selective Platinum(0)-Carbene Complexes. Efficient,

- Catalytic Hydrosilylation of Functionalised Olefins. *Adv. Synth. Catal.* **346**, 1429–1434 (2004).
29. Takeuchi, R., Nitta, S. & Watanabe, D. Cationic rhodium complex-catalysed highly selective hydrosilylation of propynylic alcohols: a convenient synthesis of (E)- γ -silyl allylic alcohols. *J. Chem. Soc., Chem. Commun.* 1777–1778 (1994).
 30. Rozenel, S. S., Padilla, R. & Arnold, J. Chemistry of reduced monomeric and dimeric cobalt complexes supported by a PNP pincer ligand. *Inorg. Chem.* **52**, 11544–11550 (2013).
 31. Scheuermann, M. L., Semproni, S. P., Pappas, I. & Chirik, P. J. Carbon dioxide hydrosilylation promoted by cobalt pincer complexes. *Inorg. Chem.* **53**, 9463–9465 (2014).
 32. Troegel, D. & Stohrer, J. Recent advances and actual challenges in late transition metal catalyzed hydrosilylation of olefins from an industrial point of view. *Coord. Chem. Rev.* **255**, 1440–1459 (2011).
 33. Karshtedt, D., Bell, A. T. & Tilley, T. D. Stoichiometric and Catalytic Reactions Involving Si–H Bond Activations by Rh and Ir Complexes Containing a Pyridylindolide Ligand. **25**, 4471–4482 (2006).
 34. Pangborn, A. B., Giardello, M. A., Grubbs, R. H., Rosen, R. K. & Timmers, F. J. Safe and Convenient Procedure for Solvent Purification. *Organometallics* **15**, 1518–1520 (1996).
 35. Brand, M. *et al.* NMR-spektroskopische untersuchungen zur hydrolyse von funktionellen trialkoxysilanen. *Zeitschrift fur Naturforsch. - Sect. B J. Chem. Sci.* **54**, 155–164 (1999).
 36. Fleming, I. *et al.* A regioselective and stereospecific synthesis of allylsilanes from secondary allylic alcohol derivatives. *J. Chem. Soc. Perkin Trans. 1* **96**, 3331–3349 (1992).

Chapter 4

Catalytic hydroboration with (^{DIPP}CCC)CoN₂: evidence for insertion, isomerization, and β-hydride elimination processes†

4.1 Introduction

Catalytic hydroboration is a powerful synthetic tool for the reduction and functionalization of unsaturated bonds, providing products that can serve as valuable synthons in a variety of chemical transformations. The widely-employed Suzuki-Miyaura coupling, for example, effectively uses organoboronates as nucleophiles for the construction of C–C bonds, cementing its status as one of the most versatile and employed reactions in the pharmaceutical industry.^{1,2} Accordingly, several catalysts have been reported for the preparation of organoboron reagents, traditionally via the hydroboration of alkenes or the borylation of olefinic or alkane substrates.^{3–5} Catalysts have typically featured noble metal centers, primarily Rh and Ir.⁵ However, the high cost, low abundance, and environmentally impacts associated with the use of such metals has motivated the development of first-row transition metal congeners.^{6,7}

Recent reports from the labs of Ritter, Chirik, Huang, and others have provided new Fe, Co, and Cu catalysts for the hydroboration of alkynes and terminal alkenes.^{8–18} Such systems boast operational simplicity and provide powerful platforms for the reduction of unsaturated bonds. Huang and coworkers reported a potent Co(PNN) (PNN = 6-[(dialkylphosphino)methyl]-2,2'-bipyridine) hydroboration catalyst that tolerates a variety of functional groups, including ketones, allyl ethers, tertiary amines, and substituted amides.¹⁹ Similarly, Chirik reported a complement of simple cobalt catalyst precursors for the hydroboration of simple alkenes, including a

† Portions of this chapter are reproduced from the following publication with permission from the authors. Ibrahim, A. D.; Entsminger, S. W.; Fout, A. R. *ACS Catal.* Submitted.

(PPh₃)₃CoH(N₂) system that is competent towards the catalytic isomerization-hydroboration of alkenes.²⁰ Recent reports from Thomas,²¹ Lu,²² and Huang²³ have paralleled such developments with Fe-based hydroboration catalysts, conferring a notable degree of functional group tolerance or enantioselectivity where applicable, as in the case of the chiral iminopyridine oxazoline iron complexes reported by Lu.²² However improvements to these reports could be the removal of activators such as Grignard reagents and NaBHET₃. The selective hydroboration of ketone-bearing alkene substrates is also not widely reported.

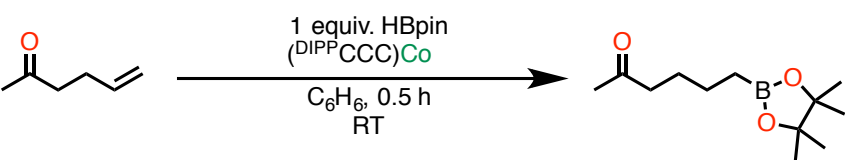
Similar functional group constraints have also been noted in copper catalysts, several of which feature the use of activated or simple alkene and alkyne substrates. Recent reports from the Ito group^{12,24} and Takaki group²⁵ have obviated some of these limitations, providing copper-based systems that can be modulated to provide interesting Markovnikov regioselectivity or that otherwise confer an improved functional group tolerance.

4.2 Results and discussion

We recently reported the hydrosilylation of terminal alkene substrates with a Co^I catalyst bearing an electron-rich CCC pincer ligand.²⁶ Mechanistic studies suggested that the catalyst engages in oxidative addition of the Si–H bond to generate a catalytically active Co^{III} hydrido silyl complex and then proceeds along a Chalk-Harrod reaction profile reminiscent of noble metal catalysts to afford the targeted alkylsilane product. This reactivity, as well as the impressive chemoselectivity of the (DIPP⁺CCC)CoN₂ (**1**) catalyst, prompted us to explore the hydroboration of alkenes bearing ketones and other traditionally challenging oxygen-containing functional groups, particularly given the paucity of earth-abundant complexes tolerant of such functionalities. Pursuant to this end, we investigated the hydroboration of 5-hexen-2-one as a model substrate. Gratifyingly, hydroboration with pinacolborane proceeded with anti-Markovnikov selectivity at

the alkene at room temperature, with no evidence of ketone hydroboration. The use of an air-stable Co^{III} analogue, $(^{\text{DIPP}}\text{CCC})\text{CoCl}_2\text{py}$, was also successful with the addition of NaHBET_3 or TMSCH_2Li activators, albeit in reduced yield. Optimization of catalytic loading led us to select 2.5 mol % of Co^{I} catalyst for catalytic reactivity (Table 4.1).

Table 4.1 Hydroboration optimization



Entry	catalyst (mol %)	Additive	GC-Yield
1	Co^{I} (5 mol %)	None	>99%
2	Co^{I} (2.5 mol %)	None	82%
3	Co^{I} (1 mol %)	None	5%
4	Co^{III} (2.5 mol %)	2 equiv. $(\text{Me}_3\text{Si})\text{CH}_2\text{Li}$	77%
5	Co^{III} (2.5 mol %)	2 equiv. NaEt_3BH	51%
6	Co^{III} (2.5 mol %)	2 equiv. MeMgBr	<1%

Following determination of catalytic conditions, we sought to investigate the substrate scope of the cobalt catalyst (Table 4.2). The hydroboration of 1-octene and styrene proceeded in excellent yield, furnishing the anti-Markovnikov product in both cases with no evidence of dehydrogenative borylation. The hydroboration of 4-vinylcyclohexene, a substrate bearing both an internal alkene and a terminal alkene, proceeded selectively at the terminal alkene position, with complete retention of the internal olefin (entry 2d). More sterically hindered substrates were not amenable to the hydroboration protocol. The hydroboration of limonene, a *gem*-disubstituted alkene, did not result in any detectable conversion while the hydroboration of cyclohexene resulted in only trace product formation after 17 hours, highlighting the steric influence on the selectivity observed. This sensitivity to steric effects was previously observed in the hydrosilylation protocol

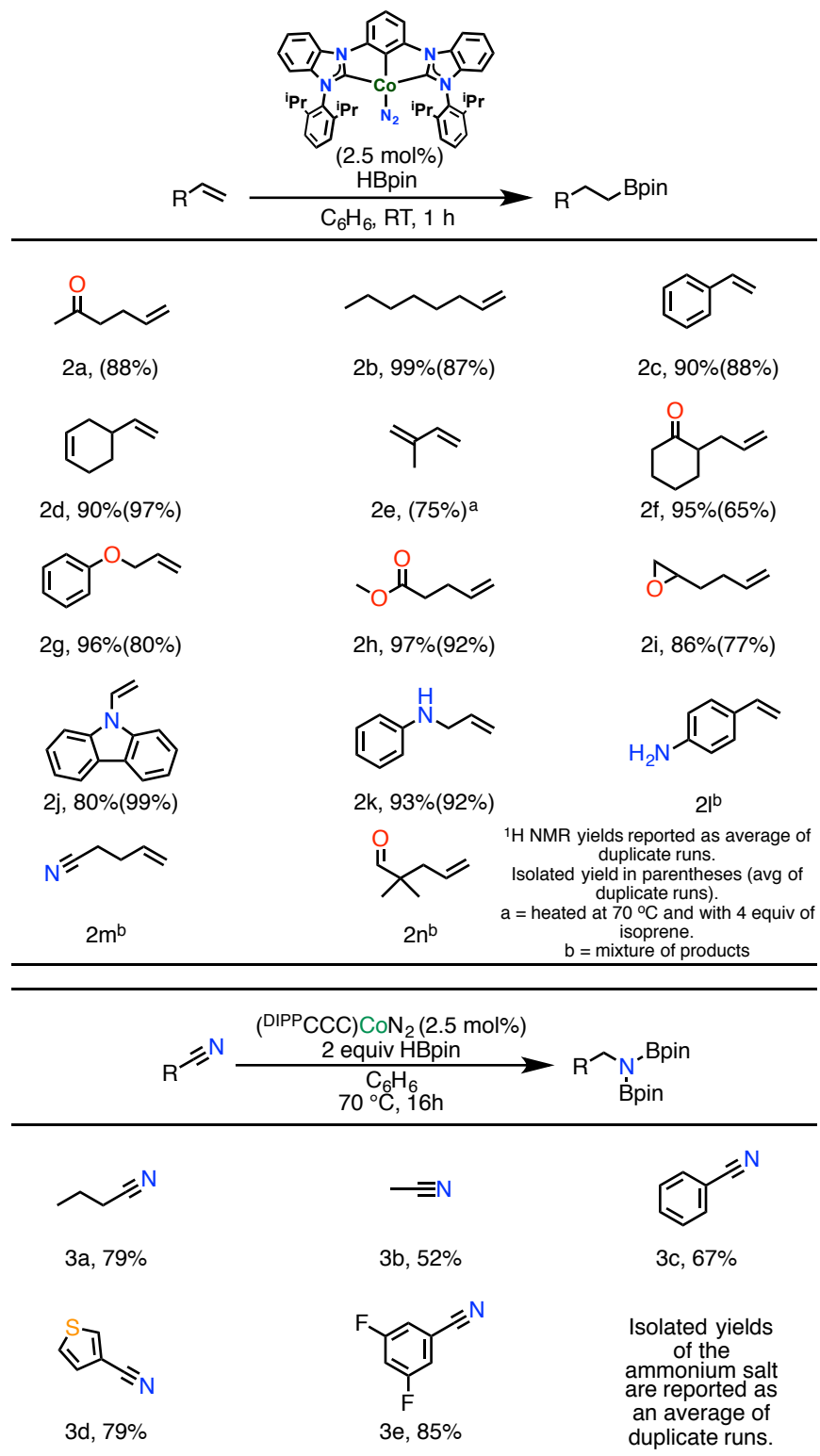
established with this Co^I system and has been observed with the PNN pincer Co system used by Huang.¹¹

Informed by the steric constraints of the catalytic system and given the difficulties associated with 1,2-selective additions to conjugated dienes,²⁷ we turned to the hydroboration of isoprene, a conjugated diene bearing both a gem-disubstituted alkene and a mono-substituted alkene. Addition was 1,2-selective across the less-substituted olefinic bond, as previously observed in our hydrosilylation studies. Such examples of 1,2-hydroboration with cobalt or iron catalysts are uncommon.²⁸ Although Ritter reports the 1,4-hydroboration of conjugated dienes with an iron iminopyridine catalyst,⁸ the analogous 1,2-addition has rarely been realized with iron or cobalt catalysts given the thermodynamic favorability of π -allyl intermediates.²⁷ Indeed, with few exceptions, general reports of 1,2-addition with conjugated dienes are infrequent.

Extension of the catalytic protocol to alkenes bearing oxygen-containing functional groups proved to be similarly successful. Allyl ethers, esters, and epoxides were found to be compatible with the catalyst with no evidence of competing dehydrogenative borylation pathways. Addition across carbonyl moieties, as in the case of 5-hexen-2-one (entry 2a) and 2-allylcyclohexenone (entry 2f), was not detected under these conditions.

Encouraged by the tolerance of oxygen-containing functional groups, we turned our attention to the hydroboration of amines. The hydroboration of 9-vinylcarbazole with pinacolborane proceeded in 80% yield after an hour. Interestingly, N-allylaniline, a secondary amine, was also tolerated under the hydroboration protocol with no concomitant formation of the N-borylated amine. To the best of our knowledge, the catalytic compatibility of unprotected amines has only been reported for a single iron hydroboration catalyst,²¹ while the use of such substrates has not been previously realized with a cobalt system. Interestingly, the corresponding

Table 4.2 Hydroboration substrate scope



reaction with 4-aminostyrene, a primary amine, did not result in the formation of the target

organoboronate ester, suggesting that the observed chemoselectivity may be sterically-modulated. Seeking to further probe the chemoselectivity of the (^{DIPP}CCC)CoN₂ system, the hydroboration of 4-pentenitrile was attempted. In contrast to the exclusive alkene-selectivity observed in the hydrosilylation protocol for this catalyst,²⁶ two organoboronate products corresponding to a single and a double addition of borane to the substrate, respectively, were detected by GC-MS. Intrigued by this reactivity, we sought to investigate the viability of nitrile reduction. Although such reductions can be accomplished stoichiometrically, established protocols typically require the use of LiAlH₄ and NaBH₄ reagents, which generate large quantities of inorganic side-products.^{29,30} The development of catalytic reduction strategies with hydrogen is also restricted, often requiring the use of poorly selective heterogeneous catalysts or the use of highly energetic conditions.³¹ Current strategies, developed by Beller,³² Milstein,^{33,34} Sabo-Etienne,³⁵ and others promise to mitigate some of these challenges but reports are otherwise limited.³¹ Alternate strategies featuring the use of silanes or boranes for the reduction of nitriles have gained traction, however Recent reports by Szymcak³⁶ and Hill³⁷ have demonstrated homogeneous reductions of nitriles using boranes. However, such hydroborations with first-row transition metals remains rare. As such, a cobalt catalyst is an attractive option for the reduction of nitriles, particularly since current strategies are mostly limited to the use of noble metal catalysts.³¹

Initial investigations into the reduction of nitriles (Table 4.2) made use of simple aliphatic nitriles (entries 3a and 3b). Heating a mixture of **1**, pinacolborane, and butyronitrile at 70 °C in benzene solvent afforded the desired bis(borylated) amine, as detected by GC-MS. Subsequent workup of the reaction mixture led to the isolation of the corresponding ammonium salt in good yields (entry 1). The reduction of acetonitrile was similarly successful, furnishing ethylammonium chloride in excellent yield following workup. To our delight, extension of the protocol to aromatic

nitriles (entries 3c-3e) also furnished the corresponding ammonium salts upon isolation, demonstrating a tolerance for thiophene moieties (entry 3d), as well as a fluorinated arene (entry 3e).

Interested in obtaining further insights into hydroboration with the (^DI^PP^PCCC)Co^I platform, we turned to labeling experiments with deuterated pinacolborane. Upon reacting styrene with an equivalent of deuterated pinacolborane, we observed deuterium incorporation into the targeted linear alkylboronate ester product at both the terminal and benzylic positions in approximately equal proportion (Figure 4.1). Moreover, deuterium resonances corresponding to incorporation at vinylic positions of the styrene starting material were also detected. These observations are consistent with the intermediacy of a cobalt hydride over the course of catalysis, as well as the negotiation of β -hydride elimination processes to regenerate alkene substrate. The absence of a deuterium resonance at 6.57 ppm, corresponding to the vinylic proton at the benzylic position of the styrene substrate suggests that 1,2 insertion is immediately followed by liberation of the targeted boronate ester while 2,1 insertion is reversible and not productive towards the formation of product, as only the linear alkylboronate ester is formed. This process is generalizable to non-vinylarene substrates. Upon reacting 1-octene with deuterated pinacolborane in the presence of the cobalt catalyst, evidence of both 2,1- and 1,2-insertions is observed; deuterium is incorporated at both the α and β carbons of the alkylboronate ester product. Additionally, the exclusive generation of the linear alkylboronate ester product, rather than a combination of the branched and linear products, suggests liberation of product immediately follows 1,2-insertion, i.e. β -hydride elimination from this insertion mode is not competitive with elimination of the target organoboronate ester while 2,1-insertion is not a productive pathway to the formation of alkylboronate ester product.

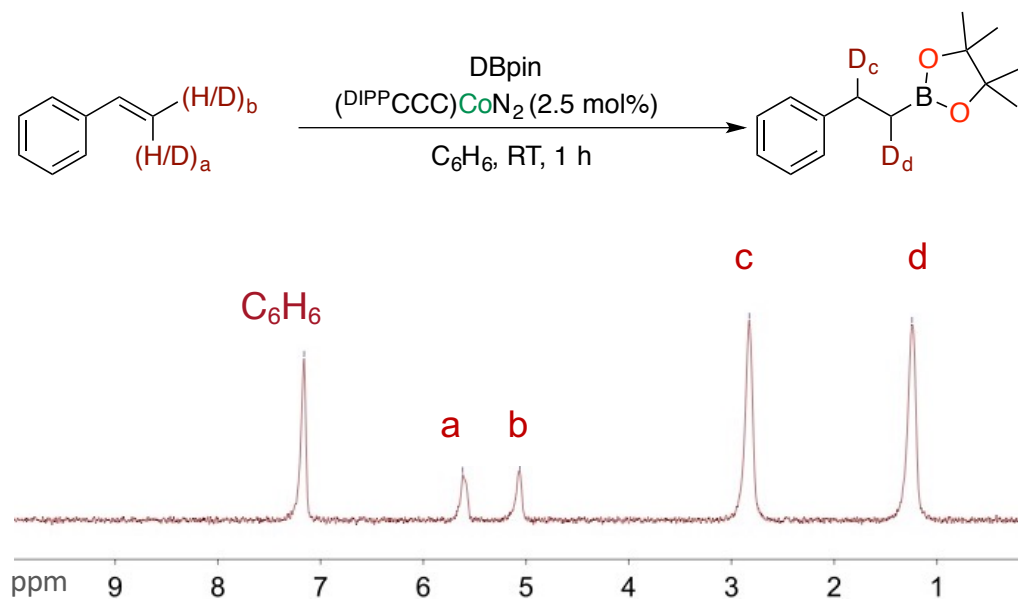


Figure 4.1 ^2H NMR spectrum of the hydroboration of styrene

The susceptibility of 2,1-insertion products to β -hydride elimination and the general lack of turnover observed for this insertion mode may be a result of the substantial steric shielding of the generated secondary alkyl cobalt intermediates, which may preclude elimination with a boryl ligand to give the target compound. The inactivity of this cobalt system toward more substituted terminal alkenes is also consistent with this possibility, as greater substitution at the substrate would provide significant steric limitations even in the event of a 1,2-insertion. To test this hypothesis, the addition of deuterated pinacolborane to cyclohexene, a substrate that generates only trace amounts of product after 24 h of stirring, was investigated. Although incorporation into the olefinic bond was not observed after 6.5 h of stirring, minor deuterium incorporation at the adjacent aliphatic carbons suggests an alkene-isomerization-type event, where insertion into the olefin is followed by β -hydride elimination from a proximal carbon to generate a deuterium-enriched cyclohexene. Importantly, the absence of the observed organoboronate product suggests the generated secondary alkyl intermediate is unreactive towards turnover, in stark contrast to

primary alkyl cobalt intermediates which can proceed along the reaction sequence. Interestingly, allowing the reaction to stir over a longer period (7 d) does eventually result in deuterium incorporation at all sites of the cyclohexene substrate, including the olefinic carbons.

Intrigued by this result, we sought to study these putative alkene isomerization events in greater detail. Accordingly, the hydroboration of the internal alkene trans-4-octene, a substrate with sterically differentiable primary and secondary alkyl sites, with deuterated pinacolborane was investigated. Deuterium incorporation was observed along the length of the substrate, consistent with alkene isomerization. In contrast to cyclohexene, however, minor resonances corresponding to the linear alkylboronate ester product were also observed in the ^2H NMR spectrum, indicating that, upon isomerization to the more sterically accessible termini of the octyl chain, i.e. upon formation of a primary alkyl cobalt intermediate, liberation of the alkylboronate ester is viable. Given the profile of the cyclohexene substrate, i.e. any insertion or hydrocobaltation step necessarily generates a sterically hindered cobalt-secondary alkyl intermediate, the opportunity to generate the analogous alkylboronate is rendered far less likely and the catalysis is effectively arrested at the insertion step.

In addition to providing a rationale for the observed regioselectivity, these data may also explain some of the chemoselectivity observed for this catalyst platform. The reduction of a ketone functionality, for example, may be disfavored given the steric profile of the insertion product. By extension, reducible functionalities such as esters and substituted amines should also be, and are, tolerated, particularly in the presence of a more sterically accessible terminal alkene that is amenable to reduction with borane. The competing reductions of the formyl group in 2,2-dimethyl-4-pentenal (entry 2n) and the nitrile moiety in 4-pentenitrile (entry 2m) are consistent, as these reducible functionalities are sterically accessible and would generate insertion products with a

comparable steric profile to mono-substituted terminal alkenes.

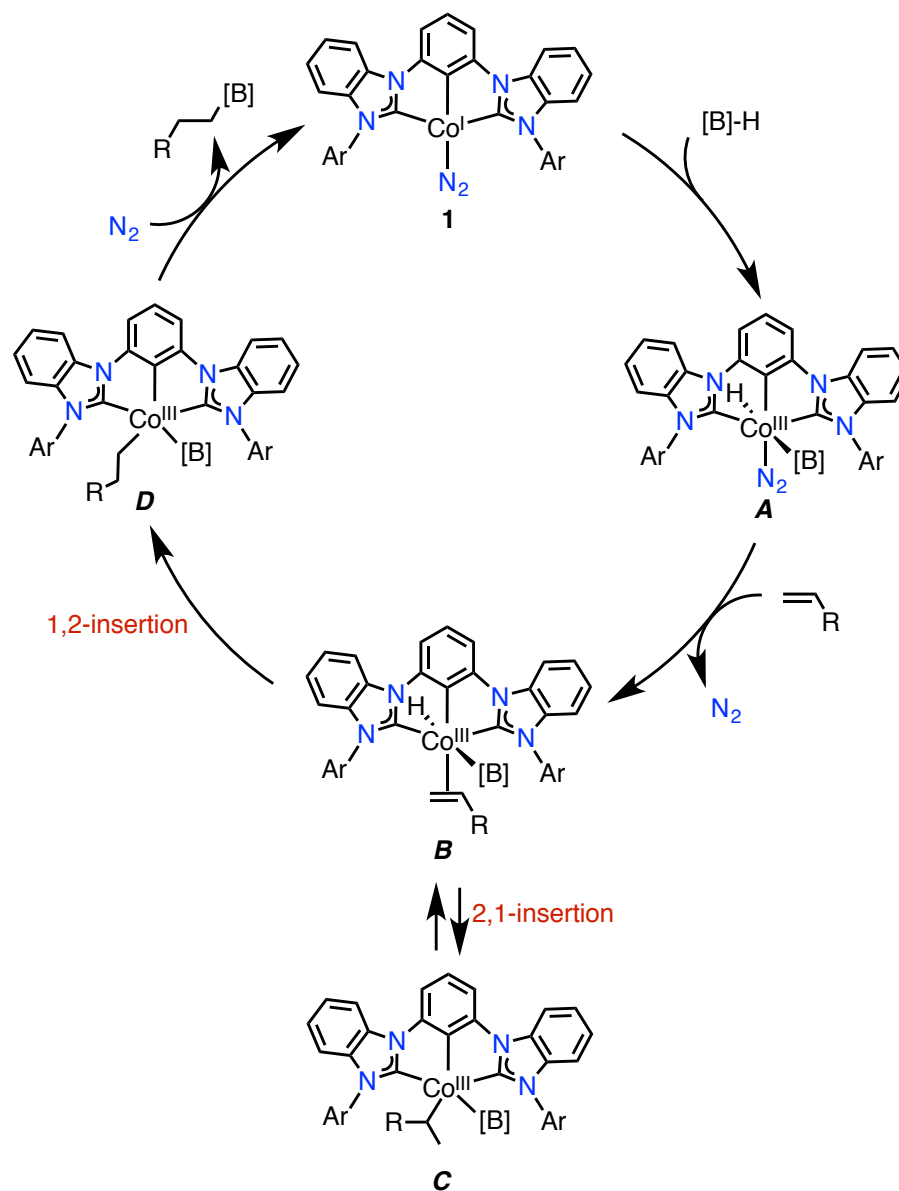


Figure 4.2 Proposed catalytic mechanism for hydroboration with $(^{DIPP}CCC)CoN_2$

Informed by these insights and given the similarities to a hydrosilylation protocol previously reported for this system,²⁶ a mechanism was proposed for the observed reactivity (Figure 4.2). Oxidative addition of borane (**A**) is proposed to commence the catalytic cycle and

generate a cobalt(III) hydrido boryl species. This is followed by coordination of an alkene or nitrile (not shown) substrate (**B**). Subsequent migratory insertion of the hydride (**D**) into the alkene affords a cobalt alkyl intermediate. This process is reversible in the event of a 2,1-insertion (**C**) or if the substrate is sufficiently sterically encumbered, regenerating the alkene via β -hydride elimination as established by deuterium labelling experiments. In the event of an internal alkene substrate, alkene isomerization to a terminal position may generate product. Finally, reductive elimination with the boryl ligand furnishes the organoboronate ester product and regenerates the Co^{I} catalyst.

In conclusion, we have developed a highly selective Co^{I} system for the hydroboration of alkenes. This reaction sequence is selective for alkenes in the presence of a number of functional groups, furnishing the anti-Markovnikov product exclusively in all observed cases. Additionally, the protocol is amenable to the reduction of nitriles to their corresponding amines, a valuable chemical reaction that is relatively underexplored with earth-abundant first-row transition metal systems. Deuterium labeling studies have provided important insights into the observed reactivity, demonstrating that the cobalt catalyst can negotiate insertion processes, β -hydride elimination pathways, and alkene isomerization events. These processes underpin the regioselectivity, and perhaps the chemoselectivity, of the system, as the generation of primary alkyl intermediates over the course of catalysis is required to liberate the alkylboronate esters.

4.3 Experimental section

General Considerations. All manipulations of air- and moisture-sensitive compounds were carried out in the absence of water and dioxygen in an MBraun inert atmosphere drybox under a dinitrogen atmosphere except where specified otherwise. All glassware was oven dried for a minimum of 8 h and cooled in an evacuated antechamber prior to use in the drybox. Solvents for

sensitive manipulations were dried and deoxygenated on a Glass Contour System (SG Water USA, Nashua, NH) and stored over 4 Å molecular sieves purchased from Strem following drying via a literature procedure prior to use.³⁸ Chloroform-*d*₁, water- *d*₂, dimethyl sulfoxide- *d*₆, benzene-*d*₆ were purchased from Cambridge Isotope Labs and were degassed and stored over 4 Å molecular sieves prior to use. Celite® 545 (J. T. Baker) was used as received. NMR Spectra were recorded at room temperature on a Varian or Bruker spectrometer operating at 500 MHz or 400 MHz (¹H NMR), 126 MHz or 101 MHz (¹³C NMR), and 119 MHz (²H NMR) (U500, VXR500, UI500NB, CB500, U400) and referenced to the residual CHCl₃, C₆D₅H, HDO, or C₂D₅HSO₂ resonances (δ in parts per million, and *J* in Hz). Electrospray ionization mass spectrometry (ESI) was recorded on a Waters Q-TOF Ultima ESI instrument. Electron ionization mass spectrometry (EI) was recorded on a Waters 70-VSE EI instrument. Allyl phenyl ether were purchased from Alfa Aesar. 4-pentenitrile was purchased from TCI Chemicals, N-allylaniline was purchased from Alfa Aesar, and the remainder of the alkene substrates were purchased from Sigma-Aldrich. All liquids were dried over 4 Å molecular sieves prior to use.

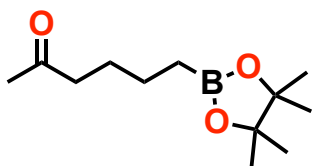
General Hydroboration Procedure for Alkenes. A 20 mL scintillation vial is charged with mesitylene or naphthalene standard (0.140 mmol), olefin (0.140 mmol), and pinacolborane (0.140 mmol) inside a glove box. Using benzene-*d*₆, the resulting mixture is then transferred to a vial containing the catalyst (^DI^PP^PCCC)CoN₂ (**1**) (0.0025 g, 0.00349 mmol), which was prepared according to literature procedure.³⁹ A final rinse and transfer with the deuterated benzene solvent, for a total solvent volume of ca. 2 mL, completes the setup and the reaction is stirred at room temperature for 1 h. Upon completion, an NMR aliquot of the reaction is taken and the yield is determined by integration relative to the resonances of the internal standard.

Isolation Protocol for Alkylboronate Esters. A 20 mL scintillation vial is charged with **1** (10

mg, 0.0140 mmol), olefin (0.558 mmol), pinacolborane (0.558 mmol), and benzene (1.5 mL). The crude reaction was taken outside of the glovebox, concentrated under reduced pressure, and purified by flash chromatography with an ethyl acetate:hexanes solvent mixture (1:20) to afford the product.

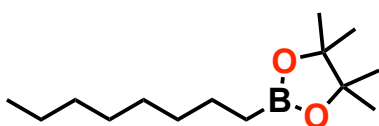
General Hydroboration Procedure for Nitriles. A 20 mL scintillation vial is charged with nitrile (0.558 mmol) and a separate vial is charged pinacolborane (1.116 mmol) inside a glove box. Using benzene solvent, the pinacolborane is transferred to a vial containing the catalyst (^{DIPP}CCC)CoN₂ (**1**)² (0.010 g, 0.0140 mmol), followed by the nitrile. A final rinse and transfer of the resulting solution to a high-pressure glass vessel with the benzene solvent gives a total solvent volume of ca. 1.5 mL and completes the setup. The vessel is sealed, taken outside of the glovebox and heated at 70 C for 16 h. Upon completion, the crude reaction is transferred to a vial and the volatiles are removed using a rotary evaporator. Aqueous hydrochloric acid (0.95 mL of 37 wt%) is subsequently added to the vial, followed by 1 mL of deionized water, and the mixture is stirred for approximately 10 mins. The water is then removed using a rotary evaporator and the solid is filtered over Celite, using solvent to wash off impurities. The remaining solid is then flushed with methanol into a separate container and the filtrate is dried under reduced pressure to give a solid.

Characterization Data.

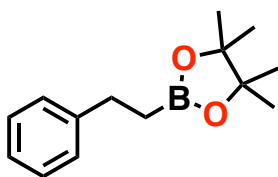


6-(4,4,5,5-tetramethyl-1,3,2-dioxaborolan-2-yl)hexan-2-one (2a). The isolation protocol was followed to afford **2a** as an oil (0.111 g, 0.491 mmol, 88%). ¹H NMR (500 MHz, Chloroform-*d*) δ 2.40 (t, *J* = 7.5 Hz, 2H), 2.11 (s, 3H), 1.62 – 1.52 (m, 3H), 1.46 – 1.33 (m, 2H), 1.23 (s, 12H), 0.81 – 0.74 (m, 2H). ¹³C

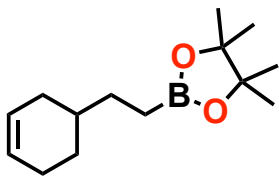
NMR (126 MHz, CDCl₃) δ 209.4, 83.1, 43.8, 29.9, 26.6, 25.0, 23.8, 11.2 (broad). ¹¹B NMR (161 MHz, CDCl₃) δ 33.9. ¹H, ¹³C, and ¹¹B NMR spectroscopy data match literature values.⁴⁰ HRMS (ES), calc. for C₁₂H₂₃BO₃Na (M + Na)⁺: 249.1638; found 225.1635.



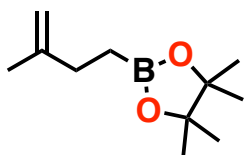
4,4,5,5-tetramethyl-2-octyl-1,3,2-dioxaborolane (2b). The general procedure was followed using naphthalene as the internal standard, 1-octene, pinacolborane, and benzene-*d*₆ (2.5 mL) (¹H NMR yield: 99%). The isolation protocol was followed to yield **2b** as an oil (Isolated yield: 87%). ¹H NMR (400 MHz, Benzene-*d*₆) δ 1.71 – 1.59 (m, 2H), 1.47 – 1.34 (m, 2H), 1.36 – 1.19 (m, 8H), 1.08 (s, 12H), 1.03 (t, *J* = 7.7 Hz, 2H), 0.94 – 0.83 (m, 3H). ¹³C NMR (101 MHz, Benzene) δ 86.2, 82.7, 32.9, 32.3, 30.0, 29.8, 25.0, 24.7, 23.1, 14.4. ¹¹B NMR (161 MHz, CDCl₃) δ 34.1. ¹H, ¹³C, and ¹¹B NMR spectroscopy data in CDCl₃ solvent match literature values.⁴¹ HRMS (EI), calc. for C₁₃H₂₆O₂B (M – CH₃)⁺: 225.2026; found 225.2036.



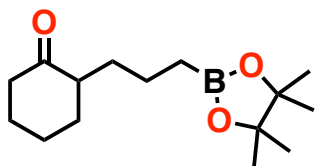
4,4,5,5-tetramethyl-2-phenethyl-1,3,2-dioxaborolane (2c). The general procedure was followed using naphthalene as the internal standard, styrene, pinacolborane, and benzene-*d*₆ (¹H NMR yield: 99%). The isolation protocol was followed to yield **2c** as an oil (Isolated yield: 88%). ¹H NMR (500 MHz, Benzene-*d*₆) δ 7.17 – 7.10 (m, 4H), 7.04 – 6.99 (m, 1H), 2.83 (t, *J* = 8.0 Hz, 2H), 1.25 (t, *J* = 7.9 Hz, 2H), 0.97 (s, 12H). ¹³C NMR (126 MHz, Benzene-*d*₆) δ 144.8, 128.5, 128.5, 125.9, 83.0, 30.6, 25.0. ¹¹B NMR (161 MHz, CDCl₃) δ 33.9. ¹H, ¹³C, and ¹¹B NMR spectroscopy data in CDCl₃ solvent match literature values.⁴² HRMS (EI), calc. for C₁₄H₂₁O₂B (M[⊖])⁺: 232.1635; found 232.1637.



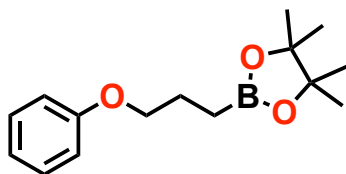
2-(2-(cyclohex-3-en-1-yl)ethyl)-4,4,5,5-tetramethyl-1,3,2-dioxaborolane (2d). The general procedure was followed using mesitylene as the internal standard, 4-vinyl-1-cyclohexene, pinacolborane, and benzene- d_6 (^1H NMR yield: 90%). The isolation protocol was followed to yield **2d** as an oil (Isolated yield: 97%). ^1H NMR (400 MHz, Benzene- d_6) δ 5.82 – 5.54 (m, 2H), 2.18 – 2.05 (m, 1H), 2.04-1.88 (m, 2H), 1.78 – 1.48 (m, 5H), 1.28 – 1.14 (m, 1H), 1.06 (s, 12H), 1.03 – 0.96 (m, 2H). ^{13}C NMR (101 MHz, Benzene- d_6) δ 127.2, 127.0, 82.8, 36.1, 32.1, 31.3, 29.1, 25.7, 25.0, 25.0. ^{11}B NMR (161 MHz, CDCl_3) δ 34.1. ^1H , ^{13}C , and ^{11}B NMR spectroscopy data in CDCl_3 solvent match literature values.⁴³ HRMS (EI), calc. for $\text{C}_{14}\text{H}_{25}\text{O}_2\text{B}$ (M^{\oplus}): 236.1948; found 236.1955.



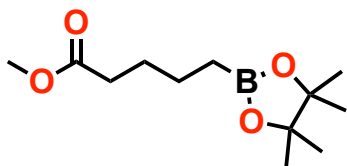
4,4,5,5-tetramethyl-2-(3-methylbut-3-en-1-yl)-1,3,2-dioxaborolane (2e). A modified isolation protocol was followed using **1** (10 mg, 0.0140 mmol), isoprene (2.232 mmol), pinacolborane (0.558 mmol), and benzene (2.5 mL). The reaction was conducted in a high-pressure vessel and sealed following addition of the borane and olefin mixture to the catalyst. The sealed vessel was then taken outside of the glove box and heated to 70 °C for 2 h. The crude reaction was concentrated under reduced pressure and purified by flash chromatography with hexanes to afford **2e** as a colorless oil (0.082 g, 0.419 mmol, 75%). ^1H NMR (500 MHz, Chloroform- d) δ 4.69 – 4.59 (m, 2H), 2.10 (t, $J = 7.8$ Hz, 2H), 1.71 (s, 3H), 1.23 (s, 12H), 0.91 (t, $J = 7.9$ Hz, 2H). ^{13}C NMR (126 MHz, CDCl_3) δ 147.9, 108.6, 83.1, 31.8, 24.9, 22.7, 9.7. ^{11}B NMR (161 MHz, CDCl_3) δ 34.0. ^1H , ^{13}C , and ^{11}B NMR spectroscopy data match literature values.⁴⁴



2-(3-(4,4,5,5-tetramethyl-1,3,2-dioxaborolan-2-yl)propyl)cyclohexan-1-one (2f). The general procedure was followed using naphthalene as the internal standard, 2-allylcyclohexanone (0.140 mmol), pinacolborane (0.140 mmol), and benzene-*d*₆ (¹H NMR yield: 95%). The isolation protocol was followed to yield **2f** as an oil (Isolated yield: 65%). ¹H NMR (500 MHz, Benzene-*d*₆) δ 2.21 (dtd, *J* = 13.4, 4.3, 1.5 Hz, 1H), 2.08 – 1.90 (m, 2H), 1.83 (dddd, *J* = 13.4, 12.4, 5.8, 1.2 Hz, 1H), 1.77 – 1.67 (m, 1H), 1.65 – 1.55 (m, 2H), 1.54 – 1.47 (m, 1H), 1.38 – 1.32 (m, 1H), 1.31 – 1.18 (m, 2H), 1.08 (s, 12H), 1.04 – 0.94 (m, 4H). ¹³C NMR (126 MHz, Benzene-*d*₆) δ 210.5, 82.8, 50.6, 42.0, 33.9, 32.6, 28.0, 25.1, 25.0, 22.3. ¹¹B NMR (161 MHz, CDCl₃) δ 33.8. ¹H and ¹³C NMR spectroscopy data in CDCl₃ solvent match literature values.¹⁹ HRMS (ES), calc. for C₁₅H₂₇BO₃ (M + H)⁺: 267.2132; found 267.2130.

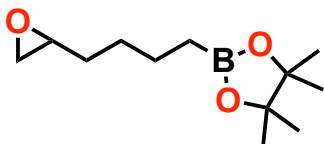


4,4,5,5-tetramethyl-2-(3-phenoxypropyl)-1,3,2-dioxaborolane (2g). The general procedure was followed using naphthalene as the internal standard, allyl phenyl ether, pinacolborane, and benzene-*d*₆ (¹H NMR yield: 96%). The isolation protocol was followed to yield **2g** as an oil (Isolated yield: 80%). ¹H NMR (500 MHz, Benzene-*d*₆) δ 7.15 – 7.10 (m, 2H), 6.89 (d, *J* = 8.1 Hz, 2H), 6.84 (t, *J* = 7.3 Hz, 1H), 3.75 (t, *J* = 6.7 Hz, 2H), 1.98 (p, *J* = 7.1 Hz, 2H), 1.10 – 0.97 (m, 14H). ¹³C NMR (126 MHz, Benzene-*d*₆) δ 159.9, 129.7, 120.6, 115.0, 83.0, 69.6, 25.0, 24.4. ¹¹B NMR (161 MHz, CDCl₃) δ 34.0. ¹H, ¹³C, and ¹¹B NMR spectroscopy data in CDCl₃ solvent match literature values.⁴⁵ HRMS (ES), calc. for C₁₅H₂₃BO₃Na (M + Na)⁺: 285.1638; found 285.1648.



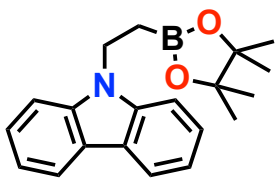
methyl 5-(4,4,5,5-tetramethyl-1,3,2-dioxaborolan-2-yl)pentanoate (2h). The general procedure was followed using naphthalene as the internal standard, methyl 4-

pentenoate, pinacolborane, and benzene- d_6 (^1H NMR yield: 97%). The isolation protocol was followed to yield **2h** as an oil (Isolated yield: 92%). ^1H NMR (400 MHz, Benzene- d_6) δ 3.31 (s, 3H), 2.13 (p, $J = 7.4$ Hz, 2H), 1.72 – 1.62 (m, 2H), 1.52 (p, $J = 7.6$ Hz, 2H), 1.04 (s, 12H), 0.90 (t, $J = 7.6$ Hz, 2H). ^{13}C NMR (101 MHz, Benzene- d_6) δ 173.4, 128.1, 86.2, 82.8, 50.9, 34.1, 27.9, 25.0, 24.2. ^{11}B NMR (161 MHz, CDCl_3) δ 33.8. ^1H and ^{13}C NMR spectroscopy data in CDCl_3 solvent match literature values.⁴⁶ HRMS (ES), calc. for $\text{C}_{12}\text{H}_{23}\text{BO}_4\text{Na}$ ($\text{M} + \text{Na}$) $^+$: 265.1587; found 265.1582.

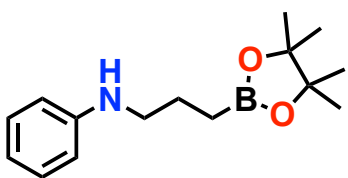


4,4,5,5-tetramethyl-2-(4-(oxiran-2-yl)butyl)-1,3,2-dioxaborolane (2i). The general procedure was followed using

naphthalene as the internal standard, 1,2-epoxy-5-hexene, pinacolborane, and benzene- d_6 (^1H NMR yield: 86%). The isolation protocol was followed to yield **2i** as an oil (Isolated yield: 77%). ^1H NMR (500 MHz, Benzene- d_6) δ 2.66 – 2.50 (m, 1H), 2.33 (t, $J = 4.6$ Hz, 1H), 2.08 (dd, $J = 5.3$, 2.6 Hz, 1H), 1.60 – 1.49 (m, 2H), 1.47 – 1.23 (m, 4H), 1.06 (s, 12H), 0.93 (t, $J = 7.7$ Hz, 2H). ^{13}C NMR (126 MHz, Benzene- d_6) δ 82.8, 51.8, 46.4, 32.8, 29.0, 25.0, 24.4. ^{11}B NMR (161 MHz, CDCl_3) δ 34.0. ^1H , ^{13}C , and ^{11}B NMR spectroscopy data in CDCl_3 solvent match literature values.⁴⁷ HRMS (ES), calc. for $\text{C}_{12}\text{H}_{23}\text{BO}_3\text{Na}$ ($\text{M} + \text{Na}$) $^+$: 249.1638; found 249.1649.



9-(2-(4,4,5,5-tetramethyl-1,3,2-dioxaborolan-2-yl)ethyl)-9H-carbazole (2j). The general procedure was followed using mesitylene as the internal standard, 9-vinylcarbazole, pinacolborane, and benzene- d_6 (^1H NMR yield: 80%). The compound was also isolated in a modified procedure using **1** (10 mg, 0.0140 mmol), 9-vinylcarbazole (0.558 mmol), pinacolborane (0.558 mmol), and benzene (2 mL) whereby the crude reaction was taken outside of the glovebox after 3 h of stirring, concentrated under reduced pressure, and purified by flash chromatography with an ethyl acetate:hexanes solvent mixture (1:20) to afford **2j** as a white solid (0.177 g, 0.552 mmol, 99%). ^1H NMR (499 MHz, Chloroform- d) δ 8.15 (d, $J = 7.8$ Hz, 2H), 7.58 – 7.47 (m, 4H), 7.27 (t, $J = 7.2$ Hz, 2H), 4.57 – 4.45 (m, 2H), 1.26 (s, 12H). ^{13}C NMR (126 MHz, CDCl_3) δ 140.1, 125.5, 123.0, 120.4, 118.7, 109.1, 83.6, 38.8, 24.9, 12.1. ^{11}B NMR (161 MHz, CDCl_3) δ 33.4. ^1H and ^{13}C NMR spectroscopy data in CDCl_3 solvent match literature values.¹⁹ HRMS (ES), calc. for $\text{C}_{20}\text{H}_{25}\text{NO}_2\text{B}$ ($\text{M} + \text{H}$) $^+$: 322.1978; found 322.1971.



4,4,5,5-tetramethyl-2-(4-(oxiran-2-yl)butyl)-1,3,2-dioxaborolane (2k). The general procedure was followed using mesitylene as the internal standard, N-allylaniline, pinacolborane, and benzene- d_6 (^1H NMR yield: 93%). The isolation protocol was followed to yield **2k** as a viscous oil (Isolated yield: 92%). ^1H NMR (400 MHz, Benzene- d_6) δ 7.22 – 7.15 (m, 2H), 6.75 (t, $J = 7.3$ Hz, 1H), 6.50 (d, $J = 7.6$ Hz, 2H), 3.35 (s, 1H), 3.00 – 2.85 (m, 2H), 1.65 (p, $J = 7.3$ Hz, 2H), 1.04 (s, 12H), 0.89 (t, $J = 7.5$ Hz, 2H). ^{13}C NMR (101 MHz, Benzene- d_6) δ 149.2, 129.5, 117.2, 113.0, 83.0, 46.2, 25.0, 25.0, 24.3.

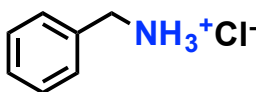
^1H NMR (500 MHz, Chloroform-*d*) δ 7.21 – 7.13 (m, 2H), 6.68 (tt, $J = 7.3, 1.2$ Hz, 1H), 6.64 – 6.59 (m, 2H), 3.78 (s, 2H), 3.11 (t, $J = 7.1$ Hz, 2H), 1.69 – 1.83 (m, 2H), 0.89 (t, $J = 7.6$ Hz, 2H). ^{13}C NMR (126 MHz, CDCl_3) δ 148.7, 129.3, 117.0, 112.7, 83.2, 46.2, 25.0, 24.0. ^{11}B NMR (161 MHz, CDCl_3) δ 33.9. HRMS (ES), calc. for $\text{C}_{15}\text{H}_{25}\text{BNO}_2$ ($\text{M} + \text{H}$) $^+$: 262.1978; found 262.1979.



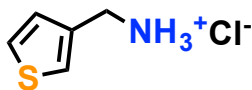
4,4,5,5-tetramethyl-2-octyl-1,3,2-dioxaborolane (3a). The general procedure for nitriles was followed with ethyl acetate (15 mL) used for washes (isolated yield: 79%). ^1H NMR (400 MHz, Chloroform-*d*) δ 8.09 (s, 3H), 2.97 (t, $J = 7.5$ Hz, 2H), 1.73 (t, $J = 7.6$ Hz, 2H), 1.39 (q, $J = 7.5$ Hz, 2H), 0.91 (t, $J = 7.3$ Hz, 3H). ^{13}C NMR (101 MHz, CDCl_3) δ 40.1, 29.6, 20.0, 13.6. ^1H and ^{13}C NMR spectroscopy data match literature values.⁴⁸



4,4,5,5-tetramethyl-2-octyl-1,3,2-dioxaborolane (3b). The general procedure for nitriles was followed with ethyl acetate (5 mL) and DCM (10 mL) used for washes (isolated yield: 52%). ^1H NMR (500 MHz, Deuterium Oxide) δ 2.87 (q, $J = 7.0$ Hz, 2H), 1.10 (t, $J = 7.3$ Hz, 3H). ^{13}C NMR (126 MHz, D_2O) δ 35.1, 12.0. ^1H and ^{13}C NMR spectroscopy data match literature values.⁴⁹

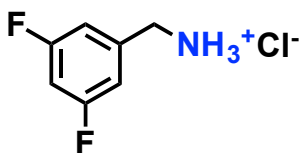


4,4,5,5-tetramethyl-2-octyl-1,3,2-dioxaborolane (3c). The general procedure for nitriles was followed with ethyl acetate (18 mL) and DCM (3 mL) used for washes (isolated yield: 67%). ^1H NMR (400 MHz, D_2O) δ 7.44, 4.15. ^{13}C NMR (101 MHz, D_2O) δ 132.5, 129.1, 128.7, 43.0. ^1H and ^{13}C NMR spectroscopy data match literature values.³⁶



4,4,5,5-tetramethyl-2-octyl-1,3,2-dioxaborolane (3d). The

general procedure for nitriles was followed with ethyl acetate (18 mL) and DCM (12 mL) used for washes (isolated yield: 79%). ^1H NMR (400 MHz, DMSO- d_6) δ 8.64 (s, 3H), 7.68 – 7.62 (m, 1H), 7.57 (dd, J = 4.9, 2.9 Hz, 1H), 7.38 – 7.23 (m, 1H), 3.99 (s, 2H). ^{13}C NMR (101 MHz, DMSO) δ 134.8, 128.2, 126.9, 125.1, 37.2. ^1H NMR spectroscopy data match literature values.⁵⁰



4,4,5,5-tetramethyl-2-octyl-1,3,2-dioxaborolane (3e). The

general procedure for nitriles was followed with ethyl acetate (8 mL) and DCM (3 mL) used for washes (isolated yield: 85%). ^1H NMR (500 MHz, Deuterium Oxide) δ 7.11 – 7.04 (m, 2H), 7.06 – 6.98 (m, 1H), 4.20 (s, 2H). ^{13}C NMR (126 MHz, Deuterium Oxide) δ 164.1 (d, J = 13.3 Hz), 162.1 (d, J = 12.9 Hz), 136.2 (t, J = 9.6 Hz), 112.1 (q), 104.7 (t, J = 25.5 Hz), 42.4. HRMS (EI), calc. for $\text{C}_7\text{H}_8\text{NF}_2$ (M)⁺: 144.0625; found 144.0624.

General Protocol for Deuterium Labelling Experiments. A 20 mL scintillation vial is charged with olefin (0.140 mmol) and deuterated pinacolborane (0.140 mmol), which was prepared according to literature procedure,⁹ inside a glove box. Using benzene solvent, the resulting mixture is then transferred to a vial containing the catalyst ($^{\text{DIPP}}\text{CCC}$)CoN₂ (**1**) (0.0025 g, 0.00349 mmol), which was prepared according to literature procedure. A final rinse and transfer with the benzene solvent, for a total solvent volume of ca. 2 mL, completes the setup and the reaction is stirred. Upon completion, an NMR aliquot of the reaction is taken.

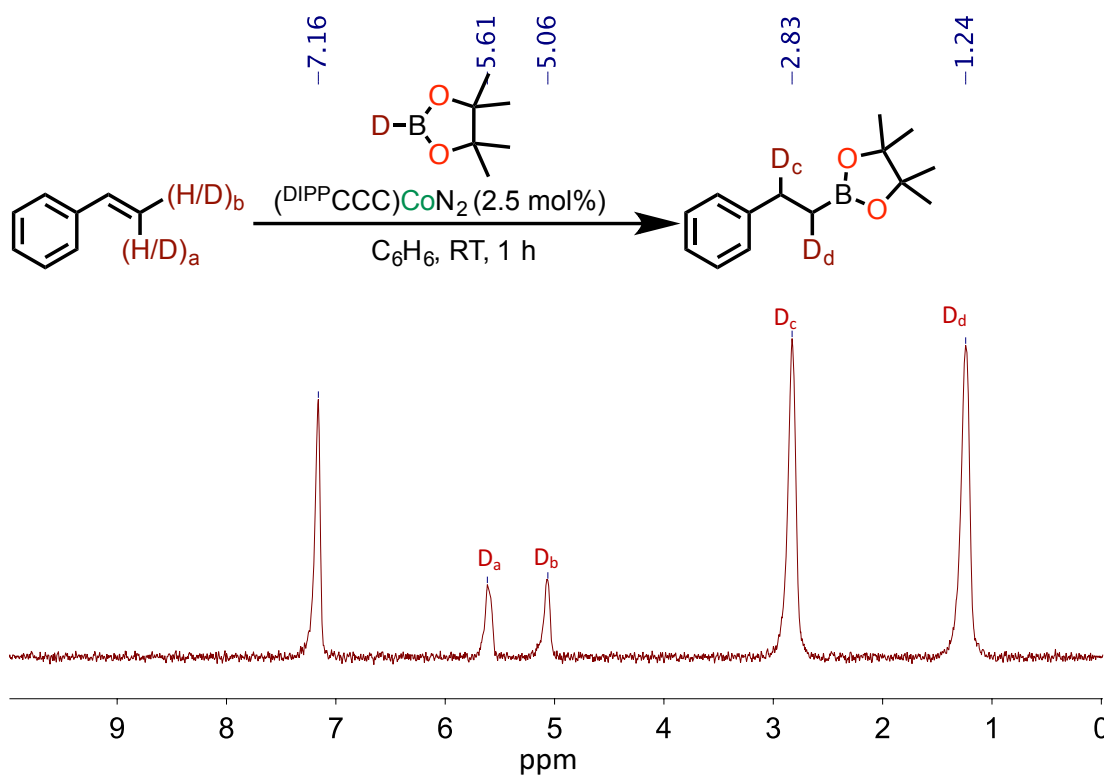


Figure 4.3 Hydroboration of styrene with DBpin

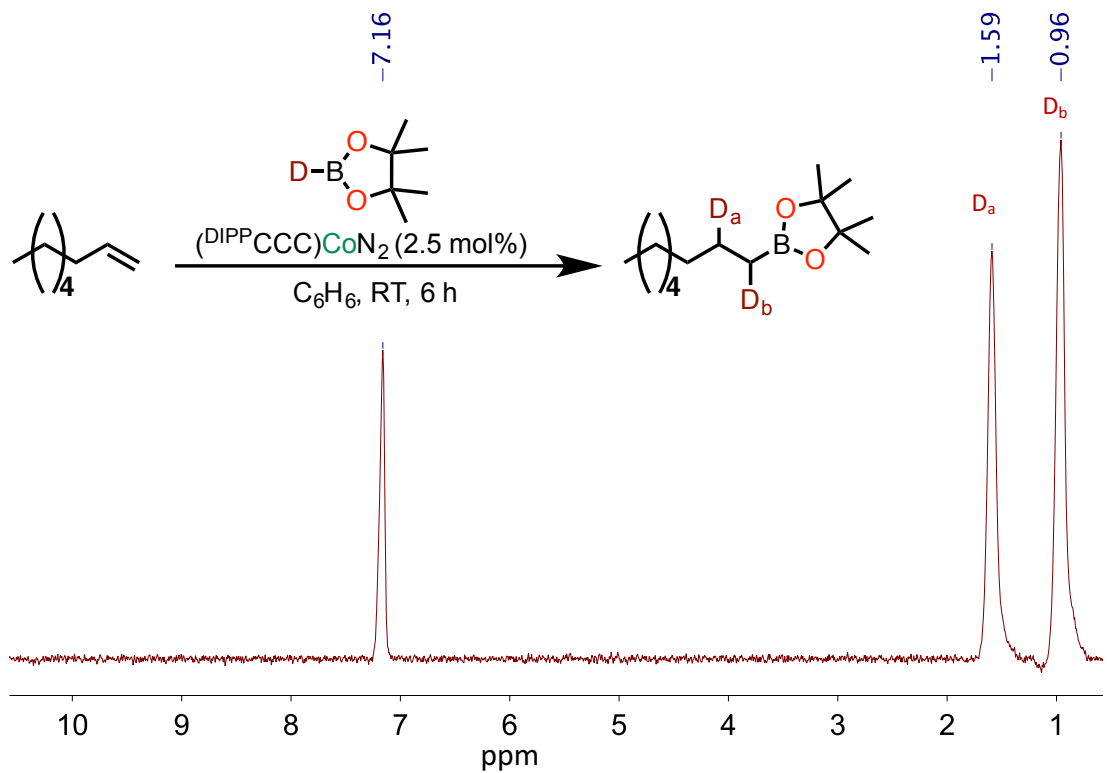


Figure 4.4 Hydroboration of 1-octene with DBpin

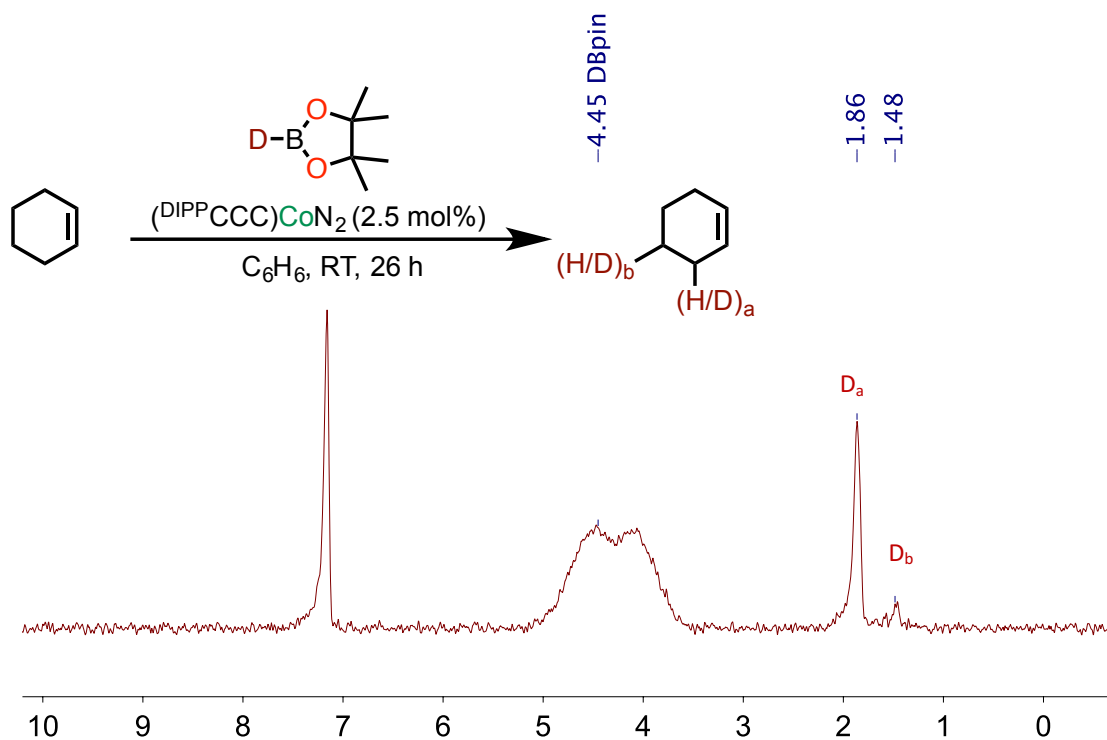


Figure 4.5 Deuterium labeling of cyclohexene with DBpin at 26 h

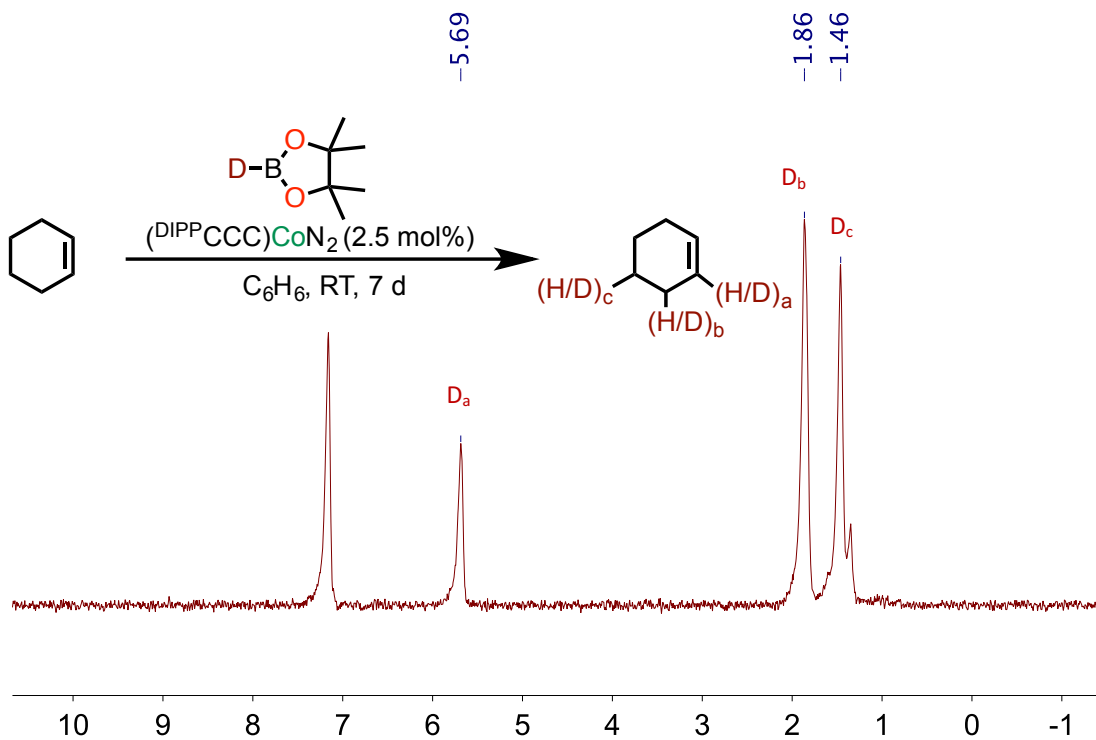


Figure 4.6 Deuterium labeling of cyclohexene with DBpin at 7 days

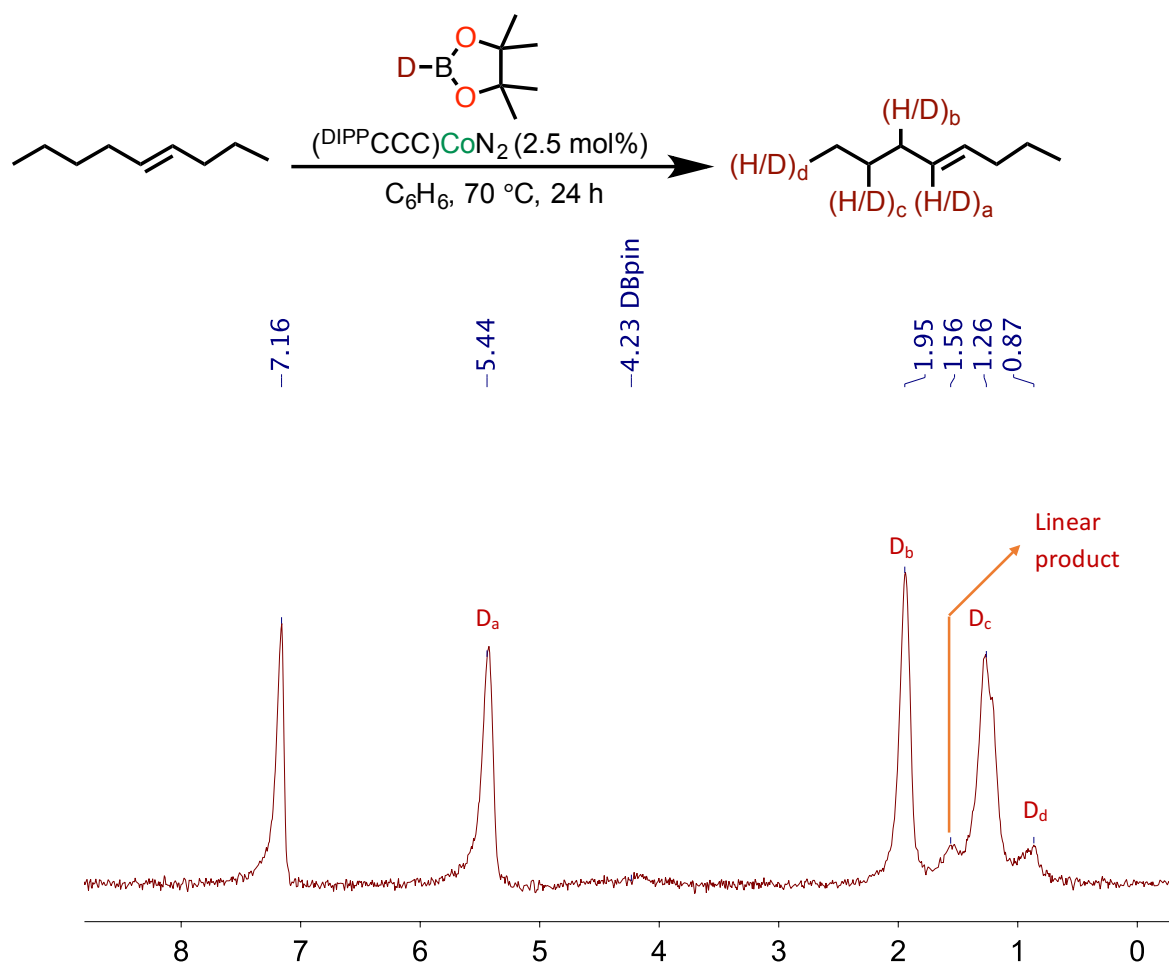


Figure 4.7 Hydroboration of trans-4-octene with DBpin

4.4 References

1. Martin, R. & Buchwald, S. L. Palladium-Catalyzed Suzuki–Miyaura Cross-Coupling Reactions Employing Dialkylbiaryl Phosphine Ligands. *Acc. Chem. Res.* **41**, 1461–1473 (2008).
2. Torborg, C. & Beller, M. Recent Applications of Palladium-Catalyzed Coupling Reactions in the Pharmaceutical, Agrochemical, and Fine Chemical Industries. *Adv. Synth. Catal.* **351**, 3027–3043 (2009).
3. Burgess, K. & Ohlmeyer, M. J. Enantioselective hydroboration mediated by homochiral rhodium catalysts. *J. Org. Chem.* **53**, 5178–5179 (1988).

4. Mkhaliid, I. A. I. *et al.* Rhodium catalysed dehydrogenative borylation of alkenes: Vinylboronates via C–H activation. *Dalt. Trans.* **95**, 1055–1064 (2008).
5. Zaidlewicz, M., Wolan, A. & Budny, M. 8.24 *Hydrometallation of C=C and C≡C Bonds. Group 3. Comprehensive Organic Synthesis II* (Elsevier, 2014). doi:10.1016/B978-0-08-097742-3.00826-0
6. Enthaler, S., Junge, K. & Beller, M. Sustainable Metal Catalysis with Iron: From Rust to a Rising Star? *Angew. Chemie Int. Ed.* **47**, 3317–3321 (2008).
7. Chirik, P. J. in *Catalysis without Precious Metals* 83–110 (Wiley-VCH Verlag GmbH & Co. KGaA, 2010). doi:10.1002/9783527631582.ch4
8. Wu, J. Y., Moreau, B. & Ritter, T. Iron-catalyzed 1,4-hydroboration of 1,3-dienes. *J. Am. Chem. Soc.* **131**, 12915–12917 (2009).
9. Obligacion, J. V & Chirik, P. J. Highly selective bis(imino)pyridine iron-catalyzed alkene hydroboration. *Org. Lett.* **15**, 2680–2683 (2013).
10. Palmer, W. N., Diao, T., Pappas, I. & Chirik, P. J. High-Activity Cobalt Catalysts for Alkene Hydroboration with Electronically Responsive Terpyridine and α -Diimine Ligands. *ACS Catal.* **5**, 622–626 (2014).
11. Zhang, L., Zuo, Z., Leng, X. & Huang, Z. A cobalt-catalyzed alkene hydroboration with pinacolborane. *Angew. Chem. Int. Ed. Engl.* **53**, 2696–2700 (2014).
12. Iwamoto, H., Kubota, K. & Ito, H. Highly selective Markovnikov hydroboration of alkyl-substituted terminal alkenes with a phosphine-copper(i) catalyst. *Chem. Commun. (Camb).* **52**, 5916–5919 (2016).
13. Kerchner, H. A. & Montgomery, J. Synthesis of Secondary and Tertiary Alkylboranes via Formal Hydroboration of Terminal and 1,1-Disubstituted Alkenes. *Org. Lett.* **18**, 5760–5763 (2016).
14. Zhang, L., Zuo, Z., Wan, X. & Huang, Z. Cobalt-Catalyzed Enantioselective Hydroboration of 1,1-Disubstituted Aryl Alkenes. *J. Am. Chem. Soc.* **136**, 15501–15504 (2014).
15. Chen, J. *et al.* Asymmetric cobalt catalysts for hydroboration of 1,1-disubstituted alkenes. *Org. Chem. Front.* **1**, 1306–1309 (2014).
16. Haberberger, M. & Enthaler, S. Straightforward Iron-Catalyzed Synthesis of Vinylboronates by the Hydroboration of Alkynes. *Chem. - An Asian J.* **8**, 50–54 (2013).
17. Zhang, L., Peng, D., Leng, X. & Huang, Z. Iron-catalyzed, atom-economical, chemo- and regioselective alkene hydroboration with pinacolborane. *Angew. Chem. Int. Ed. Engl.* **52**, 3676–80 (2013).
18. Zheng, J., Sortais, J.-B. & Darcel, C. [(NHC)Fe(CO)₄] Efficient Pre-catalyst for Selective Hydroboration of Alkenes. *ChemCatChem* **6**, 763–766 (2014).
19. Zhang, L., Zuo, Z., Leng, X. & Huang, Z. A Cobalt-Catalyzed Alkene Hydroboration with

- Pinacolborane. *Angew. Chemie Int. Ed.* **53**, 2696–2700 (2014).
20. Scheuermann, M. L., Johnson, E. J. & Chirik, P. J. Alkene isomerization-hydroboration promoted by phosphine-ligated cobalt catalysts. *Org. Lett.* **17**, 2716–2719 (2015).
 21. Greenhalgh, M. D. & Thomas, S. P. Chemo-, regio-, and stereoselective iron-catalysed hydroboration of alkenes and alkynes. *Chem. Commun. (Camb)*. **49**, 11230–11232 (2013).
 22. Chen, J., Xi, T. & Lu, Z. Iminopyridine oxazoline iron catalyst for asymmetric hydroboration of 1,1-disubstituted aryl alkenes. *Org. Lett.* **16**, 6452–6455 (2014).
 23. Peng, D. *et al.* Phosphinite-iminopyridine iron catalysts for chemoselective alkene hydrosilylation. *J. Am. Chem. Soc.* **135**, 19154–19166 (2013).
 24. Kubota, K., Yamamoto, E. & Ito, H. Copper(I)-catalyzed borylative exo-cyclization of alkenyl halides containing unactivated double bond. *J. Am. Chem. Soc.* **135**, 2635–2640 (2013).
 25. Yoshida, H., Takemoto, Y. & Takaki, K. Direct Synthesis of Boron-Protected Alkenyl- and Alkylborons via Copper-Catalyzed Formal Hydroboration of Alkynes and Alkenes. *Asian J. Org. Chem.* **3**, 1204–1209 (2014).
 26. Ibrahim, A. D., Entsminger, S. W., Zhu, L. & Fout, A. R. A Highly Chemoselective Cobalt Catalyst for the Hydrosilylation of Alkenes using Tertiary Silanes and Hydrosiloxanes. *ACS Catal.* **6**, 3589–3593 (2016).
 27. Parker, S. E., Börgel, J. & Ritter, T. 1,2-selective hydrosilylation of conjugated dienes. *J. Am. Chem. Soc.* **136**, 4857–4860 (2014).
 28. Zaidlewicz, M. & Meller, J. Syntheses with organoboranes. VII. Monohydroboration of conjugated dienes with catecholborane catalyzed by complexes of nickel(II) chloride and cobalt(II) chloride with diphosphines. *Tetrahedron Lett.* **38**, 7279–7282 (1997).
 29. Amundsen, L. H. & Nelson, L. S. Reduction of Nitriles to Primary Amines with Lithium Aluminum Hydride. *J. Am. Chem. Soc.* **73**, 242–244 (1951).
 30. Prasad, A. S. B., Kanth, J. V. B. & Periasamy, M. Convenient methods for the reduction of amides, nitriles, carboxylic esters, acids and hydroboration of alkenes using NaBH₄/I₂ system. *Tetrahedron* **48**, 4623–4628 (1992).
 31. Bagal, D. B. & Bhanage, B. M. Recent Advances in Transition Metal-Catalyzed Hydrogenation of Nitriles. *Adv. Synth. Catal.* **357**, 883–900 (2015).
 32. Lange, S. *et al.* Selective catalytic hydrogenation of nitriles to primary amines using iron pincer complexes. *Catal. Sci. Technol.* **6**, 4768–4772 (2016).
 33. Mukherjee, A., Srimani, D., Chakraborty, S., Ben-David, Y. & Milstein, D. Selective Hydrogenation of Nitriles to Primary Amines Catalyzed by a Cobalt Pincer Complex. *J. Am. Chem. Soc.* **137**, 8888–8891 (2015).
 34. Chakraborty, S., Leitus, G. & Milstein, D. Selective hydrogenation of nitriles to primary

- amines catalyzed by a novel iron complex. *Chem. Commun.* **52**, 1812–1815 (2016).
35. Reguillo, R., Grellier, M., Vautravers, N., Vendier, L. & Sabo-Etienne, S. Ruthenium-Catalyzed Hydrogenation of Nitriles: Insights into the Mechanism. *J. Am. Chem. Soc.* **132**, 7854–7855 (2010).
 36. Geri, J. B. & Szymczak, N. K. A Proton-Switchable Bifunctional Ruthenium Complex That Catalyzes Nitrile Hydroboration. *J. Am. Chem. Soc.* **137**, 12808–12814 (2015).
 37. Weetman, C. *et al.* Magnesium-catalysed nitrile hydroboration. *Chem. Sci.* **7**, 628–641 (2016).
 38. Pangborn, A. B., Giardello, M. A., Grubbs, R. H., Rosen, R. K. & Timmers, F. J. Safe and Convenient Procedure for Solvent Purification. *Organometallics* **15**, 1518–1520 (1996).
 39. Ibrahim, A. D. *et al.* Monoanionic bis(carbene) pincer complexes featuring cobalt(I–III) oxidation states. *Dalt. Trans.* **45**, 9805–9811 (2016).
 40. Mori-Quiroz, L. M., Shimkin, K. W., Rezazadeh, S., Kozlowski, R. A. & Watson, D. A. Copper-Catalyzed Amidation of Primary and Secondary Alkyl Boronic Esters. *Chem. - A Eur. J.* **22**, 15654–15658 (2016).
 41. Clary, J. W. *et al.* Hydride as a Leaving Group in the Reaction of Pinacolborane with Halides under Ambient Grignard and Barbier Conditions. One-Pot Synthesis of Alkyl, Aryl, Heteroaryl, Vinyl, and Allyl Pinacolboronic Esters. *J. Org. Chem.* **76**, 9602–9610 (2011).
 42. Wen, Y., Xie, J., Deng, C. & Li, C. Selective Synthesis of Alkylboronates by Copper(I)-Catalyzed Borylation of Allyl or Vinyl Arenes. *J. Org. Chem.* **80**, 4142–4147 (2015).
 43. Zhang, L., Peng, D., Leng, X. & Huang, Z. Iron-Catalyzed, Atom-Economical, Chemo- and Regioselective Alkene Hydroboration with Pinacolborane. *Angew. Chemie Int. Ed.* **52**, 3676–3680 (2013).
 44. Fletcher, C. J., Blair, D. J., Wheelhouse, K. M. P. & Aggarwal, V. K. The total synthesis of (–)-aplysin via a lithiation–borylation–propenylation sequence. *Tetrahedron* **68**, 7598–7604 (2012).
 45. Yi, J. *et al.* Alkylboronic Esters from Palladium- and Nickel-Catalyzed Borylation of Primary and Secondary Alkyl Bromides. *Adv. Synth. Catal.* **354**, 1685–1691 (2012).
 46. Falck, J. ., Kumar, P. S., Reddy, Y. K., Zou, G. & Capdevila, J. H. Stereospecific synthesis of EET metabolites via Suzuki–Miyaura coupling. *Tetrahedron Lett.* **42**, 7211–7212 (2001).
 47. Espinal-Viguri, M., Woof, C. R. & Webster, R. L. Iron-Catalyzed Hydroboration: Unlocking Reactivity through Ligand Modulation. *Chem. - A Eur. J.* **22**, 11605–11608 (2016).
 48. Ni, M. *et al.* Improved recognition of alkylammonium salts by ion pair recognition based on a novel heteroditopic pillar[5]arene receptor. *Tetrahedron Lett.* **53**, 6409–6413 (2012).
 49. Jackson, D. M., Ashley, R. L., Brownfield, C. B., Morrison, D. R. & Morrison, R. W. Rapid

Conventional and Microwave-Assisted Decarboxylation of L-Histidine and Other Amino Acids via Organocatalysis with R-Carvone Under Superheated Conditions. *Synth. Commun.* **45**, 2691–2700 (2015).

50. Hays, S. J. *et al.* 2-Amino-4H-3,1-benzoxazin-4-ones as Inhibitors of C1r Serine Protease. **41**, 1060–1067 (1998).

Chapter 5

Reactivity of (^{DIPP}CCC)CoN₂ towards dichalcogenides and other potential two-electron oxidants

5.1 Introduction

The use of highly electron-donating ligands with cobalt has been a successful approach to “ennobling” the base metal. Recent examples of cobalt-mediated oxidative addition or reductive elimination reactions, observed with substrates such as silanes,^{1,2} dihydrogen,³⁻⁵ and even arenes,^{5,6} underlie the tenability of two-electron redox events with base metals in the proper electron-rich ligand environment. Interestingly, although these cobalt-mediated processes are likely to proceed along two-electron pathways reminiscent of second- and third-row transition metal compounds, they can nevertheless provide orthogonal selectivities or reactivity to precious metal congeners.^{7,8} Accordingly, a study of the reactivity of electron-rich cobalt complexes towards various potential oxidants can provide meaningful insights into what factors impact observed selectivities and/or what factors dictate whether two-electron or single-electron redox events will be operative over the course of a reaction.

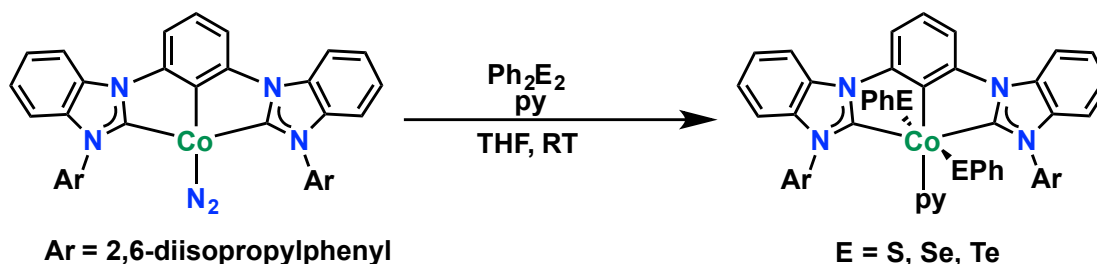
Using the electron-rich (^{DIPP}CCC) ligand platform (^{DIPP}CCC = bis(diisopropylphenylbenzimidazol-2-ylidene)phenyl), our laboratory has also investigated the ability of a strong-field ligand environment to support two-electron processes at a cobalt metal center. Using a Co^I compound, (^{DIPP}CCC)CoN₂, we reported a highly chemoselective hydrosilylation process with evidence of the oxidative addition of silane as the initial catalytic step.⁹ This process’ selectivity is dictated in many cases by the steric profile of the substrates, although the unique ability of the base metal to tolerate functionalities such as hydroxyl groups, amino groups, and nitriles, suggests electronic factors likely play an important role as well. Similarly, catalytic hydroboration with

$(^{\text{DIPP}}\text{CCC})\text{CoN}_2$ has highlighted the prominent role that sterics play in determining selectivity, in addition to establishing the viability of insertion, alkene isomerization, and β -hydride elimination processes at the metal under catalytic conditions.

Seeking to further elaborate on the reactivity of $(^{\text{DIPP}}\text{CCC})\text{CoN}_2$, we sought to explore the reactivity of the complex towards potential oxidants, such as diphenyl dichalcogenides and methyl iodide. These oxidants are regularly reacted with transition metal complexes and may, in theory, oxidize the metal by either a single electron or two electrons, providing a useful means with which to better understand the redox reactivity of the cobalt center.

5.2 The reactivity of $(^{\text{DIPP}}\text{CCC})\text{CoN}_2$ towards diphenyl dichalcogenides

To commence our studies, we investigated the reaction of $(^{\text{DIPP}}\text{CCC})\text{CoN}_2$ with diphenyl disulfide. Treatment of $(^{\text{DIPP}}\text{CCC})\text{CoN}_2$ (**1**) with diphenyl disulfide in the presence of pyridine resulted in the formation of a brown Co(III) bis(thiophenolate) complex, $(^{\text{DIPP}}\text{CCC})\text{Co}(\text{SPh})_2(\text{py})$, **2**, in excellent yields (81%) (Scheme 5.1).



Scheme 5.1 Reaction of $(^{\text{DIPP}}\text{CCC})\text{CoN}_2$ with diphenyl dichalcogenides

The ^1H NMR spectrum of **2** revealed a C_2 -symmetric diamagnetic compound consistent with cleavage of the sulfur-sulfur bond of the oxidant. ^1H NMR resonances corresponding to the

methyl protons of the ¹Pr moiety appear at 0.85 and 1.23 ppm and are slightly shifted from those of starting material, 0.02 ppm and 0.03 ppm respectively. Similarly, the methine protons of the ¹Pr moieties are shifted from those of the Co^I, appearing at 3.73 ppm vs. 2.71 ppm for **1**, (DIPP⁺CCC)CoN₂⁻. Such a downfield shift for the methine proton septet has been regularly observed with a higher oxidation state at the metal for this platform.

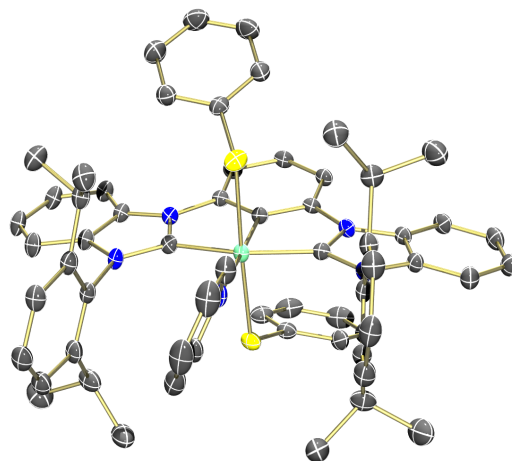


Figure 5.1. Crystal Structure of **2**

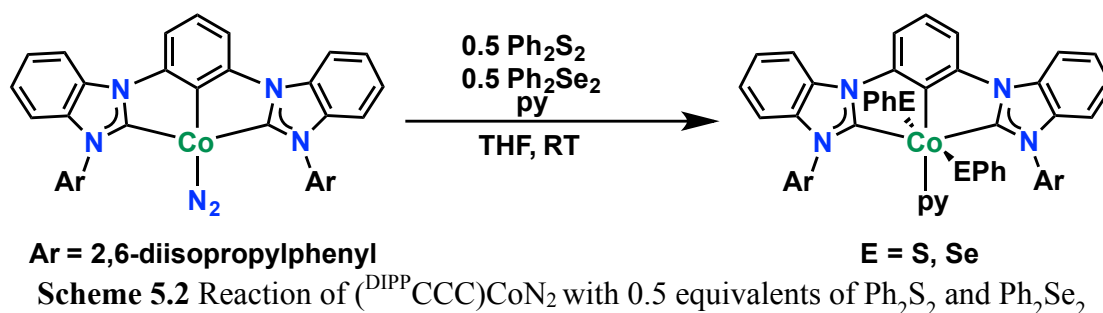
This formulation was corroborated by X-ray diffraction studies; characterization of the crystalline product, obtained by slow evaporation of a concentrated solution of **2** from benzene, indicates the presence of two thiophenolate ligands and a pyridine coordinated to the metal center in an octahedral geometry, establishing a formal +3 oxidation state at the metal (Figure 5.1).

Reactions of **1** with diphenyl diselenide and diphenyl ditelluride produced similar NMR spectra and verify the successful formation of the selenide (**3**) and telluride (**4**) analogues to the bis(thiophenolate) complex. ¹H NMR resonances of **3** corresponding to the methyl protons of the ¹Pr moiety appear at 0.85 and 1.23 ppm and are again shifted from those of starting material. Similarly, the methine protons of the ¹Pr moieties are shifted from those of the Co^I, appearing at 3.76 ppm vs. 2.71 ppm. Similar shifts are observed in the ¹H NMR resonances of **4**. Methyl protons of the ¹Pr moiety appear at 0.89 and 1.21 ppm, while a resonance at 3.78 ppm is attributed to the methine protons of the ¹Pr group.

Complex **2** is a rare example of a cobalt(III) bis(thiophenolate) compound. A search for similar complexes in the Cambridge Structural Database at the time of this isolation yielded only 7 other examples of crystallographically characterized mononuclear Co(III) centers featuring two

thiophenolate moieties.¹⁰

Mechanistic investigations suggest radical events may be operative in the cleavage of the dichalcogenide bonds. Treatment of **1** with 0.5 equivalents of Ph₂S₂ resulted in the formation of a complex mixture of diamagnetic products, which includes the bis(thiophenolate) species **2**, in addition to paramagnetic species whose ¹H NMR resonances are similar to those reported for the Co^{II} complex (DIPP^{CCC})CoClpy. Similarly, treatment of **1** with 0.5 equivalent of Ph₂S₂ and 0.5 equivalents of Ph₂Se₂ resulted in the formation of three products by ¹H NMR spectroscopy, assigned to the bis(sulfide), bis(selenide), and a presumed mixed species bearing both thiophenolate and selenophenolate ligands (Scheme 5.2).

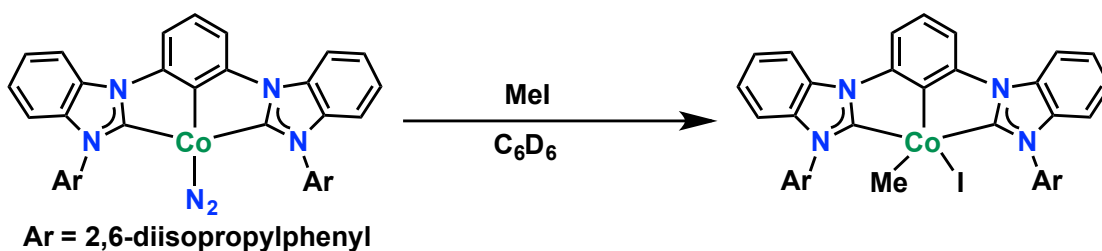


5.3 Synthesis of (DIPP^{CCC})Co(Me)I

In an attempt to investigate the potential of **1** to undergo oxidative addition, MeI, a substrate that can either undergo S_N2 type reactivity or homolytically cleave in the presence of a nucleophilic metal species, was reacted with a thawing solution of **1** in C₆D₆ (Scheme 5.3). The solution took on a yellow-green color and was immediately characterized by ¹H NMR spectroscopy (Figure 5.2). A new upfield singlet in the ¹H NMR integrating to three protons was observed at -0.26 ppm and was assigned to the newly appended methyl moiety. The appearance of four doublets and two septets corresponding to the methyl and methine protons of the ¹Pr moieties of the ligand also confirmed the presence of a dissymmetric environment about the metal center, suggesting the

compound was a Co(III) iodomethyl species, $(^{\text{DIPP}}\text{CCC})\text{Co}(\text{Me})\text{I}$ (**5**), rather than a C_2 -symmetric Co^{III} bis(iodide) or bis(methyl) compound. Thermal instability of product **5** has precluded further characterization.

The transient nature of **5** is not unusual given the significant trans effect of the aryl backbone carbon of the pincer. The presence of strongly-donating alkyl or aryl ligands is often difficult to detect with the $(^{\text{DIPP}}\text{CCC})$ ligand. Indeed, transmetalation attempts with $(^{\text{DIPP}}\text{CCC})\text{CoCl}_2\text{py}$ and MesMgBr have resulted in the formation of bimesitylene and $(^{\text{DIPP}}\text{CCC})\text{CoN}_2$ (**1**) products, rather than targeted $(^{\text{DIPP}}\text{CCC})\text{Co}(\text{Mes})\text{Clpy}$.



Scheme 5.3 Reaction of $(^{\text{DIPP}}\text{CCC})\text{CoN}_2$ with MeI

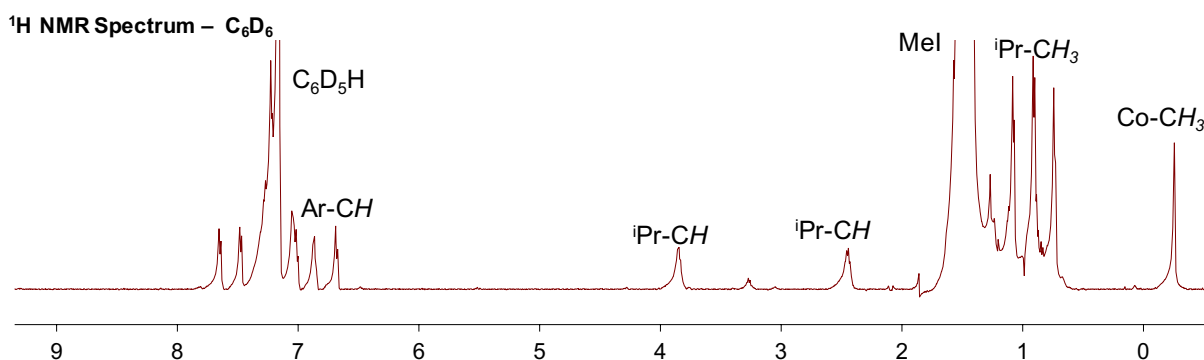


Figure 5.2 ^1H NMR spectrum of Co(III) iodomethyl species

5.4 Dehydrocoupling of ammonia-borane: Isolation of $(^{\text{DIPP}}\text{CCC})\text{Co}(\eta^2\text{-BH}_3)(\text{H})$ (**10**)

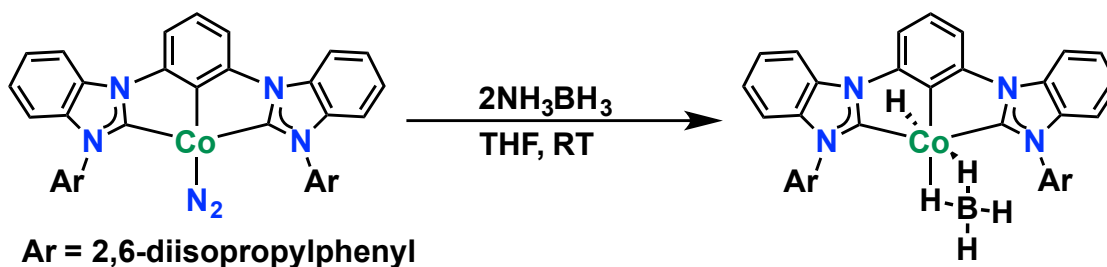
Intrigued by a recent report of a hydridoborane cobalt tetrahydridoborate complex¹¹ generated from the addition of an amine borane to a Co(I) starting material and mindful of the

limited number of homogeneous dehydrocoupling catalysts featuring first-row transition metals^{12,13}, we sought to explore the reactivity of **1** towards ammonia-borane. We reasoned that the absence of a coordinating atom capable of directly assisting in the cleavage of the amine-borane bonds may result in an entirely metal-mediated process to generate a Co^{III} product.

Addition of NH₃BH₃ to a solution of **1** in benzene and subsequent stirring at room temperature overnight afforded a light brown-yellow reaction mixture. Subsequent workup of the reaction afforded a light yellow solid **6** (Scheme 5.4).

The presence of a cobalt hydride and an η²-BH₄ was established by ¹H NMR and infrared spectroscopies (Figure 5.3). Upfield singlets at -14.52, -8.56, and -0.11 ppm, integrating in a 1:1:2 ratio, were assigned to a cobalt-hydride, a bridging hydride, and the two hydrides exclusive to the BH₄ moiety. Additionally, the presence of a dissymmetric environment, reflected in the presence of additional doublets and septets corresponding to the ¹Pr moieties of the ligand, lend credence to the formation of (DIPP^{CCC})Co(η²-BH₄)(H).

Similarly, the presence of B–H stretches at 1879 cm⁻¹, 2431 cm⁻¹, and 2452 cm⁻¹ by infrared spectroscopy establish an η² coordination mode for the BH₄ ligand, comparing favorably to values observed for a cobalt tetrahydroborate complex reported by Peters¹¹, as well for other transition metal tetrahydroborate complexes.¹⁴ In addition to the significance of this chemistry to hydrogen storage and the formation of inorganic polymers,¹⁵ such molecules may provide insight into the dehydrogenation of ammonia-borane.^{16,17}



Scheme 5.4 Reaction of $(^{\text{DIPP}}\text{CCC})\text{CoN}_2$ with NH_3BH_3

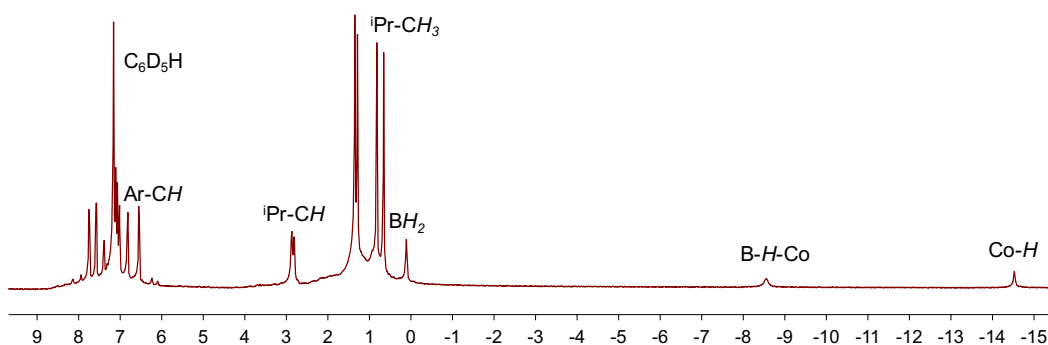


Figure 5.3 ^1H NMR spectrum of Co(III) tetrahydridoborate species

5.5 Conclusions

In conclusion, the reactivity of the $(^{\text{DIPP}}\text{CCC})\text{CoN}_2$ species towards a variety of oxidants may largely be dictated by the bond strengths of the particular substrate. The cleavage of bonds with a higher bond dissociation energy, such as Si–H and B–H bonds for example,¹⁸ appears to proceed along two-electron pathways, as observed in the case of ammonia borane, diphenylsilane,⁹ and pinacolborane (see Chapters 3 and 4). In contrast, the lower BDE of the E–E bond in dichalcogenide substrates is coincident with apparent homolytic cleavage pathways.¹⁸ Finally, the apparent oxidative addition of the weak C–I bond in methyl iodide suggests that the accessibility of alternative pathways (perhaps $\text{S}_{\text{N}}2$ substitution for a sterically unencumbered alkyl halide)¹⁹ may eclipse simple BDE metrics of the targeted bond in determining operant mechanisms, i.e. one-electron or two-electron pathways, for certain substrates. These results, while requiring further

elaboration, may provide a framework to rationalize reactivity observed with the (^{DIPP}CCC) system and should inform future experiments with this platform.

5.6 Experimental section

General Considerations. All manipulations of air- and moisture-sensitive compounds were carried out in the absence of water and dioxygen in an MBraun inert atmosphere drybox under a dinitrogen atmosphere except where specified otherwise. All glassware was oven dried for a minimum of 8 h and cooled in an evacuated antechamber prior to use in the drybox. Solvents for sensitive manipulations were dried and deoxygenated on a Glass Contour System (SG Water USA, Nashua, NH) and stored over 4 Å molecular sieves purchased from Strem following drying via a literature procedure prior to use.¹ Benzene-*d*₆ were purchased from Cambridge Isotope Labs and was degassed and stored over 4 Å molecular sieves prior to use. Celite® 545 (J. T. Baker) was used as received. NMR Spectra were recorded at room temperature on a Varian or Bruker spectrometer operating at 500 MHz or 400 MHz (¹H NMR), 126 MHz or 101 MHz (¹³C NMR), and 119 MHz (²H NMR) (U500, VXR500, UI500NB, CB500, U400) and referenced to the residual C₆D₅H resonances (δ in parts per million, and *J* in Hz). (^{DIPP}CCC)CoN₂ was prepared according to literature procedure.²⁰ Diphenyl disulfide, diphenyl diselenide, and diphenyl ditelluride were obtained from Sigma-Aldrich and used as received. All liquids were dried over 4 Å molecular sieves prior to use.

Preparation of (^{DIPP}CCC)Co(SPh)₂(py) (2). A solution of (^{DIPP}CCC)Co(N₂) (1) (0.035 g, 0.0488 mmol) in approximately 1 mL of THF was prepared and cooled to -35 °C. To this mixture was added a similarly chilled solution of diphenyl disulfide (0.0107 g, 0.0490 mmol) in THF (1 mL).

Additional solvent (1 mL) was used to rinse and complete the transfer, a drop of pyridine was added, and the reaction mixture was stirred overnight at room temperature. Upon completion of the stirring period, volatiles were removed in vacuo to yield the pure brown solid (0.039 g, 0.0395 mmol, 81%). Crystals suitable for X-ray diffraction were grown by slow evaporation from benzene. ^1H NMR (500 MHz, Benzene- d_6) δ 8.74 (d, $J = 5.2$ Hz, 2H), 7.75 (d, $J = 8.2$ Hz, 2H), 7.12-7.03 (m), 7.01 (d, $J = 7.8$ Hz, 4H), 6.91 (d, $J = 8.0$ Hz, 6H), 6.85 (dd, $J = 14.8, 7.4$ Hz, 6H), 6.72 (d, $J = 8.0$ Hz, 1H), 6.61 (dd, $J = 18.6, 7.9$ Hz, 6H), 6.47 (t, $J = 7.4$ Hz, 4H), 6.16 – 6.06 (m, 2H), 3.82 – 3.65 (m, 4H), 1.23 (d, $J = 6.6$ Hz, 12H), 0.85 (d, $J = 6.7$ Hz, 12H). ^{13}C NMR (126 MHz, Benzene) δ 154.21, 148.38, 145.88, 144.56, 139.62, 137.53, 132.14, 130.05, 128.36, 128.25, 128.12, 128.06, 127.92, 127.87, 126.68, 124.39, 123.94, 123.28, 121.76, 112.60, 111.21, 108.84, 28.25, 26.07, 23.48.

Preparation of ($^{\text{DIPP}}\text{CCC})\text{Co}(\text{SePh})_2(\text{py})$ (3**).** Inside a glovebox, a solution of **1** (0.030 g, 0.0419 mmol) in approximately 1 mL of THF was prepared and cooled to -35 °C. To this mixture was added a similarly chilled solution of diphenyl diselenide (0.0131 g, 0.0420 mmol) in THF (1 mL). Additional solvent (1 mL) was used to rinse and complete the transfer, a drop of pyridine was added, and the reaction mixture was stirred overnight at room temperature. Upon completion of the stirring period, volatiles were removed under reduced pressure to yield the green-brown solid (0.0392 g, 0.0363 mmol, 87%). ^1H NMR (500 MHz, Benzene- d_6) δ 8.63 – 8.55 (m, 2H), 7.72 (d, $J = 8.1$ Hz, 2H), 7.51 (dd, $J = 7.2, 2.2$ Hz, 4H), 7.11 – 7.00 (m), 6.93-6.83 (m, 14H), 6.71 (d, $J = 7.5$ Hz, 4H), 6.67 (t, $J = 7.8$ Hz, 2H), 6.57 (d, $J = 8.0$ Hz, 2H), 6.45 (t, $J = 7.5$ Hz, 3H), 6.02 (t, $J = 6.7$ Hz, 1H), 3.76 (sept, $J = 6.7$ Hz, 4H), 1.22 (d, $J = 6.6$ Hz, 12H), 0.85 (d, $J = 6.8$ Hz, 12H). The product was not sufficiently pure to definitively assign the product compound's resonances in the ^{13}C NMR spectrum. Accordingly, the following values are tentatively assigned. ^{13}C NMR (126

MHz, C₆D₆) δ 206.3, 164.2, 155.3, 148.5, 145.6, 139.9, 138.5, 134.7, 134.1, 132.6, 131.7, 131.4, 130.1, 129.4, 127.9, 126.6, 124.7, 124.5, 123.0, 121.8, 121.5, 121.5, 28.2, 26.2, 23.6.

Preparation of (^{DIPP}CCC)Co(TePh)₂(py) (4). Inside a glovebox, a solution of **1** (0.005 g, 0.00698 mmol) in approximately 1 mL of THF was prepared at room temperature. To this mixture was added a solution of diphenyl ditelluride (0.0029 g, 0.00696 mmol) in THF (1 mL). Additional solvent (1 mL) was used to rinse and complete the transfer, a drop of pyridine was added, and the reaction mixture was stirred overnight at room temperature. Upon completion of the stirring period, volatiles were removed under reduced pressure to yield the green-brown solid (0.0068 g, 0.00600 mmol, 86%). ¹H NMR (499 MHz, Benzene-*d*₆) δ 8.61 (d, *J* = 5.4 Hz, 2H), 7.64 (d, *J* = 8.4 Hz, 2H), 7.11 – 6.77 (m), 6.77– 6.61 (m), 6.55 (t, *J* = 8.9 Hz, 4H), 6.44 (t, *J* = 7.5 Hz, 6H), 5.86 (t, *J* = 6.8 Hz, 1H), 3.78 (sept, *J* = 6.8 Hz, 4H), 1.21 (d, *J* = 6.6 Hz, 12H), 0.89 (d, *J* = 6.7 Hz, 12H). The product was not sufficiently pure to definitively assign the product compound's resonances in the ¹³C NMR spectrum.

Reaction of (^{DIPP}CCC)Co(N₂) with 0.5 equiv. of Ph₂S₂ and 0.5 equiv. of Ph₂Se₂. Inside a glovebox, a solution of **1** (0.0248 g, 0.0346 mmol) in approximately 1 mL of THF was prepared in a 20 mL scintillation vial and chilled to -35 °C. To this solution, was added a solution of diphenyl disulfide (0.0038 g, 0.0174 mmol) and diphenyl diselenide (0.0054 g, 0.0173 mmol) in THF (2 mL). Additional solvent (1 mL) was used to rinse and complete the transfer, a drop of pyridine was added, and the reaction mixture was stirred overnight at room temperature. Upon completion of the stirring period, volatiles were removed under reduced pressure to yield a brown residue. An

NMR of this compounds revealed both **2** and **3**, in addition to a presumed mixed species assigned as the (^{DIPP}CCC)Co(SPh)(SePh)(py).

Reaction of (^{DIPP}CCC)Co(N₂) with 0.5 equiv. of Ph₂S₂. Inside a glovebox, a solution of **1** (0.040 g, 0.0558 mmol) in approximately 2 mL of THF was prepared in a 20 mL scintillation vial and chilled to -35 °C. To this solution, was added a solution of diphenyl disulfide (0.0061 g, 0.0279 mmol) in THF (1 mL). Additional solvent (1 mL) was used to rinse and complete the transfer, a drop of pyridine was added, and the reaction mixture was stirred overnight at room temperature. Upon completion of the stirring period, volatiles were removed under reduced pressure to yield a brown residue. An NMR of this compounds revealed **2**, as well as a complex mixture of diamagnetic and paramagnetic compounds.

Preparation of (^{DIPP}CCC)Co(Me)I (5**).** Inside a glovebox, a solution of **1** (0.005 g, 0.00698 mmol) in approximately 0.5 mL of C₆D₆ was prepared and frozen -35 °C. To this thawing solution was added a drop of methyl iodide and the resulting mixture quickly turned a yellow-green color, whose ¹H NMR spectrum was rapidly recorded. ¹H NMR (500 MHz, Benzene-*d*₆) δ 7.65 (d, *J* = 8.4 Hz, 2H), 7.48 (d, *J* = 7.9 Hz, 2H), 7.37 – 7.20 (m), 7.13 – 6.97 (m, 3H), 6.93 – 6.81 (m, 3H), 6.68 (d, *J* = 8.9 Hz, 2H), 3.98 – 3.75 (m, 2H), 2.62 – 2.33 (m, 2H), 1.53 (d, *J* = 6.4 Hz), 1.08 (d, *J* = 6.6 Hz, 6H), 0.91 (d, *J* = 6.8 Hz, 6H), 0.74 (d, *J* = 6.8 Hz, 6H), -0.25 (s, 3H).

Preparation of (^{DIPP}CCC)Co(η²-BH₄)(H) (6**).** A 20 mL scintillation vial was charged with NH₃BH₃ (0.0018 g, 0.0583 mmol). To this vial was added a solution of **1** (0.00205 g, 0.0286 mmol) in ca. 1 mL of THF. Additional solvent (1 mL) was used to rinse and complete the transfer, and the reaction mixture was stirred overnight at room temperature. Upon completion of the

stirring period, volatiles were removed under reduced pressure and the residue was taken up in benzene, filtered over Celite, and dried under reduced pressure to afford a light brown-yellow solid. (0.020 g, 0.0284 mmol, 99%). $^1\text{H NMR}$ (500 MHz, Benzene- d_6) δ 7.74 (d, $J = 8.0$ Hz, 2H), 7.58 (d, $J = 7.7$ Hz, 2H), 7.39 (t, $J = 7.7$ Hz, 1H), 7.13 (d, $J = 7.7$ Hz, 2H), 7.11 – 7.08 (m, 2H), 7.05 (dd, $J = 7.6, 1.8$ Hz, 2H), 7.01 (t, $J = 7.4$ Hz, 2H), 6.81 (t, $J = 7.6$ Hz, 2H), 6.54 (d, $J = 8.0$ Hz, 2H), 2.91 – 2.84 (m, 2H), 2.84 – 2.78 (m, 2H), 1.35 (d, $J = 6.5$ Hz, 6H), 1.28 (d, $J = 6.8$ Hz, 6H), 0.81 (d, $J = 6.7$ Hz, 6H), 0.65 (d, $J = 6.9$ Hz, 6H), 0.11 (s, 2H), -8.57 (s, 1H), -14.52 (s, 1H). IR: 1879 cm^{-1} , 2431 cm^{-1} , 2452 cm^{-1} .

5.7 References

1. Rozenel, S. S., Padilla, R. & Arnold, J. Chemistry of reduced monomeric and dimeric cobalt complexes supported by a PNP pincer ligand. *Inorg. Chem.* **52**, 11544–11550 (2013).
2. Scheuermann, M. L., Semproni, S. P., Pappas, I. & Chirik, P. J. Carbon dioxide hydrosilylation promoted by cobalt pincer complexes. *Inorg. Chem.* **53**, 9463–9465 (2014).
3. Ingleson, M., Fan, H., Pink, M., Tomaszewski, J. & Caulton, K. G. Three-Coordinate Co(I) Provides Access to Unsaturated Dihydrido-Co(III) and Seven-Coordinate Co(V). *J. Am. Chem. Soc.* **128**, 1804–1805 (2006).
4. Rozenel, S. S., Padilla, R., Camp, C. & Arnold, J. Unusual activation of H_2 by reduced cobalt complexes supported by a PNP pincer ligand. *Chem. Commun. (Camb)*. **50**, 2612–2614 (2014).
5. Semproni, S. P., Hojilla Atienza, C. C. & Chirik, P. J. Oxidative addition and C–H activation chemistry with a PNP pincer-ligated cobalt complex. *Chem. Sci.* **5**, 1956–1960 (2014).
6. Obligacion, J. V., Semproni, S. P. & Chirik, P. J. Cobalt-catalyzed C–H borylation. *J. Am. Chem. Soc.* **136**, 4133–4136 (2014).
7. Obligacion, J. V., Semproni, S. P., Pappas, I. & Chirik, P. J. Cobalt-Catalyzed $\text{C}(\text{sp}^2)$ -H Borylation: Mechanistic Insights Inspire Catalyst Design. *J. Am. Chem. Soc.* **138**, 10645–10653 (2016).
8. Obligacion, J. V., Bezdek, M. J. & Chirik, P. J. $\text{C}(\text{sp}^2)$ -H Borylation of Fluorinated Arenes Using an Air-Stable Cobalt Precatalyst: Electronically Enhanced Site Selectivity Enables Synthetic Opportunities. *J. Am. Chem. Soc.* **139**, 2825–2832 (2017).
9. Ibrahim, A. D., Entsminger, S. W., Zhu, L. & Fout, A. R. A Highly Chemoselective Cobalt

- Catalyst for the Hydrosilylation of Alkenes using Tertiary Silanes and Hydrosiloxanes. *ACS Catal.* **6**, 3589–3593 (2016).
10. Allen, F. H. The Cambridge Structural Database: a quarter of a million crystal structures and rising. *Acta Crystallogr. Sect. B Struct. Sci.* **58**, 380–388 (2002).
 11. Lin, T. & Peters, J. C. Boryl-Mediated Reversible H₂ Activation at Cobalt: Catalytic Hydrogenation, Dehydrogenation, and Transfer Hydrogenation. **135**, 15310–15313 (2013).
 12. Clark, T. J., Russell, C. A. & Manners, I. Homogeneous, Titanocene-Catalyzed Dehydrocoupling of Amine-Borane Adducts. 9582–9583 (2006).
 13. Vogt, M., de Bruin, B., Berke, H., Trincado, M. & Grützmacher, H. Amino olefin nickel(i) and nickel(0) complexes as dehydrogenation catalysts for amine boranes. *Chem. Sci.* **2**, 723–727 (2011).
 14. Besora, M. & Lledós, A. *Coordination Modes and Hydride Exchange Dynamics in Transition Metal Tetrahydroborate Complexes*. (Springer-Verlag Berlin Heidelberg, 2008).
 15. Baker, R. T. *et al.* Iron complex-catalyzed ammonia-borane dehydrogenation. A potential route toward B-N-containing polymer motifs using earth-abundant metal catalysts. *J. Am. Chem. Soc.* **134**, 5598–5609 (2012).
 16. Duman, S. & Özkar, S. Hydrogen generation from the dehydrogenation of ammonia-borane in the presence of ruthenium(III) acetylacetonate forming a homogeneous catalyst. *Int. J. Hydrogen Energy* **38**, 180–187 (2013).
 17. Murugesan, S. & Kirchner, K. Non-precious metal complexes with an anionic PCP pincer architecture. *Dalt. Trans.* **45**, 416–439 (2016).
 18. Blanksby, S. J. & Ellison, G. B. Bond Dissociation Energies of Organic Molecules. **36**, 255–263 (2003).
 19. Crabtree, R. H. *The Organometallic Chemistry of the Transition Metals*. (John Wiley & Sons, Inc., 2009).
 20. Ibrahim, A. D. *et al.* Monoanionic bis(carbene) pincer complexes featuring cobalt(I–III) oxidation states. *Dalt. Trans.* **45**, 9805–9811 (2016).